Electronic Thesis and Dissertation Repository

3-25-2020 3:30 PM

Smouldering Combustion Treatment of Soils and Granular Activated Carbon Contaminated with Per- and Polyfluoroalkyl Substances

Alexandra L. Duchesne, *The University of Western Ontario*

Supervisor: Gerhard, Jason I., *The University of Western Ontario*
A thesis submitted in partial fulfillment of the requirements for the Master of Engineering Science degree in Civil and Environmental Engineering
© Alexandra L. Duchesne 2020

Follow this and additional works at: https://ir.lib.uwo.ca/etd

Part of the Environmental Engineering Commons

Abstract

Per- and polyfluoroalkyl substances (PFAS) are emerging contaminants, ubiquitous in the environment, and are challenging to remediate. Self-sustaining Treatment for Active Remediation (STAR) destroys organic contaminants embedded in porous media using smouldering combustion. Self-sustaining smouldering conditions allow the reaction to propagate through the contaminated media without external energy. This study explored STAR as a remediation option for PFAS-impacted granular activated carbon (GAC) and PFAS-contaminated soil. Three smouldering mixtures were used (i) PFAS-spiked GAC and sand, (ii) PFAS-spiked soil and GAC, (iii) PFAS-contaminated field site soil and GAC. Smouldering temperatures were greater than 900°C, destroying the GAC. Post-treatment PFAS concentrations of the sand, soil, and ash were near or below detection limits (0.5 μg/kg). Analysis of emissions demonstrated hydrogen fluoride and shorter-chain PFAS were produced suggesting PFAS had been mineralized and altered during smouldering. Results suggest STAR is an effective remediation technique for PFAS-impacted soils and PFAS-saturated GAC.

Summary for Lay Audience

Non-stick pans, waterproof clothing, fast-food wrappers, and stain-resistant carpets are some of the countless products that are made with a group of man-made chemicals called PFAS. PFAS are also included in foams used at airports and military sites to extinguish fires. The sites that have used the foam and manufactured PFAS has led to PFAS getting into the environment. PFAS chemicals do not naturally breakdown so they accumulate in the environment and people, where they are suspected to cause various health problems. To remove PFAS from drinking water, carbon filters are most commonly used. However, at the end of their lifespan, few disposal options are available. Also, no methods currently exist that are effective at removing PFAS compounds attached to soil. STAR is a heat-based treatment option for soils that has been shown to destroy other contaminants. STAR requires little energy to operate, allowing STAR to be cheap and useful method to clean-up contaminated soils. This research, for the first time, explored using STAR as a treatment option to remove PFAS from polluted soils and carbon filter material. STAR technology can bring contaminated soils and carbon filter material to extreme temperature (900˚C or greater), destroying the carbon filter material and breaking down the PFAS. Results showed that after using STAR, no PFAS remained in the soil. Compounds released into the air were either non-toxic or could be absorbed to other carbon filters that could be treated later. This research demonstrated STAR is an option to treat carbon filter material and soil contaminated with PFAS, removing these toxic compounds from the environment.

Co-Authorship

This thesis was written in accordance with regulations and guidelines set by the Faculty of Graduate and Postdoctoral Studies at the University of Western Ontario. All experiments and data were conducted, collected, and analyzed by the candidate with the supervision and guidance of Dr. Jason I. Gerhard. The candidate wrote the thesis and was the main author on the manuscript chapter, which is expected to be submitted for publication:

Chapter 3: Smouldering Combustion Treatment of Soils and Granular Activated Carbon Contaminated with Per- and Polyfluoroalkyl Substances

By   Alexandra L. Duchesne, Jason I. Gerhard, David Major, Joshua Brown, Kela Weber, and David Patch

Alexandra L. Duchesne: helped design experiments, performed all experiments, coordinated all sampling and analytical work, completed analysis and interpretation of all results, and wrote the draft chapter.

Jason I. Gerhard: initiated the research topic, funded the research, helped design and supervised the project, assisted in data interpretation, and reviewed/revised the drafter chapter.

David Major: initiated the research topic, helped obtain funding, assisted with data interpretation, and reviewed/revised the draft chapter.

Joshua Brown: assisted with experiments and data interpretation, and reviewed/revised the drafter chapter.

iv

Kela P. Weber: helped design sampling and analytical protocols, assisted with data interpretation and reviewed/revised the draft chapter.

David Patch: analyzed PFAS samples, improved sampling and analytical protocols, assisted with data interpretation, and reviewed/revised the draft chapter.

Table of Contents

List of Tables

List of Figures

List of Abbreviations and Symbols

AFFF:	aqueous film forming foams
B.D.L.:	below detection limit
B.Q.L.:	below quantification limit
CF_4:	tetrafluoromethane
C_2F_6:	hexafluoroethane
CIC:	combustion ion chromatography
cm:	centimeter
CO_2:	carbon dioxide
CO:	carbon monoxide
DoH:	Department of Health
ECCC:	Environment and Climate Change Canada
g:	gram
GAC:	granular activated carbon
GC-MS:	gas chromatography - mass spectrometry
HC:	Health Canada
HF:	hydrofluoric acid
HPLC:	high performance liquid chromatography
ISE:	ion-selective electrode
kg:	kilogram
L:	liter
LC-MS/MS:	liquid chromatography with tandem mass spectrometry
min:	minute
mg:	milligram
O_2:	oxygen
PFAA:	perfluoroalkyl acids
PFAS:	per- and polyfluoroalkyl substance
PFBA:	perfluorobutanoic acid
PFBS:	perfluorobutanesulfonic acid
PFCA:	perfluorinated carboxylic acids
PFDA:	perfluorodecanoic acid
PFHpA:	perfluoroheptanoic acid
PFHxS:	perfluorohexanesulfonic acid
PFPA:	perfluoropropanoic acid
PFPeA:	perfluoropentanoic acid
PFOA:	perfluorooctanoic acid
PFOS:	perfluorooctanesulfonic acid
PFNA:	perfluorononanoic acid
PFSA:	perfluorinated sulfonic acids
RPD:	relative percent difference
s:	second
STAR:	Self-Sustaining Treatment for Active Remediation
TC:	thermocouple
TCE:	trichloroethylene
TFA:	thrifluoroacetic
TOF:	total organic fluorine

XAD: sorbent tube
VOF: volatile organic fluorine
  ≈ : approximately equal to
  ˚C : degrees Celsius
  > : greater than
  ≤ : less than or equal to
  µg : microgram
  % : percent

Chapter 1

Introduction

1.1. Problem Overview

Per- and polyfluoroalkyl substances (PFAS) are a group of emerging contaminants, known for persistence in the environment (Espana et al., 2015; Kuroda et al., 2014; Wang et al., 2015). PFAS are comprised of a partially or fully fluorinated carbon chain and a functional head group, with sulfonic and carboxylic being two of the most common (Buck et al., 2011; Pabon & Corpart, 2002). The unique properties of PFAS and their structure makes them resistant to thermal and chemical degradation (3M Corporation, 1999; Buck et al., 2011; Kissa, 2001). These properties make PFAS ideal for manufacturing and industrial uses, such as aqueous film forming foam (AFFF), waterproof clothing, and textiles (Paul et al., 2009; Schaider et al., 2017). Long-term use of PFAS at manufacturing facilities and AFFF at airports, military and training sites has led to widespread contamination of PFAS in the environment (Cousins et al., 2016; Hu et al., 2016; Rayne & Forest, 2009).

Increasingly stringent regulations for drinking water and soil and the health concerns relating to PFAS are driving the need for remediation technologies (Trojanowicz et al., 2018). Granular activated carbon (GAC) is the most common option for removing PFAS from contaminated drinking water (Espana et al., 2015; Hale et al., 2017; Kucharzyk et al., 2017). However, the spent GAC will need to be regenerated or disposed. This requires incineration or thermal treatment to destroy or regenerate the GAC (Espana et al., 2015). Incineration is expensive due to the energy required for treatment and facilities licensed to

accept PFAS-laden materials are not widely available, and as a result is not an ideal disposal option (Dorrance et al., 2017).

Existing remediation technologies for soil have proven inadequate for remediating PFAS contamination (Brusseau, 2018; Schaefer et al., 2015). The range of PFAS compounds at contaminated sites create challenges since many technologies cannot breakdown all types of PFAS (Dorrance et al., 2017). Landfilling, incineration, and soil washing are the most popular options for PFAS-contaminated soils (Crownover et al., 2019; Dorrance et al., 2017; Ross et al., 2018). Landfilling creates a long-term liability and is becoming more restricted by regulations (Hale et al., 2017; Ross et al., 2018). Soil washing, like incineration, is expensive, creates an additional waste stream, and is impractical for large volumes of contaminated soils (Dorrance et al., 2017; Ross et al., 2018).

Self-Sustaining Treatment for Active Remediation (STAR) has been shown to be a promising remediation option for liquid organic wastes, such as coal tar and crude oil (Pironi et al., 2011; Switzer et al., 2009). STAR uses smouldering combustion, which is a flameless, exothermic, oxidation reaction that occurs on the surface of a solid fuel when exposed to oxygen (Ohlemiller, 1985). The smouldering reaction creates a hot, thin front where the oxidation reaction destroys the fuel, leaving clean sand (Pironi et al., 2009). Smouldering conditions can create a self-sustaining smouldering reaction allowing STAR to be energy-efficient (Hasan et al., 2015). For some fuels, the volatility or low concentration in the soil prevent self-sustaining smouldering and therefore require a surrogate fuel (Kinsman et al., 2017; Salman et al., 2015). Fuels like vegetable oil and wood chips have been mixed into contaminated soils to allow for remediation to be

successful (Gianfelice et al., 2019; Salman et al., 2015). Smouldering temperatures are commonly between 500-1200˚C, depending largely on the energy content and concentration of the fuel (Zanoni et al., 2019).

Heating PFAS-contaminated soils at 400-500˚C has been shown to remove the PFAS from the soil but will not destroy them (Ross et al., 2018). During GAC regeneration, temperatures greater than 700˚C are required to remove PFAS, however, temperatures greater than 900˚C are needed to mineralize the PFAS compounds (Ross et al., 2018; Wang et al., 2015; Watanabe et al., 2016; Yamada et al., 2005). PFAS mineralization is evident when hydrofluoric acid (HF) is produced (Ross et al., 2018; Trautmann et al., 2015). Temperatures lower than 900˚C can cause undesired shorter-chain PFAS or volatile organic fluorine (VOF) by-products to form (Ross et al., 2018; Wang et al., 2015; Watanabe et al., 2016). Studies have demonstrated mixing of carbon particles into porous media can reach self-sustaining smouldering temperatures over 1000˚C (Baud et al., 2015; Martins et al., 2010). Therefore, smouldering can achieve the temperatures required for PFAS mineralization. Smouldering remediation has not been tested on PFAS-contaminated soils or GAC.

1.2. Research Objectives

The main objective of this research was to explore the ability for smouldering to remediate PFAS-contaminated soils and PFAS-impacted GAC. To achieve this, a series of laboratory scale experiments were first conducted, without PFAS, to learn the GAC concentrations needed to achieve smouldering temperatures required for PFAS mineralization. The main objective of this research was then completed by conducting a

serious of laboratory scale smouldering experiments with three types of PFAS-contaminated media, GAC, spiked soil, and field soil.

The sub-objective was to begin identification of emission products to complete a fluorine mass balance. To achieve this objective, a suite of analytical methods were used during smouldering to measure the fraction of PFAS completely mineralized and shorter-chain fluorine compounds that could be produced.

1.3. Thesis Outline

This thesis is written in an integrated article format in accordance with the guidelines and regulations stipulated by the Facility of Graduate Studies at the University of Western Ontario. Chapters included in this thesis are described below.

Chapter 2 is a review of the available literature pertaining to a background on PFAS, environmental contamination, and a review of the common remediation technologies for PFAS contamination. An introduction to smouldering remediation is also included, discussing the conditions typically required for successful remediation and smouldering characteristics.

Chapter 3 presents the results from laboratory experiments exploring the ability for smouldering remediation to successfully remove PFAS from contaminated soils and to destroy PFAS-contaminated GAC. This chapter is written in a manuscript format with the intention of submission to a peer reviewed journal.

Chapter 4 summarizes the research conducted, conclusions from this work, and the recommendations for continuing work.

Appendices provide additional information which is referenced throughout the thesis.

1.4. References

3M. (1999). The Science of organic fluorochemistry. AR226-0527.

Baud, G., Salvador, S., Debenest, G., & Thovert, J.-F. (2005). New Granular Model Medium To Investigate Smouldering Fronts Propagation – Experiments. *Energy & Fuels, 29*(10), 6780-6792. doi: 10.1021/acs.energyfuels.5b01325

Brusseau, M.L. (2018). Assessing the potential contributions of additional retention processes to PFAS retardation in the subsurface. *Science of the Total Environment, 613-614,* 176-185. doi: 10.1016/j.scitotenv.2017.09.065

Buck, R.C., Franklin, J., Berger, U., Conder, J.M., Cousins, I.T., de Voogt, P., Jensen, A.A., Kannan, K., Mabury, S.A., & van Leeuwen, S.P. (2011). Perfluoroalkyl and Polyfluoroalkyl Substances in the Environment: Terminology, Classification, and Origins. *Integrated Environmental Assessment and Management, 7*(4), 513-541. doi: 10.1002/ieam.258

Cousins, I.T., Vestergren, R., Wang, Z., Scheringer, M., & McLachlan, M.S. (2016). The precautionary principle and chemicals management: The example of perfluoroalkyl acids in groundwater. *Environment International, 94,* 331-340. doi: 10.1016/j.envint.2016.04.044

Crownover, E., Oberle, D., Kluger, M., & Heron, G. (2019). Perfluoroalkyl and polyfluoroalkyl substances thermal desorption evaluation. *Remediation, 29*(4), 77-81. doi: 10.1002/rem.21623

Dorrance, L.R., Kellogg, S., Love, A.H. (2017). What You Should Know About Per- and Polyfluoroalkyl Substances (PFAS) for Environmental Claims. *Environmental Claims Journal, 29*(4), 290-304. doi: 10.1080/10406026.2017.1377015

Espana V.A.A., Mallavarapu, M., & Naidu, R. (2015). Treatment technologies for aqueous perfluorooctanesulfonate (PFOS) and perfluorooctanoate (PFOA): A critical review with an emphasis on field testing. *Environmental Technology & Innovation,* 4, 168-181. doi: 10.1016/j.eti.2015.06.001

Gianfelice, G., Della Zassa, M., Biasin, A., & Canu B.P. (2019). Onset and propagation of smouldering in pine bark controlled by addition of inert solids. *Renewable Energy, 132,* 596-614. doi: 10.1016/j.renene.2018.08.028

Hale, S.E., Arp, H.P.H., Slinde, G.A., Wade, E.J., Bjørseth, Breedveld, G.D., Straith, B.F., Moe, K.G., Jartun, M., & Høisæter, Å. (2017). Sorbent amendment as a remediation strategy to reduce PFAS mobility and leaching in a contaminated sandy soil from a Norwegian firefighting training facility. *Chemosphere, 171,* 9-18. doi: 10.1016/j.chemosphere.2016.12.057

Hasan, T., Gerhard, J.I., Hadden, R., & Rein, G. (2015). Self-sustaining smouldering combustion of coal tar for the remediation of contaminated sand: Two-dimensional experiments and computation simulations. *Fuel, 150,* 288-297. doi: 10.1016/j.fuel.2015.02.014

Hu, X.C., Andrews, D.Q., Lindstrom, A.B., Bruton, T.A., Schaider, L.A., Grandjean, P., Lohmann, R., Carignan, C.C., Blum, A., Balan, S.A., Higgins, C.P., & Sunderland, E.M. (2016). Detection of Poly- and Perfluoroalkyl Substances (PFASs) in U.S. Drinking Water Linked to Industrial Sites, Military Fire Training Areas, and Wastewater Treatment Plants. *Environmental Science & Technology Letters, 3*(10), 344-350. doi: 10.1021/acs.estlett.6b00260

Kinsman, L., Torero, J.L., & Gerhard, J.I. (2017). Organic liquid mobility induced by smoldering remediation. *Journal of Hazardous Materials, 325,* 101-112. doi: 10.1016/j.jhazmat.2016.11.049

Kissa, E. (2001). *Fluorinated Surfactants and Repellants* (2nd ed.). New York, NY: Marcel Dekker, Inc.

Kucharzyk, K.H., Darlington, R., Benotti, M., Deeb, R., & Hawley, E. (2017). Novel treatment technologies for PFAS compounds: A critical review. *Journal of Environmental Management, 204,* 757-764. doi: 10.1016/j.jenvman.2017.08.016

Kuroda, K., Murakami, M., Oguma, K., Takada, H., & Takizawa, S. (2014). Investigating sources and pathways of perfluoroalkyl acid (PFAAs) in aquifers in Tokyo using multiple tracers. *Science of the Total Environment, 488-489,* 51-60. doi: 10.1016/j.scitotenv.2014.04.066

Martins, M.F., Salvador, S., Thovert, J.-F., & Debenest, G. (2010). Co-current combustion of oil shale – Part 2: Structure of the combustion front. *Fuel, 89*(1), 133-143. doi: 10.1016/j.fuel.2009.06.040

Ohlemiller, T.J. (1985). Modeling of smoldering combustion propagation. *Progress in Energy and Combustion Science, 11*(4), 277-310. doi: 10.1016/0360-1285(85)90004-8

Pabon, M., & Corpart J.M. (2002). Fluorinated surfactants: synthesis, properties, effluent treatment. *Journal of Fluorine Chemistry, 114*(2)*,* 149-156. doi: 10.1016/S0022-1139(02)00038-6

Paul, A.G., Jones, K.C., & Sweetman, A.J. (2009). A First Global Production, Emissions, And Environmental Inventory for Perfluorooctane Sulfonate. *Environmental Science & Technology, 43*(2), 386-392. doi: 10.1021/es802216n

Pironi, P., Switzer, C., Gerhard, J.I., Rein, G., & Torero, J.L. (2011). Self-Sustaining Smoldering Combustion for NAPL Remediation: Laboratory Evaluation of Process Sensitivity to Key Parameters. *Environmental Science & Technology, 45*(7), 2980-2986. doi: 10.1021/es102969z

Pironi, P., Switzer, C., Rein, G., Gerhard, J.I., Torero, J.L., & Fuentes, A. (2009). Small-Scale Forward Smouldering Experiments for Remediation of Coal Tar in Inert Media. *Proceedings of the Combustion Institute, 32*(2), 1957-1964. doi: 10.1016/j.proci.2008.06.184

Rayne, S., & Forest, K. (2009). Perfluoroalkyl sulfonic and carboxylic acids: A critical review of physiochemical properties, levels and patterns in waters and wastewaters, and treatment methods. *Journal of Environmental Science and Health Part A, 44*(12), 1145-1199. doi: 10.1080/10934520903139811

Ross, I., McDonough, J., Miles, J., Storch, P., Kochunarayanan, P.T., Kalve, E., Hurst, J., Dasgupta, S.S., & Burdick, J. (2018). A review of emerging technologies for remediation of PFASs. *Remediation Journal, 28*(2), 101-126. doi: 10.1002/rem.21553

Salman, M., Gerhard, J.I., Major, D.W., Pironi, P., & Hadden, R. (2015). Remediation of trichloroethylene-contaminated soils by star technology using vegetable oil

smoldering. *Journal of Hazardous Materials, 285,* 346-355. doi: 10.1016/j.jhazmat.2014.11.042

Schaider, L.A., Balan, S.A., Blum, A., Andrews, D.Q., Strynar, M.J., Dickinson, M.E., Lunderberg, D.M., Lang, J.R., & Peaslee, G.F. (2017). Fluorinated Compounds in U.S. Fast Food Packaging. *Environmental Science & Technology Letters, 4*(3), 105-111. doi: 10.1021/acs.estlett.6b00435

Switzer, C., Pironi, P., Gerhard, J.I., Rein, G., & Torero, J.L. (2009). Self-Sustaining Smoldering Combustion: A Novel Remediation Process for Non-Aqueous-Phase Liquids in Porous Media. *Environmental Science & Technology, 43,* 5871-5877. doi: 10.1021/es803483s

Trautmann, A.M., Schell, H., Schmidt, K.R., Mangold, K.M. & Tiehm, A. (2015). Electrochemical degradation of perfluoroalkyl and polyfluoroalkyl substances (PFASs) in groundwater. *Water Science & Technology, 71*(10), 1569-1575. doi: 10.2166/wst.2015.143

Trojanowicz, M., Bojanowska-Czajka, A., Bartosiewicz, I., & Kulisa, K. (2018). Advanced Oxidation/Reduction Processes treatment for aqueous perfluorooctanoate (PFOA) and perfluorooctanesulfonate (PFOS) – A review of recent advances. *Chemical Engineering Journal, 336,* 170-199. doi: 10.1016/j.cej.2017.10.153

Wang, F., Lu, X., Li, X., & Shih, K. (2015). Effectiveness and Mechanisms of Defluorination of Perfluorinated Alkyl Substances by Calcium Compounds during Waste Thermal Treatment. *Environmental Science & Technology, 45 (9),* 5672-5680. doi: 10.1021/es506234b

Watanabe, N., Takata, M., Takemine, S., & Yamamoto, K. (2016). Residual organic fluorinated compounds from thermal treatment of PFOA, PFHxA and PFOS adsorbed onto granular activated carbon (GAC). *Journal of Material Cycles and Waste Management, 18,* 625-630. doi: 10.1007/s10163-016-0532-x

Yamada, T., Taylor, P.H., Buck, R.C., Kaiser, M.A., Giraud, R.J. (2005). Thermal degradation of fluorotelomer treated articles and related materials. *Chemosphere, 61,* 974-984. doi: 10.1016/j.chemosphere.2005.03.025

Zanoni, M.A.B., Torero, J.L., & Gerhard, J.I. (2019). Delineating and explaining the limits of self-sustained smouldering combustion. *Combustion and Flame, 201,* 78-92. doi: 10.1016/j.combustflame.2018.12.00

Chapter 2

Literature Review

2.1. Introduction

Concerns of PFAS contamination have increased in recent years (Buck et al., 2011). Release of PFAS at AFFF sites and manufacturing facilities has caused widespread contamination of soil and water (Houtz et al., 2013; Hu et al., 2016). GAC is most commonly used to treat PFAS-contaminated water but this results in an additional waste stream being created (Dorrance et al., 2017). This means the spent GAC must either be destroyed or regenerated and both options are expensive (Carter & Farrell, 2010). Current remediation options for PFAS-contaminated soils are excavation and landfilling or incineration (Hale et al., 2017). Regulations are beginning to restrict landfilling, limiting it as an option for PFAS-contaminated soils (Ross et al., 2018). Emerging remediation options for PFAS-contaminated soil and water are expensive, cannot effectively treat a variety of PFAS, or have not been tested at a field scale (Ross et al., 2018; Vecitis et al., 2009). The growing concerns with health problems linked to PFAS and increasingly stringent regulations, require alternative remediation options to be developed**.**

Smouldering combustion is a proven remediation option for hazardous organic liquid wastes in inert porous media (Pironi et al., 2011; Switzer et al., 2009). After a short heating period, the injection of a forced air will initiate the smouldering reaction (Pironi et al., 2009). As the smouldering front propagates upward, it destroys the contaminant leaving clean sand (Switzer et al., 2009). While the contaminant is usually the fuel for this remediation technique, in situations where the contaminant concentration is too low to provide enough energy to smoulder or is too volatile, a surrogate fuel can be added to

promote smouldering combustion (Gianfelice et al., 2019; Salman et al., 2015). This chapter includes the relevant literature to provide background for supporting the possibility of smouldering combustion as a remediation option for treating PFAS-contaminated soil and PFAS-impacted GAC.

2.2. PFAS Contamination

2.2.1. PFAS Structure

Per- and polyfluoroalkyl substances (PFAS) are a group of synthetic compounds which are now classified as emerging contaminants (Kucharzyk et al., 2017; Xiao et al., 2015). Perfluorinated PFAS, or perfluoroalkyl acids (PFAA), contain chains of fully fluorinated moieties with an attached functional group (Kuroda et al., 2014; Pabon & Corpart, 2002). Two common subgroups of PFAA are perfluorinated carboxylic acids (PFCA) and perfluorinated sulfonic acids (PFSA) (Buck et al., 2011). PFAA compounds are further differentiated based on their carbon chain length; PFCA are considered long-chain when they contain seven or more carbon atoms and PFSA with six or more (Ross et al., 2018). For example, perfluorooctanoic acid (PFOA) and perfluorooctanesulfonic acid (PFOS) are both considered long-chain PFAA with an eight-carbon chain and have a carboxylic and sulfonic functional group, respectively. Table 2.1 includes examples of PFAS discussed in this research and their chemical structures. Polyfluorinated compounds can be significantly more complex than PFAA. They can have carbon with fluorine or hydrogen atoms, a wide range of functional groups, and a variety of heteroatoms (Ross et al., 2018). Polyfluorinated compounds are often referred to as PFAA precursors (Buck et al., 2011).

Table 2.1: Information for PFAS Compounds Discussed in this Research (PFAS Are Listed by Increasing Chain-Length in their Respective Categories)

PFAS Name	Acronym	Chemical Formula	Boiling Point (°C)[a]	Vapour Pressure (Pa)	Water Solubility (g/L)	Chemical Structure
Short Chain Fluorinated Compounds						
Trifluoracetic acid	TFA	CF_3COOH	72[b]	10700[b]	Micible with water[b]	
Perfluoropropanoic acid	PFPA	$F(CF_2)_2COOH$	96[c]	5333[c]	n/a[c]	
Perfluorinated Carboxylic Acids (PFCA)						
Perfluorobutanoic acid	PFBA	$F(CF_2)_3COOH$	121	1307	Micible with water	
Perfluoropentanoic acid	PFPeA	$F(CF_2)_4COOH$	124.4	1057	112.6	
Perfluorohexanoic acid	PFHxA	$F(CF_2)_5COOH$	143	457	21.7	
Perfluoroheptanoic acid	PFHpA	$F(CF_2)_6COOH$	175	158	4.2	
Perfluorooctanoic acid	PFOA	$F(CF_2)_7COOH$	188-192	4-1300	3.4-9.5	
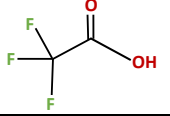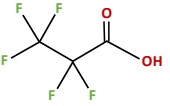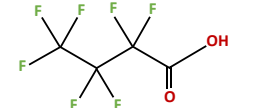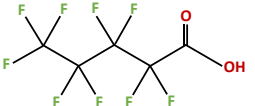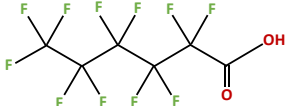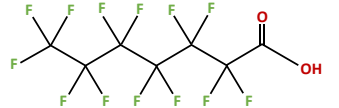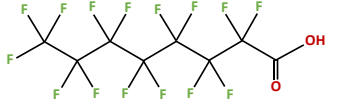
PFAS Name	Acronym	Chemical Formula	Boiling Point (°C)[a]	Vapour Pressure (Pa)	Water Solubility (g/L)	Chemical Structure
Perfluorinated Carboxylic Acids (PFCA)						
Perfluorononanoic acid	PFNA	$F(CF_2)_8COOH$	218	1.3	9.5	
Perfluorodecanoic acid	PFDA	$F(CF_2)_9COOH$	218	0.2	9.5	
Perfluoroundecanoic acid	PFUnA	$F(CF_2)_{10}COOH$	160-230	0.1	0.004	
Perfluorododecanoic acid	PFDoA	$F(CF_2)_{11}COOH$	245	0.01	0.0007	
Perfluorinated Sulfonic Acids (PFSA)						
Perfluorobutanesulfonic acid	PFBS	$F(CF_2)_4SO_3H$	211	631	51.4	
Perfluorohexanesulfonic acid	PFHxS	$F(CF_2)_6SO_3H$	238-239[d]	58.9	2.3	
Perfluorooctanesulfonic acid	PFOS	$F(CF_2)_8SO_3H$	258-260[e]	6.7	1.52-1.57	

[a]Unless otherwise noted, values were retrieved from SGS (2018).
[b](Fisher Scientific, 2014)
[c](ThermoFisher Scientific, 2018)
[d](Persistent Organic Pollutants Review Committee, 2018)
[e](EPA, 2017)

2.2.2. PFAS Properties

PFAS have interesting properties due to their chemical structure (Hale et al., 2017). The carbon-fluorine bond is one of the strongest bonds in nature, allowing PFAS compounds to be incredibly stable (Brusseau, 2018; Wei et al., 2017). These bonds make PFAS resistant to chemical, thermal, and biological degradation (3M Corporation, 1999; Buck et al., 2011; Pabon & Corpart, 2002). Additionally, the carbon-fluorine chain is both hydrophobic and oleophobic, while the functional group is hydrophilic and oleophilic (Figure 2.1 is an example of the components for PFOS) (Brusseau, 2018; Pabon & Corpart, 2002; Pan et al., 2009; Yeung et al., 2013). These characteristics allow PFAS to repel water and oil (Kissa, 2001; Lindstrom et al., 2011).

F- fluorine atom, O- oxygen atom, H- hydrogen atom, S- sulfur atom (within oxygen atoms) , C - carbon atoms (within fluorine atoms)

Note that on more complex compounds, the sulfur atom can act as a linkage connecting the hydrophobe to a different hydro (or oleo)phyl.
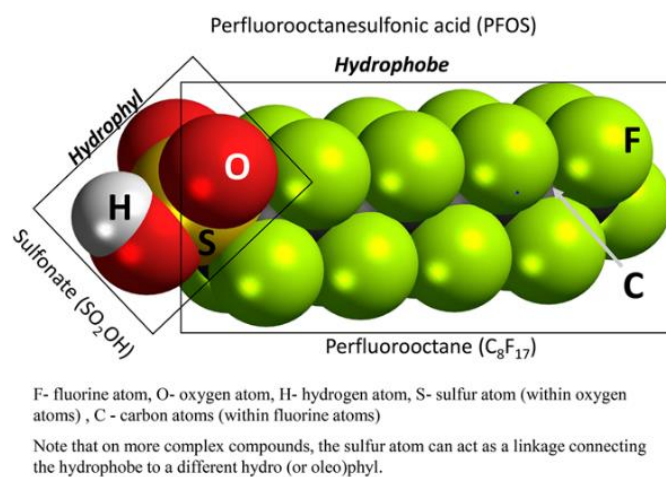
Figure 2.1: Chemical structure of PFOS (Hatton et al., 2018).

Studies have demonstrated PFAA are resistant to biodegradation and will accumulate in the environment (Buck et al., 2011; Espana et al., 2015; Pabon & Corpart, 2002). PFAA precursors, in certain aerobic or anaerobic environments, can degrade to PFAA (McGuire et al., 2014; Zhang et al., 2013). However, once degraded to PFAA these compounds experience no additional natural degradation due to their stability (Buck et al., 2011; Pabon & Corpart, 2002; Ross et al., 2018).

The adsorption behaviour of PFAS is influenced by both the chain-length and the functional group (Higgins & Luthy, 2006). For example, numerous studies have demonstrated the adsorption increased with increasing chain length, this is attributed to the hydrophobic properties of the C-F chain (Crownover et al., 2019; Ross et al., 2018). Higgins & Luthy (2006) discovered PFSA tend to have a higher adsorption to subsurface media than PFCA, showing the influence of the functional groups.

Research suggests PFAA solubilities increase as the chain-length decreases (Table 2.1) (Pancras et al., 2016; Ross et al., 2018). Their solubility is attributed to the hydrophilic functional group (Wei et al., 2017). PFAA precursors tend to have lower solubilities than PFAA, causing them to accumulate in the soils closer to the source zone (Hatton et al., 2018).

PFAS volatility also depends on the chain length and function groups (Table 2.1) (Crownover et al., 2019). PFAA are typically not volatile, however some polyfluorinated compounds will volatilize (Ross et al., 2018).

Recently, there has been a transition from the more common long-chain PFAS to alternatives due to the environmental and health concerns relating to long-chain PFAS. However, there is a lack of research and understanding of the replacement compounds. Some studies have shown that these replacements could have similar environmental persistence and be equally as hazardous as the compounds they are replacing (Gomis et al., 2015; Wang et al., 2015).

2.2.3. PFAS Uses

PFAS resistance to thermal degradation and being able to repel water and oil lead to their use in many manufacturing, industrial, and consumer applications. Examples of

consumer products containing PFAS include non-stick cookware, waterproof clothing, cosmetics, packaging, paper, and aqueous film forming foam (AFFF) (Giesy & Kannan, 2002; Paul et al., 2009; Prevedouros et al., 2006).

PFAS resistance to thermal degradation and surfactant properties made them ideal for AFFF (Rahman et al., 2014). AFFF has been used since the 1960s at military bases, firefighting training facilities, and airports (Moody & Field, 2000; Pabon & Corpart, 2002). AFFF containing PFAS was most frequently used on hydrocarbon fires (Pabon & Corpart, 2002). The hydrophobic properties provide stability in the foam solution and the oleophobic properties prevent mixing with hydrocarbons and instead allow the foam to supress the flames and prevent oxygen from reaching the fire (Chemguard, 2005). The PFAS compounds in AFFF are unique to the manufacturer and the production date (Dauchy et al., 2019).

Phase out of PFOS began in the early 2000s and production halted entirely in 2015 (ECCC, 2019). As a result, alternative PFAS compounds, such as shorter-chain PFAS and PFAA precursors, are being used for consumer products and AFFF (Birnbaum & Grandjean, 2015; Hatton et al., 2018).

2.2.4. Environmental Contamination & Health Concerns

PFAS contamination is most commonly caused from using AFFF, however manufacturing facilities, landfills, and wastewater treatment plants are also sources of contamination (Houtz et al., 2013; Hu et al., 2016; Schultz et al., 2004). Widespread use of AFFF has caused substantial contamination due to the lack of mitigating measures put into place when the AFFF was used, allowing it to seep into the subsurface (Milley et al., 2018). Release of PFAS into the environment has led to researchers finding PFAS in ground and

surface waters, sediments and soils, animals, plants, and biota worldwide (Boulanger et al., 2004; Codling et al., 2014; Inoue et al., 2004; Kannan et al., 2002). Contamination has caused fishing bans, closure of drinking water wells, and increasing concerns with health implications (Hatton et al., 2018). Groundwater concentrations at AFFF sites were reported to be greater than 2000 μg/L of PFOS and 300 μg/L PFOA (Cousins et al., 2016). Without intervention, the groundwater at these contaminated sites pose a risk to drinking water sources in the surrounding regions (Cousins et al., 2016). A study completed by Hu et al. (2016), tested public drinking water sources in U.S. and the drinking water supplied to approximately six million people exceeded the health advisory (0.07 μg/L for PFOS and PFOA combined).

PFAS concentrations and compounds vary greatly between contaminated sites. Table 2.2 includes a summary of PFAS concentrations found at numerous contaminated sites. When compared to normal background PFAS concentrations, it is evident that the contaminated sites have high and variable concentrations.

Health concerns from PFAS began in the early 2000s (Espana et al., 2015). Bioaccumulation of PFAS have increased health concerns in humans (Conder et al., 2008; Kuroda et al., 2014; Martin et al., 2004). During a U.S. national survey, PFOS and PFOA were found in 95% of the human blood serum samples analyzed with concentrations as high as 33 μg/L (U.S. Centers for Disease Control and Prevention, 2019). Krafft and Riess (2015) determined the longer chain PFSA and PFCA will bioaccumulate and biomagify more than their shorter chain counterparts and can lead to numerous health problems. Most health studies have focused on PFOS and PFOA (Melzer et al., 2010). Together, they are considered likely carcinogens and have been linked numerous health problems such as

lower immune system responses to vaccines, low birth weight, thyroid disease, and attention deficit/hyperactivity disorder in children (Barry et al., 2013; Fei et al., 2008; Grandjean et al., 2017; Hoffman et al., 2010; Melzer et al., 2010). Less information is available for health concerns of shorter chain PFAS or the precursor compounds (Birnbaum & Grandjean, 2015).

Table 2.2: PFAS Concentrations Measured at Contaminated Sites

Location	Sample Type	PFOS (µg/kg)	PFOA (µg/kg)	PFNA (µg/kg)	PFBS (µg/kg)	PFHxS (µg/kg)	PFHpA (µg/kg)	Reference
Contaminated Sites								
Firefighting training facility at airport (Norway)	Soil (depths 0-3.8 m)	6.4-2400	<2.8-67.3	<2.5 2.8-41.3	<2.4	<2.4 3.0-25.3	<1.8-34.4	Hale et al., 2017
Old fire station (Sweden)	Soil (0.5-1.0)	35.7-287	<0.3 – 1.2	n/a	n/a	1.6-6	n/a	Filipovic et al., 2015
	Soil Core (increments)	2.2-85.7	<0.12-1.37	n/a	n/a		n/a	
Main training facility	Soil (0.5-1.0)	2.12 – 379	<0.3-65.8	n/a	n/a	0.10-21.3	n/a	
	Soil Core (increments)	118-8520	5.89-287	n/a	n/a	n/a	n/a	
Intermediate Soil Depot	Soil (0.5-1.0)	<0.5 – 6.1	<0.1-0.49	n/a	n/a	<0.02-3.1	n/a	
Soil Depot	Soil (0.5-1.0)	<0.5-1.6	<0.1-0.16	n/a	n/a	<0.02-0.33	n/a	
Napalm-training ground	Soil Core (increments)	6.6-140	0.51-1.51	n/a	n/a	n/a	n/a	
Ellsworth Air Force Base (South Dakota, US)	Soil (0.6 m below surface)	11-20000 (median 2400)	BDL-5200	BDL-20	BDL-620	3-13000	BDL-320	Houtz et al., 2013
	Aquifer solids (5-6m below surface)	98-1000	11-130	BDL-2	2-88	40-870	3-31	
Ellsworth Air Force Base (South Dakota, US)	Soil samples	0.953-36000	B.D.L. - 11484	B.D.L. - 59.4	B.D.L. - 968	B.D.L. - 23875	B.D.L. - 323	McGuire et al., 2014
Multiple Norwegian airports	Soil	700-2900	<10-23	<10-10	<10	14-34	<10-15	Kupryianchyk et al., 2016
Firefighting training site (Stockholm Arlanda Airport, Sweden)	Soil samples (0.1-0.3 m below surface)	28	1.0	<0.33	0.34	3.4	0.99	Sorengard et al., 2019
Uncontaminated Sites								
America, China, Norway, Japan, Greece, Mexico (average)	Soil	0.47	0.124	n/a	n/a	n/a	n/a	Strynar et al., 2012
Multiple locations around Lake Ontario	Surface sediment	0.684-51.8	0.079-4.99	0.66 – 3.86	B.D.L.	B.D.L.- 0.549	B.D.L. – 0.516	Yeung et al., 2013
	Sediment core	0.591-30.1	0.057 – 3.75	0.041-2.96	B.D.L.	B.D.L. – 0.451	B.D.L.	

n/a: not analyzed

2.2.5. Characterization of PFAS-Contaminated Sites

Characterizing PFAS contaminated sites are challenging due to the various parameters that will influence the behaviour, such as transformation of PFAA precursors, the variability of the PFAS compounds present and their properties, presence of co-contaminants, and subsurface conditions (Dauchy et al., 2019; Guelfo & Higgins, 2013; Hale et al., 2017; Higgins & Luthy, 2006). Transformation of precursor compounds to PFAA impedes the ability to characterize PFAS-contaminated sites. Their slow transformation creates a long-term source of PFAS with varying solubilities and adsorption properties (Dauchy et al., 2019; Kuroda et al., 2014). Multiple field studies have attempted to identify PFAS at former AFFF sites (Backe et al., 2013; Dauchy et al., 2019; Houtz et al., 2013). The results found the PFAA precursors in the AFFF were mainly absent from the field samples tests, however, precursors not in the AFFF were found on site. This indicated the initial PFAA precursors had undergone transformation and the presence of these precursors shows the transformation process is very slow (Backe et al., 2013; Houtz et al., 2013).

The surfactant properties of longer-chain PFAS cause them to accumulate at air-water interfaces (Brusseau, 2018; Hatton et al., 2018). With some PFAS having a higher solubility, their presence at the site will cause long groundwater plumes to form (Ross et al., 2018). Dauchy et al. (2019), found no PFAA in the shallow subsurface suggesting these compounds are mobile in the subsurface and the lack of degradation allows PFAA to travel far distances with time. Even with clay layers present, PFAS were measured as far as 15m from the AFFF release (Dauchy et al., 2019).

Co-contaminants also need to be factored into site characterization as these have shown to impact the adsorption and solubility of PFAS; for example, when PFOS mixed with non-aqueous phase liquids (NAPLs) at an AFFF site, this caused the sorption of PFOS to increase (Guelfo & Higgins, 2013). The properties of the subsurface and groundwater will also influence the adsorption capacity of PFAS. Organic carbon tends have the largest impact on the adsorption of PFAS to the subsurface media, higher organic carbon in soil will increase the adsorption of PFAS (Aly et al., 2019; Higgins & Luthy, 2006). The presence of clay particles can alter the adsorption behaviour because clay is positively charged creating electrostatic interactions with the negatively charged PFAA (Hatton et al., 2018). pH and ionic strength of the groundwater will also change the adsorption of PFAS to the subsurface media (Aly et al., 2019; Barzen-Hanson et al., 2017). Figure 2.2 is a conceptual release of PFAS and the factors which influence its movement in the subsurface. Overall, studies have confirmed it is nearly impossible to generalize the expected PFAS compounds, their concentrations, or their behaviour in the subsurface (Dauchy et al., 2019; Guelfo & Higgins, 2013). The PFAS variability complicates remediation efforts as sites will need to be classified on an individual basis.
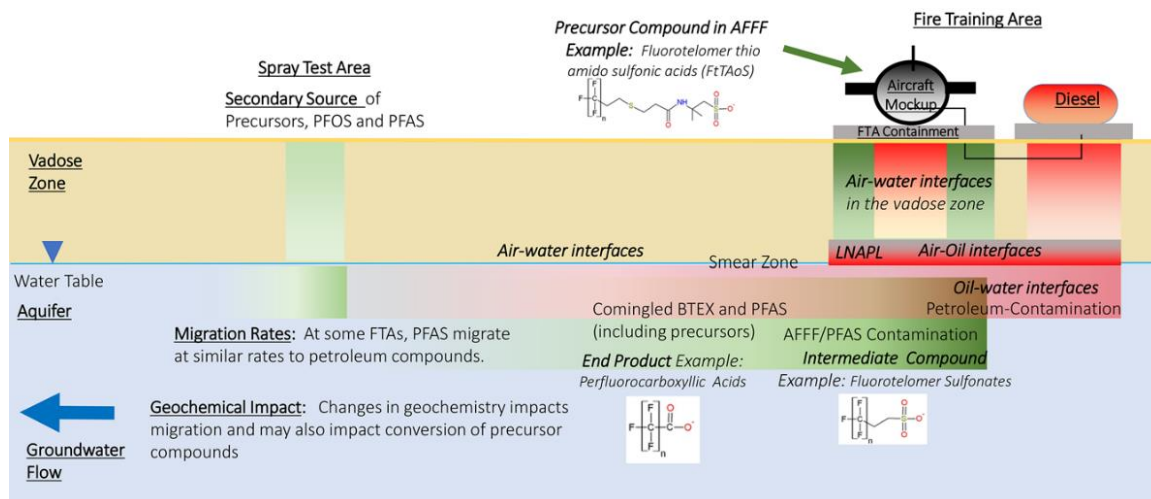
Figure 2.2: Conceptual release of PFAS and their movement in the subsurface (Hatton et al., 2018).

2.2.6. Regulations

With increasing concerns with PFOS and PFOA, due to their bioaccumulation and toxicity, governments have begun to set regulations for drinking water. In Canada, Health Canada (HC) has implemented maximum acceptable concentration (MAC) in drinking water of 0.2 µg/L and 0.6 µg/L for PFOA and PFOS, respectively (HC, 2016). There are nine additional PFAS, as of 2019, with a drinking water screening value ranging from 0.2 – 30 µg/L (HC, 2016). Screening values for the PFAS compounds were established using PFOS and PFOA as surrogates due to limited information being available for the toxicity of these PFAS (Government of Canada, 2019). In 2016, the U.S. EPA set a drinking water advisory of 0.07 µg/L for PFOS and PFOA combined (U.S. EPA, 2016). Numerous states have implemented their own, more stringent, regulations which unlike the advisories set by the EPA, are enforceable. For example, Michigan has proposed maximum contaminant levels (MCLs) of 8 ng/L for PFOA, and 16 ng/L for PFOS, as well as, MCLs for five other PFAS (Michigan Department of Environment, Great Lakes, and Energy, 2019).

Environment and Climate Change Canada (ECCC) has implemented federal environmental quality guidelines (FEQGs). FEQGs provide benchmarks for contaminants in the ambient environment. For surface water, ECCC has set a FEQG of 6.8 μg/L and 10 μg/kg for residential and agricultural soils for PFOS (ECCC, 2017). Screening levels set by the U.S. EPA for PFOS is 6000 ng/g and for PFOA is 16000 ng/g in 2009 (U.S. EPA, 2009). Exceeding the screening levels prompt additional site assessments. Screening levels are set to limit the adverse effect from direct exposure to the soil and do not consider the possible impact PFAS may have on groundwater (U.S. EPA, 2009). For this reason, there are concerns regarding PFAS-contaminated soils becoming a long-term problem for groundwater (Hatton et al., 2018). Increasingly stringent regulations have driven the need to determine remediation options for contaminated drinking water and soils (Trojanowicz et al., 2018).

2.2.7. Remediation Options

Remediation options for treating PFAS-contaminated drinking water and soils are limited (Hale et al., 2017). When selecting remediation technologies, it is vital to know which PFAS are present since many existing technologies tend to be ineffective for varying chain-lengths and functional groups (Brusseau, 2018; Ross et al., 2018; Schaefer et al., 2015). In many situations, multiple remediation technologies will be needed together to effectively remove PFAS from contaminated water and soils (Dorrance et al., 2017).

2.2.7.1. Remediation Options for PFAS-Contaminated Water

GAC is the most common method used to remove PFAS from contaminated water (Espana et al., 2015; Hale et al., 2017; Kucharzyk et al., 2017; Pabon & Corpart, 2002). The emerging remediation options for PFAS-contaminated water are limited because many

create an additional waste stream, cannot treat a wide range of PFAS, or are expensive (Dorrance et al., 2017; Ross et al., 2018).

There are some disadvantages of using GAC as a remediation option. GAC is not effective at removing all PFAS, large volumes are required, and an additional waste stream is produced (Milley et al., 2018). Studies have determined GAC is most effective for longer-chain PFAS and sulfonic functional group. Appleman et al. (2014) found GAC is better at removing PFAS with a sulfonic functional group than a carboxylic functional group with the same chain-length. GAC is most effective for PFAS like PFOA and PFOS and becomes gradually worse as the chain-length becomes shorter (Appleman et al., 2014; McCleaf et al., 2017). More frequent regeneration or replacement of the GAC is needed if high concentrations of shorter-chain PFAS are present (Espana et al., 2015). Therefore, if large amounts of water must be treated or shorter-chain PFAS are in high concentrations, significant amounts of GAC may be required (Appleman et al., 2014). Incineration or thermal regeneration are the most common methods for treating the spent GAC (Dorrance et al., 2017; Watanabe et al., 2016). Overall, disposal and regeneration of GAC can be challenging due to the costs associated with incineration, access to the licensed facilities, and harmful by-products that can be emitted (discussed in more detail in Section 2.2.8.) (Carter & Farrell, 2010; Watanabe et al., 2016).

2.2.7.2.   Remediation Options for PFAS-Contaminated Soils

Excavation and landfilling or incineration at off-site facilities are the most common remediation options for PFAS-contaminated soils (Dorrance et al., 2017; Hale et al., 2017). Complexity of field soils and the regulatory limits prevent many existing and emerging remediation technologies as viable options (Dorrance et al., 2017; Vecitis et al., 2009).

With increasing regulation and long-term liability, landfilling contaminated soils is becoming less appealing and more expensive (Ross et al., 2018). The problems discussed for incineration of GAC, in terms of costs, access, and emission concerns also apply to PFAS-contaminated soils (Crownover et al., 2019).

Thermal desorption of PFAS from contaminated soils has been explored as a possible remediation option. Crownover et al. (2019) found heating PFAS-contaminated soils at 350˚C for 10 days can achieve a 99.91% removal efficiency. During these experiments, PFSA remained on the soil longer than PFCA, suggesting the functional group influences the temperatures required for removal from soil (Crownover et al., 2019). Thermal desorption could possibly be achieved using rotary kilns because the operating temperatures are 500-600˚C. The effectiveness of rotary kilns to treat PFAS-contaminated soils has not been tested. The mobilization cost, energy requirements, and emissions treatment are also limiting factors for the feasibility of rotary kilns (Ross et al., 2018). Vapor energy generator (VEG) process is another thermal remediation option which injects steam at 1100˚C into contaminated soils ex situ (Ross et al., 2018). At this time, the bench-scale experiments have achieved a >99% removal of PFAS and full-scale experiments have not been completed (Endpoint, 2017). Overall, limited options are available to treat PFAS-contaminated soils. Of the options available, thermal remediation techniques appear to show great potential (Ross et al., 2018).

2.2.8. Thermal Destruction of PFAS

Numerous studies have been completed to better understand the capabilities of using thermal destruction to breakdown PFAS compounds. When PFOS was heated, in reagent form, to 600˚C or more it will begin to thermally breakdown but will produce

tetrafluoromethane (CF_4), hexafluoroethane (C_2F_6) and other volatile organofluoride compounds (Taylor & Yamada, 2003). Incomplete breakdown of PFAS compounds are problematic because many of these compounds are harmful greenhouse gases (Taylor & Yamada, 2003; Watanabe et al., 2016).

A series of studies were completed which explored thermally treatment PFAS-contaminated GAC in a nitrogen gas atmosphere using PFOS, PFOA and PFHxA (Wang et al., 2011; Wang et al., 2013; Watanabe et al., 2018). These studies provide a number of valuable insights on the outcomes of heating PFAS compounds: (i) complete removal of PFAS from the GAC can be achieved at temperatures greater than 700˚C, (ii) increased mineralization will occur when PFAS is adsorbed to GAC than in reagent form, (iii) release of shorter-chain PFAS and undesired volatile organic fluorine compounds are minimized when the emissions are kept at 1000˚C (Wang et al., 2011, 2013; Watanabe et al., 2018; Yamada et al., 2005). Greater mineralization was achieved when PFAS was adsorbed to GAC because the volatilization of the PFAS was prevented as temperatures increased beyond their boiling points (Table 2.1) (Watanabe et al., 2018). Between 700˚C and 900˚C shorter-chain PFAS, PFBA and PFPeA, were captured in the emissions, which were not originally on the GAC. The production of these shorter-chain PFAS suggests stepwise degradation may occur during thermal destruction (Watanabe et al., 2016). Thermal oxidation may also improve PFAS destruction, instead of using a nitrogen atmosphere, since incineration has been successfully shown to breakdown PFAS at 1000˚C (Vecitis et al., 2009; Watanabe et al., 2016; Yamada et al., 2005). Limited information is available regarding thermal degradation of PFAA precursors (Ross et al., 2018).

2.2.9. Breakdown Mechanisms

Limited literature is available which identifies the breakdown mechanisms that occur during thermal oxidation. However, Bentel et al. (2019) identified the breakdown mechanisms that occur when UV-generated hydrated electrons are used to degrade PFAS compounds. Results suggested chain length and functional group are important in determining the breakdown mechanisms that will occur (Bentel et al., 2019). H/F exchange, which is the replacement of a fluorine atom with a hydrogen atom, can occur without shortening the chain length of the PFAS. Once degradation begins and a hydrogen atom has replaced a fluorine atom, less energy is required for this to continue (Bentel et al., 2019). It is also possible for the functional group to break off from the carbon chain or spontaneous C-F bond cleavage to occur, shortening the chain length (Bentel et al., 2019). Su et al. (2019) also studied the breakdown mechanisms using UV-generated hydrated electrons. The results from this study also found chain-shortening and loss of functional group of PFOS will occur. Though these studies explored breakdown mechanisms using UV-generated hydrated electrons, it is expected that these results could provide insight on breakdown mechanisms that may occur during thermal oxidation.

2.3. Smouldering Combustion

2.3.1. Smouldering of Porous Solid Fuels

Smouldering combustion is slow-moving, low-temperature, and flameless (Rein, 2009). The focus of smouldering research has primarily been for use in enhanced oil recovery (Akkutlu & Yortsos, 2003; Greaves et al., 2000), understanding peat smouldering fires (Hadden et al., 2013; Rein, 2009), and porous solid fuels (e.g., polyurethane foam) for fire safety (Bar-Ilan et al., 2005; Dodd et al., 2012; Ohlemiller, 2002; Torero & Fernandez-Pello, 1995, 1996). During smouldering combustion, two main types of reactions occur: a pyrolysis and oxidation, which can be simplified into two equations (Rein, 2016; Torero & Fernandez-Pello, 1996):

$Pyrolysis$:

$$Fuel\,(solid) + Heat\ \rightarrow Pyrolyzate\,(gas) + Char\,(solid) + Ash\,(solid) \qquad 2.1$$
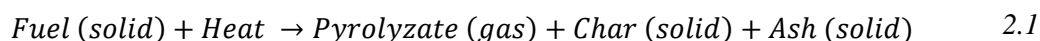
$Heterogeneous\ oxidation$:

$$Char\,(solid) +\ O_2(gas)\ \rightarrow Heat + CO_2 +\ H_2O + other\ gases + Ash\,(solid) \quad 2.2$$
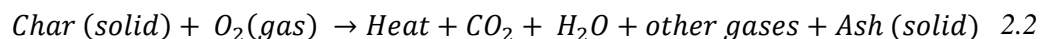
The endothermic, nonoxidative pyrolysis reaction begins when a fuel is heated to temperatures exceeding 200-250°C (Rein, 2009). In the pyrolysis region, the heat is absorbed by the fuel, decomposing it, releasing volatiles, water vapour, polyaromatic hydrocarbons, and low levels of CO and CO_2 (Rein, 2009). As the pyrolysis reaction passes, the decomposed fuel becomes mainly carbon-rich char and ash (Eqn 2.1) (Ohlemiller, 2002; Rein, 2009). The production of char during pyrolysis is important because the char releases more heat than the remaining fuel during the oxidation reaction (Rein, 2016).

As temperatures increase beyond 300˚C, the char and fuel remaining after pyrolysis is consumed during the oxidation reaction (Rein, 2009). The exothermic oxidation occurs on the surface of the condensed fuel, which ultimately can be either a solid or liquid, releasing heat, carbon dioxide (CO_2), water vapour, ash, and other gases (Eqn 2.2) (Ohlemiller, 2002; Rein, 2016; Bar-Ilan & Rein, 2004). When compounds containing largely carbon are smouldered, they will produce primarily CO_2 and water vapour (Ohlemiller, 2002). The highest temperatures and greatest mass loss occurs in the oxidation region because of the exothermic nature of the reaction and the destruction of the char and fuel (Rein, 2009). Heat released during the oxidation reaction will move to the unburned fuel promoting the continuation of the pyrolysis and oxidation reactions (Yermán et al., 2015).

Two factors which can limit the smouldering reaction are the supply of oxygen to the oxidation region and the heat losses to the surroundings (Rein, 2009). When sufficient heat is released during the oxidation reaction, to overcome the heat consumed during pyrolysis and heat losses to the environment, smouldering propagation will occur (Rein, 2009; Yermán et al., 2015). When sufficient heat is produced, the supply of oxygen is still vital for the smouldering reaction to continue (Rein, 2016). The rate of oxygen diffusion onto the surface the of the fuel during the oxidation reaction will control the overall rate of the reaction (Bar-Ilan & Rein, 2004; Ohlemiller, 2008; Rein, 2016; Switzer et al., 2009, 2011).

A porous matrix is essential for smouldering to propagate, as this will allow for sufficient oxygen to transport from the edge of the system to the smouldering zone through both convection and diffusion (Ohlemiller, 1985; Rein, 2009). Additionally, the porous matrix will increase the area per unit volume which in turn increases the oxidation reaction since it occurs on the surface of the material (Ohlemiller, 1985; Rein, 2009). Lastly, the

matrix acts as an insulator which prevents heat losses during smouldering, strengthening the reaction (Rein, 2009).

2.3.2. Smouldering Configurations

Smouldering combustion can occur in two configurations: forward and opposed (Figure 2.3) (Rein, 2009; Rein et al., 2007; Torero & Fernandez-Pello, 1996). Forward smouldering occurs when the reaction front and oxygen source move in the same direction (Yermán et al., 2015). In opposed smouldering, the reactions and supplied air are moving in opposite directions (Rein, 2009). The forward smouldering configuration allows smouldering to propagate more quickly; the heat and combustion gases released by the oxidation reaction transport forward through convection, pre-heating and drying the unburned fuel (Rein, 2016). If the same fuel and air supply were to be used in both configurations, forward smouldering would allow for a more complete combustion of the fuel (Ohlemiller & Lucca, 1983).
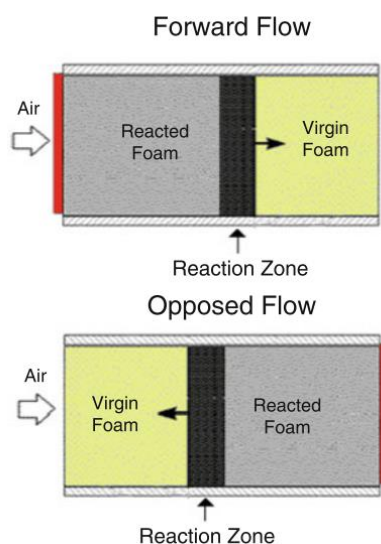
Figure 2.3: Reaction front and air supply configurations for forward and opposed smouldering (Rein, 2016).

In forward smouldering the pyrolysis and oxidation reactions form two separate fronts (Rein, 2009). The pyrolysis reaction is located at the side of the reaction zone by the

unburned fuel ahead of the oxidation reaction. When the air flow reaches the pyrolysis reaction after passing through the oxidation zone, it may have a low oxygen concentration, promoting the nonoxidative pyrolysis (Torero & Fernandez-Pello, 1996). The oxidation reaction occurs at the other end of the reaction where the oxygen concentrations are higher (Rein et al., 2007). For opposed smouldering, the pyrolysis and oxidation reactions occur together as one combined front (Bar-Ilan et al., 2004).

2.4. Smouldering as a Remediation Option

2.4.1. Laboratory Scale Columns

Smouldering is used as a commercial remediation technology called STAR (Self-Sustaining Treatment for Active Remediation). Studies have demonstrated that smouldering can successfully remediate soils contaminated with organic wastes at the laboratory and larger scales, both in situ and ex situ (Murray, 2019; Pironi et al., 2009; Scholes et al., 2015; Switzer et al., 2014). For laboratory experiments and ex situ remediation, forward smouldering in the upward direction was chosen because it takes advantage of the buoyancy effects and additional preheating (Switzer et al., 2009). This strengthens the smouldering reaction since the hot gasses released will help preheat the contaminated mixture (Ohlemiller, 1985).

Ignition protocol for the smouldering reaction at the laboratory scale, starts by introducing the heat source at the base; initiating the preheating phase (Pironi et al., 2009). During the preheating phase, the main heat transfer mechanisms are conduction and convection close to the heat source (Switzer et al., 2014). When the contaminant mixture above the heater reaches a predetermined temperature, forced air is added which initiates the smouldering reaction (Pironi et al., 2009; Torero & Fernandez-Pello, 1996). A

significant increase in the temperature above the heater indicates the smouldering reaction begins (Zone II in Figure 2.4) (Pironi et al., 2009). Rising CO_2 and CO concentrations are also an indication of a successful smouldering ignition (Pironi et al., 2009; Switzer et al., 2014). Other compounds released in emissions are unique to contaminant type and smouldering parameters (Switzer et al., 2009). Experiments using coal tar and crude oil released traces of naphthalene, toluene, and m-xylene (Switzer et al., 2009). The external energy source is removed shortly after the initiation of smouldering and the reaction will continue propagating upward (Pironi et al., 2009; Switzer et al., 2009). Maximum temperatures are typically between 500-700˚C and will last for several minutes, destroying the contaminant during that time (Switzer et al., 2009). As the smouldering front and gases move upward, the heat dries and preheats the contaminant mixture above the smouldering zone (Zone IV in Figure 2.4) (Ohlemiller, 1985). After the contaminant is destroyed, the temperatures will decrease, known as the cooling phase in the clean sand (Figure 2.4) (Switzer et al., 2014; Yermán et al., 2017). The continued airflow transfers the heat upward until the temperatures in the remediated soil returns to ambient temperature (Zone I in Figure 2.4) (Pironi et al., 2011).
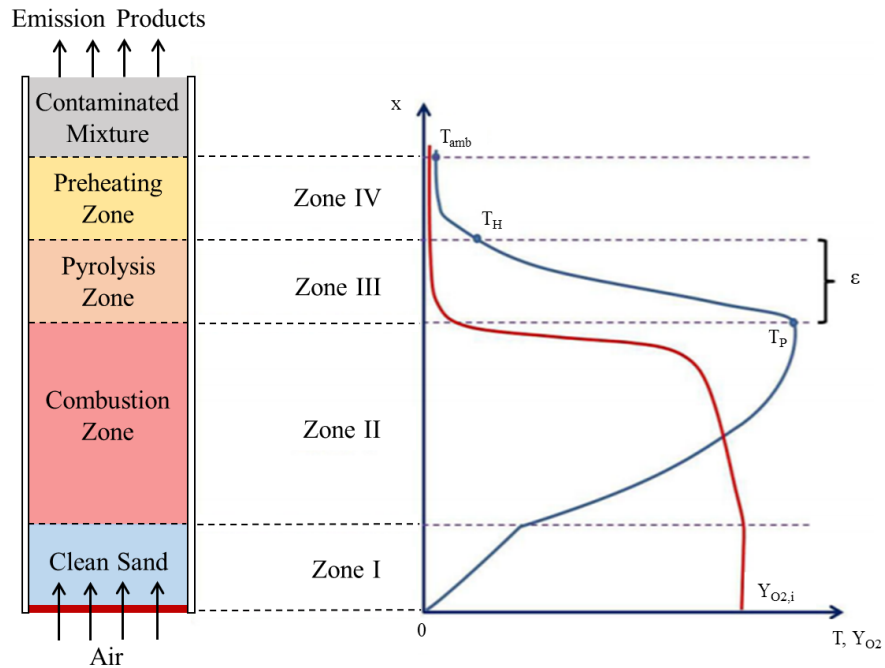
Figure 2.4: Zones in the smouldering reaction at the laboratory scale and their corresponding oxygen and temperatures profiles. $Y_{O2,I}$ is the oxygen concentrations at ambient air conditions, T_P is the temperature at the location between the smouldering front and pyrolysis zone, T_H is the temperature where pyrolysis reaction is no longer sustainable, and T_{amp} is the ambient temperature (adapted from Yermán et al., 2017).

2.4.2. Self-Sustaining Smouldering

Self-sustaining smouldering has been shown at the laboratory scale. A smouldering reaction is determined to be self-sustaining when the reaction continues throughout the contaminated mixture without additional energy being required (Pironi et al., 2009). During the experiment, self-sustaining smouldering is evident by the consistent peak temperatures exhibited by the thermocouples after the heater has been turned off (Pironi et al., 2011). Self-sustaining smouldering will continue until the fuel is completely consumed or the air supply is terminated (Pironi et al., 2011). When the thermocouples demonstrate decreasing temperatures, and therefore showing a weakening reaction, the reaction is considered non self-sustaining (Pironi et al., 2011). Non self-sustaining smouldering can

occur when the fuel does not create adequate heat to continue the reaction, the fuel concentration is too low, or there is insufficient airflow to the smouldering zone (Salman et al., 2015; Switzer et al., 2009).

2.4.3. Large Scale Experiments

Several studies have demonstrated successful remediation using STAR on large scales (Murray, 2019; Scholes et al., 2015; Solinger et al., 2020; Switzer et al., 2014). Increasing the smouldering scale can have several benefits including stronger smouldering reactions due to decreased heat losses to the environment, shorter preheating periods, and fewer ignitions required to treat large volumes of contaminated soil (Pironi et al., 2011). Experiments were conducted at a pilot field scale using coal tar and petrochemical NAPLs, achieving remediation of the contaminated soil (Switzer et al., 2014). Pilot field experiments achieve self-sustaining smouldering at lower contaminant concentrations than laboratory scale, due to less heat losses at increased scales (Switzer et al., 2009).

STAR has been successful as a commercial remediation technique for numerous sites contaminated with hydrocarbons. Scholes et al. (2015) remediated a coal-tar-contaminated site using STAR in situ. For the first time, it was shown that contaminated soils can be remediated below the water table using STAR (Scholes et al., 2015). The temperatures were less consistent due to variable subsurface conditions, such as changing moisture contents, ability for oxygen to reach the smouldering front, and properties of the subsurface material (Scholes et al., 2015). Ex situ remediation using STAR has also recently been proven successful for hydrocarbon sludge (Murray, 2019). The ex situ application of STAR allows sand or soil to be mixed with the contaminant, therefore creating a mixture with

adequate porosity to achieve self-sustaining smouldering. This concept could be extended to other contaminants which are unable to act as the fuel for the smouldering reaction.

Success of STAR at field scales, suggests there are benefits of using smouldering over incineration at the same scale. Smouldering is less energy demanding to incineration which requires a constant supply of energy to continue (Switzer et al., 2009). Success of STAR at field scales makes this remediation technique is an energy-efficient and low-cost option for contaminated soils (Hasan et al., 2015).

2.4.4. Smouldering Fuels

Smouldering remediation has proven to be effective for many liquid organic wastes, such as crude oil, coal tar, and mixed hydrocarbons (Pironi et al., 2009; Switzer et al., 2009). For these wastes, average peak temperatures of 550 – 1140˚C are possible depending on the fuel, fuel concentration, and air flux (Pironi et al., 2011, 2009; Switzer et al., 2009, 2014). Smouldering has also been shown to be an effective method for biosolids disposal (Rashwan et al., 2016; Yermán et al., 2015). However, with temperatures of approximately 390 – 660˚C, biosolid experiments were cooler than previously explored fuels (Rashwan et al., 2016; Yermán et al., 2015).

Various studies have explored the use of a surrogate fuel for smouldering remediation (Salman et al., 2015; Switzer et al., 2009). A surrogate fuel may be required when the contaminant cannot achieve self-sustaining smouldering (Salman et al., 2015). Salman et al. (2015) used vegetable oil to remediate trichloroethylene (TCE), which had exhibited non self-sustaining behaviour when smouldered alone. Temperatures during these experiments were approximately 540 – 635˚C (Salman et al., 2015). Results from these

experiments suggest an alternate surrogate fuel would be required to achieve the high temperatures needed for PFAS mineralization.

2.4.5. Smouldering Trends

Multiple smouldering studies, using a variety of fuels at the laboratory scale, have determined the smouldering velocity is linearly dependent on the supplied air flux (Pironi et al., 2011, 2009). Consistent behaviour occurred in pilot field experiments completed using coal tar and petrochemical NAPLs (Switzer et al., 2014). This relationship is attributed to higher air fluxes supplying the smouldering reaction with additional oxygen, increasing the reaction rate (Bar-Ilan et al., 2004; Rein, 2009). Therefore, the smouldering operator can control the destruction rate by adjusting the air flux during the reaction.

Greater concentrations of fuel in the smouldering mixture will increase the temperatures up to a certain threshold, which is dependent on the fuel (Pironi et al., 2011). For example, with coal tar temperatures plateaued with concentrations greater than 75 000 mg/kg (Pironi et al., 2011). Studies suggest there is fuel concentration threshold, once exceeded, will begin to decrease the smouldering velocity (Pironi et al., 2009). Below this limit, the smouldering velocity will increase, despite needing to destroy more fuel with higher fuel concentrations (Pironi et al., 2011). More fuel being available for the smouldering reaction, increases the heat released, decreasing the time require to pre-heat the contaminant mixture, and accelerating the reaction (Pironi et al., 2011). Surpassing this limit, hinders the reaction causing it to slow (Pironi et al., 2011, 2009). The dispersion of oxygen may be prevented with fuel concentrations begin to fill pore spaces and the excess heat released with higher fuel concentrations no longer exceeds the limitations of less oxygen (Pironi et al., 2011). Few solid contaminants have been studied to understand fuel

concentration and temperature relationships which are not influenced by the limited porosity experienced for liquid wastes at high concentrations.

2.5. Conclusions

PFAS contamination poses numerous remediation challenges due to their complex structures and the variety of compounds at contaminated sites. Disposal options for spent GAC using to remove PFAS from contaminated water can be expensive. There are a limited number of remediation technologies available to treatment PFAS-contaminated soils and with the increasingly restrictive regulations, there is an increasing need for alternatives options.

STAR is an effective remediation option for organic wastes, such as coal tar and crude oil. STAR shows potential for remediation option PFAS-contaminated soils and disposal option for PFAS-contaminated GAC. Temperatures greater than 1000°C can be reached during smouldering which should remove PFAS from soils and breakdown the PFAS. STAR has not been explored as a remediation option for PFAS-contaminated media.

This work includes a series of laboratory scale experiments which explore the potential STAR to remediate PFAS-contaminated soils and PFAS-contaminated GAC. To assess the success of STAR as a remediation technique, the soil must be tested following treatment and the emissions need to be monitored to ensure destruction of the PFAS. Results from these experiments may provide a fundamental understanding which can be built upon to improve STAR conditions and maximize the destruction of PFAS.

2.6. References

3M. (1999). The Science of organic fluorochemistry. AR226-0527.

Akkutlu, I. Y., & Yortsos, Y. C. (2003). The dynamics of in-situ combustion fronts in porous media. *Combustion and Flame, 134*(3), 229–247. doi: 10.1016/S0010-2180(03)00095-6

Aly, Y. H., McInnis, D. P., Lombardo, S. M., Arnold, W. A., Pennell, K. D., & Simcik, M. F. (2019). Enhanced adsorption of perfluoro alkyl substances for in situ remediation. *Environmental Science: Water Research & Technology, 5*, 1867–1875. doi: 10.1039/c9ew00426b

Appleman, T. D., Higgins, C. P., Quiñones, O., Vanderford, B. J., Kolstad, C., Zeigler-Holady, J. C., & Dickenson, E. R. V. (2014). Treatment of poly- and perfluoroalkyl substances in U.S. full-scale water treatment systems. *Water Research, 51*, 246–255. doi: 10.1016/j.watres.2013.10.067

Backe, W. J., Day, T. C., & Field, J. A. (2013). Zwitterionic, Cationic, and Anionic Fluorinated Chemicals in Aqueous Film Forming Foam Formulations and Groundwater from U.S. Military Bases by Nonaqueous Large-Volume Injection HPLC-MS/MS. *Environmental Science & Technology, 47*(10), 5226–5234. doi: 10.1021/es3034999

Bar-Ilan, A., Putzeys, O. M., Rein, G., Fernandez-Pello, A. C., & Urban, D.L. (2005). Transition from forward smoldering to flaming in small polyurethane foam samples. *Proceedings of the Combustion Institute, 30(*2), 2295–2302. doi: 10.1016/j.proci.2004.08.233

Bar-Ilan, A., Rein, G., Fernandez-Pello, A. C., Torero, J. L., & Urban, D.L. (2004). Forced forward smoldering experiments in microgravity. *Experimental Thermal and Fluid Science, 28*(7), 743–751. doi: 10.1016/j.expthermflusci.2003.12.012

Bar-Ilan, A., Rein, G., Walther, D. C., Fernandez-Pello, A. C., Torero, J. L., & Urban, D. L. (2004). The Effect of Buoyancy on Opposed Smoldering. *Combustion Science and Technology, 176*(12), 2027-2055. doi: 10.1080/00102200490514822

Barry, V., Winquist, A., & Steenland, K. (2013). Perfluorooctanoic Acid (PFOA) Exposures and Incident Cancers among Adults Living Near a Chemical Plant. *Environmental Health Perspectives, 121*(11-12), 1313–1318. doi: 10.1289/ehp.1306615

Barzen-Hanson, K. A., Roberts, S. C., Choyke, S., Oetjen, K., McAlees, A., Riddell, N., McCrindle, R., Ferguson, P.L., Higgins, C.P., Field, J. A. (2017). Discovery of 40 Classes of Per- and Polyfluoroalkyl Substances in Historical Aqueous Film-Forming Foams (AFFFs) and AFFF-Impacted Groundwater. *Environmental Science & Technology, 51*(4), 2047–2057. doi: 10.1021/acs.est.6b05843

Bentel, M.J., Yu, Y., Xu, L., Li, Z., Wong, B.M., Men, Y., & Liu, J. (2019). Defluorination of Per- and Polyfluoroalkyl Substances (PFASs) with Hydrated Electrons: Structural Dependence and Implications to PFAS Remediation and Management. *Environmental Science & Technology, 53*(7), 3718-3728. doi: 10.1021/acs.est.8b06648

Birnbaum, L. S., & Grandjean, P. (2015). Alternatives to PFASs: Perspectives on the Science. *Environmental Health Perspectives, 123*(5), 104–105. doi: 10.1289/ehp.1509944

Boulanger, B., Vargo, J., Schnoor, J. L., & Hornbuckle, K. C. (2004). Detection of Perfluorooctane Surfactants in Great Lakes Water. *Environmental Science & Technology, 38*(15), 4064–4070. doi: 10.1021/es0496975

Brusseau, M.L. (2018). Assessing the potential contributions of additional retention processes to PFAS retardation in the subsurface. *Science of the Total Environment, 613-614,* 176-185. doi: 10.1016/j.scitotenv.2017.09.065

Buck, R.C., Franklin, J., Berger, U., Conder, J.M., Cousins, I.T., de Voogt, P., Jensen, A.A., Kannan, K., Mabury, S.A., & van Leeuwen, S.P. (2011). Perfluoroalkyl and Polyfluoroalkyl Substances in the Environment: Terminology, Classification, and Origins. *Integrated Environmental Assessment and Management, 7*(4), 513-541. doi: 10.1002/ieam.258

Carter, K. E., & Farrell, J. (2010). Removal of Perfluorooctane and Perfluorobutane Sulfonate from Water via Carbon Adsorption and Ion Exchange Removal of Perfluorooctane and Perfluorobutane Sulfonate from Water via Carbon Adsorption and Ion Exchange. *Separation Science and Technology, 45*(6), 762–767. doi: 10.1080/01496391003608421

Chemguard (2005, September). General Foam Information (Data Sheet #D10D03010). Retrieved January 15, 2020, from https://www.chemguard.com/pdf/General-Foam-Information.pdf

Codling, G., Halsall, C., Ahrens, L., Del Vento, S., Wiberg, K., Bergknut, M., Laudon, H., Ebinghaus, R. (2014). The fate of per- and polyfluoroalkyl substances within a melting snowpack of a boreal forest. *Environmental Pollution, 191*, 190–198. doi: 10.1016/j.envpol.2014.04.032

Conder, J. M., Hoke, R. A., de Wolf, W., Russell, M. H., & Buck, R. C. (2008). Are PFCAs Bioaccumulative? A Critical Review and Comparison with Regulatory Criteria and Persistent Lipophilic Compounds. *Environmental Science & Technology, 42*(4), 995–1003. doi: 10.1021/es070895g

Cousins, I.T., Vestergren, R., Wang, Z., Scheringer, M., & McLachlan, M.S. (2016). The precautionary principle and chemicals management: The example of perfluoroalkyl acids in groundwater. *Environment International, 94*, 331-340. doi: 10.1016/j.envint.2016.04.044

Crownover, E., Oberle, D., Kluger, M., & Heron, G. (2019). Perfluoroalkyl and polyfluoroalkyl substances thermal desorption evaluation. *Remediation, 29*(4), 77-81. doi: 10.1002/rem.21623

Dauchy, X., Boiteux, V., Colin, A., Hémard, J., Bach, C., Rosin, C., & Munoz, J.-F. (2019). Deep seepage of per- and polyfluoroalkyl substances through the soil of a fire fighter training site and subsequent groundwater contamination. *Chemosphere, 214*, 729–737. doi: 10.1016/j.chemosphere.2018.10.003

Dodd, A. B., Lautenberger, C., & Fernandez-Pello, C. (2012). Computational modeling of smolder combustion and spontaneous transition to flaming. *Combustion and Flame, 159*(1), 448–461. doi: 10.1016/j.combustflame.2011.06.004

Dorrance, L.R., Kellogg, S., Love, A.H. (2017). What You Should Know About Per- and Polyfluoroalkyl Substances (PFAS) for Environmental Claims. *Environmental Claims Journal, 29*(4), 290-304. doi: 10.1080/10406026.2017.1377015

Environment and Climate Change Canada. (2019, September). Perfluorooctane sulfonate (PFOS), its salts and precursors - information sheet. Retrieved January 7, 2020,

from https://www.canada.ca/en/health-canada/services/chemical-substances/fact-sheets/chemicals-glance/perfluorooctane-sulfonate-public-summary.html

Environment and Climate Change Canada. (2017). *Federal Environmental Quality Guidelines: Perfluorooctane Sulfonate (PFOS).*

Endpoint. (2016, February). Bench-Scale VEG Research & Development Study: Implementation Memorandum for Ex-Situ Thermal Desorption of Perfluoroalkyl Compounds (PFCs) in Soils. Retrieved January 10, 2020, from https://www.endpoint-inc.com/wp-content/uploads/2016/05/VEG-Bench-Scale-PFCs-Soil.pdf

EPA. (2017, November). *Technical Fact Sheet – Perflurooctane Sulfonate (PFOS) and Perfluorooctanoic Acid (PFOA).* Retrieved April 5, 2020, from https://www.epa.gov/sites/production/files/2017-12/documents/ffrrofactsheet_contaminants_pfos_pfoa_11-20-17_508_0.pdf

Espana V.A.A., Mallavarapu, M., & Naidu, R. (2015). Treatment technologies for aqueous perfluorooctanesulfonate (PFOS) and perfluorooctanoate (PFOA): A critical review with an emphasis on field testing. *Environmental Technology & Innovation, 4*, 168-181. doi: 10.1016/j.eti.2015.06.001

Fabris, I., Cormier, D., Gerhard, J. I., Bartczak, T., Kortschot, M., Torero, J. L., & Cheng, Y.-L. (2017). Continuous, self-sustaining smouldering destruction of simulated faeces. *Fuel, 190*, 58–66. doi: 10.1016/j.fuel.2016.11.014

Fei, C., McLaughlin, J. K., Tarone, R. E., & Olsen, J. (2008). Fetal Growth Indicators and Perfluorinated Chemicals: A Study in the Danish National Birth Cohort. *American Journal of Epidemiology, 168*(1), 66–72. doi: 10.1093/aje/kwn095

Filipovic, M., Woldegiorgis, A., Norström, K., Bibi, M., Lindberg, M., & Österås, A.-H. (2015). Historical usage of aqueous film forming foam: A case study of the widespread distribution of perfluoroalkyl acids from a military airport to groundwater, lakes, soils, and fish. *Chemosphere, 129,* 39-45. Doi: 10.1016/j.chemosphere.2014.09.005

Fisher Scientific. (2014, October). *Safety Data Sheet (Trifluoroacetic acid).* Retrieved April 5, 2020, from https://www.criver.com/sites/default/files/resources/TrifluoroaceticAcidMaterialSafetyDataSheetMSDS.pdf

Gianfelice, G., Della Zassa, M., Biasin, A., & Canu B.P. (2019). Onset and propagation of smouldering in pine bark controlled by addition of inert solids. *Renewable Energy, 132*, 596-614. doi: 10.1016/j.renene.2018.08.028

Giesy, J. P., & Kannan, K. (2002). Perfluorochemical Surfactants in the Environment. *Environmental Science & Technology, 36*(7), 146A–152A. doi: 10.1021/es022253t

Gomis, M. I., Wang, Z., Scheringer, M., & Cousins, I. T. (2015). A modeling assessment of the physicochemical properties and environmental fate of emerging and novel per- and polyfluoroalkyl substances. *Science of the Total Environment, 505*, 981–991. doi: 10.1016/j.scitotenv.2014.10.062

Government of Canada. (2019, April). Water Talk – Perfluoroalkylated substances in drinking water. Retrieved January 7, 2020, from https://www.canada.ca/en/services/health/publications/healthy-living/water-talk-drinking-water-screening-values-perfluoroalkylated-substances.html

Grandjean, P., Heilmann, C., Weihe, P., Nielsen, F., Mogensen, U. B., & Budtz-Jørgensen, E.   (2017). Serum Vaccine Antibody Concentrations in Adolescents Exposed to Perfluorinated Compounds. *Environmental Health Perspectives, 125*(7), 1–7. doi: 10.1289/EHP275

Greaves, M., Young, T. J., El-Usta, S., Rathbone, R. R., Ren, S. R., & Xia, T. X. (2000). Air Injection into Light and Medium Heavy Oil Reservoirs: Combustion Tube Studies on West of Shetlands Clair Oil and Light Australian Oil. *Chemical Engineering Research and Design, 78*(5), 721-730. doi: 10.1205/026387600527905

Guelfo, J. L., & Higgins, C. P. (2013). Subsurface Transport Potential of Perfluoroalkyl Acids at Aqueous Film-Forming Foam (AFFF)-Impacted Sites. *Environmental Science & Technology, 47*(9), 4164–4171. doi: 10.1021/es3048043

Hale, S.E., Arp, H.P.H., Slinde, G.A., Wade, E.J., Bjørseth, Breedveld, G.D., Straith, B.F., Moe, K.G., Jartun, M., & Høisæter, Å. (2017). Sorbent amendment as a remediation strategy to reduce PFAS mobility and leaching in a contaminated sandy soil from a Norwegian firefighting training facility. *Chemosphere, 171*, 9-18. doi: 10.1016/j.chemosphere.2016.12.057

Hadden, R. M., Rein, G., & Belcher, C. M. (2013). Study of the competing chemical reactions in the initiation and spread of smouldering combustion in peat. *Proceedings of the Combustion Institute, 34*(2), 2547–2553. doi: 10.1016/j.proci.2012.05.060

Hasan, T., Gerhard, J.I., Hadden, R., & Rein, G. (2015). Self-sustaining smouldering combustion of coal tar for the remediation of contaminated sand: Two-dimensional experiments and computation simulations. *Fuel, 150*, 288-297. doi: 10.1016/j.fuel.2015.02.014

Hatton, J., Holton, C., & DiGuiseppi, B. (2018). Occurrence and behavior of per- and polyfluoroalkyl substances from aqueous film-forming foam in groundwater systems. *Remediation, 28,* 89–99. doi: 10.1002/rem.21552

Health Canada. (2016). Health Canada's Drinking Water Screening Values for Perfluoroalkylated Substances (PFAS).

Higgins, C. P., & Luthy, R. G. (2006). Sorption of Perfluorinated Surfactants on Sediments. *Environmental Science & Technology, 40*(23), 7251–7256. doi: 10.1021/es061000n

Hoffman, K., Webster, T. F., Weisskopf, M. G., Weinberg, J., & Vieria, V. M. (2010). Exposure to Polyfluoroalkyl Chemicals and Attention Deficit/Hyperactivity Disorder in U.S. Children 12-15 Years of Age. *Environmental Health Perspectives, 118*(12), 1762–1767. doi: 10.1289/ehp.1001898

Houtz, E.F., Higgins, C.P., Field, J.A., & Sedlak, D.L. (2013). Persistence of Perfluoroalkyl Acid Precursors in AFFF-Impacted Groundwater and Soil.

Environmental Science & Technology, 47(15), 8187-8195. doi: 10.1021/es4018877

Howell, J. R., Hall, M. J., & Ellzey, J. L. (1996). Combustion of Hydrocarbon Fuels within Porous Inert Media. *Progress in Energy and Combustion Science, 22*(2), 121–145. doi: 10.1016/0360-1285(96)00001-9

Hu, X.C., Andrews, D.Q., Lindstrom, A.B., Bruton, T.A., Schaider, L.A., Grandjean, P., Lohmann, R., Carignan, C.C., Blum, A., Balan, S.A., Higgins, C.P., & Sunderland, E.M. (2016). Detection of Poly- and Perfluoroalkyl Substances (PFASs) in U.S. Drinking Water Linked to Industrial Sites, Military Fire Training Areas, and Wastewater Treatment Plants. *Environmental Science & Technology Letters, 3*(10), 344-350. doi: 10.1021/acs.estlett.6b00260

Inoue, K., Okada, F., Ito, R., Kato, S., Sasaki, S., Nakajima, S., Uno, A., Saijo, Y., Sata, F., Yoshimura, Y., Kishi, R., & Nakazawa, N. (2004). Perfluorooctane Sulfonate (PFOS) and Related Perfluorinated Compounds in Human Maternal and Cord Blood Samples: Assessment of PFOS Exposure in Susceptible Population during Pregnancy. *Environmental Health Perspectives, 112*(11), 1204-1207. doi: 10.1289/ehp.6864

Kannan, K., Newsted, J., Halbrook, R. S., & Giesy, J. P. (2002). Perfluorooctanesulfonate and Related Fluorinated Hydrocarbons in Mink and River Otters from the United States. *Environmental Science & Technology, 36*(12), 2566–2571. doi: 10.1021/es0205028

Kissa, E. (2001). *Fluorinated Surfactants and Repellants* (2nd ed.). New York, NY: Marcel Dekker, Inc.

Kosswig, K. (2000). *Sulfonic Acids, Aliphatic. Ullman's Encyclopedia of Industrial Chemistry* (7th ed.). New York, NY: John Wiley & Sons.

Krafft, M.P., & Riess, J.G. (2015) Selected physicochemical aspects of poly- and perfluoroalklated substances relevant to performance, environment and sustainability – Part one. *Chemosphere, 129,* 4-19. doi: 10.1016/j.chemosphere.2014.08.039

Kucharzyk, K.H., Darlington, R., Benotti, M., Deeb, R., & Hawley, E. (2017). Novel treatment technologies for PFAS compounds: A critical review. *Journal of Environmental Management, 204*, 757-764. doi: 10.1016/j.jenvman.2017.08.016

Kuprianchyk, D., Hale, S.E., Breedveld, G.D., & Cornelissen, G. (2016). Treatment of sites contaminated with perfluorinated compounds using biochar amendment. *Chemosphere, 142,* 35-40. doi: 10.1016/j.chemosphere.2015.04.085

Kuroda, K., Murakami, M., Oguma, K., Takada, H., & Takizawa, S. (2014). Investigating sources and pathways of perfluoroalkyl acid (PFAAs) in aquifers in Tokyo using multiple tracers. *Science of the Total Environment, 488-489*, 51-60. doi: 10.1016/j.scitotenv.2014.04.066

Lindstrom, A. B., Strynar, M. J., & Libelo, E. L. (2011). Polyfluorinated Compounds: Past, Present, and Future. *Environmental Science & Technology, 45*(19), 7954–7961. doi: 10.1021/es2011622

Martin, J. W., Smithwick, M. M., Braune, B. M., Hoekstra, P. F., Muir, D. C. G., & Mabury, S. A. (2004). Identification of Long-Chain Perfluorinated Acids in Biota from the Canadian Arctic. *Environmental Science & Technology, 38*(2), 373–380. doi: 10.1021/es034727+

McCleaf, P., Englund, S., Östlund, A., Lindegren, K., Wiberg, K., & Ahrens, L. (2017). Removal efficiency of multiple poly- and perfluoroalkyl substances (PFASs) in drinking water using granular activated carbon (GAC) and anion exchange (AE) column tests. *Water Research, 120*, 77–87. doi: 10.1016/j.watres.2017.04.057

McGuire, M. E., Schaefer, C., Richards, T., Backe, W. J., Field, J. A., Houtz, E., Sedlak, D.L., Guelfo, J.L., Wunsch, A., & Higgins, C. P. (2014). Evidence of Remediation-Induced Alteration of Subsurface Poly- and Perfluoroalkyl Substance Distribution at a Former Firefighter Training Area. *Environmental Science & Technology, 48*(12), 6644–6652. doi: 10.1021/es5006187

Melzer, D., Rise, N., Depledge, M. H., Henley, W. E., & Galloway, T. S. (2010). Disease in the U.S. National Health and Nutrition Examination Survey. *Environmental Health Perspectives, 118*(5), 686–692. doi:/10.1289/ehp.0901584

Michigan Department of Environment, Great Lakes, and Energy. (2019, October). Michigan moves forward on drinking water standards for PFAS. Retrieved January 7, 2020, from https://www.michigan.gov/egle/0,9429,7-135--509830--,00.html

Milley, S.A., Koch, I., Fortin, P., Archer, J., Reynolds, D., Weber, K.P. (2018). Estimating the number of airports potentially contaminated with perfluoroalkyl and polyfluoroalkyl substances from aqueous film forming foam: A Canadian example. *Journal of Environmental Management, 222*, 122-131. doi: 10.1016/j.jenvman.2018.05.028

Moody, C. A., & Field, J. A. (2000). Perfluorinated Surfactants and the Environmental Implications of Their Use in Fire-Fighting Foams. *Environmental Science & Technology, 34*(18), 3864–3870. doi: 10.1021/es991359u

Murray, C. (2019). Field Trials of Ex Situ Smouldering Treatment (STARx) of Oil Sludge (Master's thesis). Retrieved from Western Electronic Thesis and Dissertation Repository.

Ohlemiller, T.J. (1985). Modeling of smoldering combustion propagation. *Progress in Energy and Combustion Science, 11*(4), 277-310. doi: 10.1016/0360-1285(85)90004-8

Ohlemiller, T.J. (2002). Smoldering Combustion. In P.J. DiNenno, D. Drysdale, W.D. Walton, R.L.P. Custer, J.R. Hall Jr., & J.M. Watts Jr. (Eds.), *SFPE Handbook of Fire Protection Engineering (3rd ed.)* (pp. 200-210). Quincy, Massachusetts: National Fire Protection Association

Ohlemiller, T.J. (2008) Smouldering combustion. In: DiNenno PJ, Drysdale D, Beyler CL, Walton WD, (Eds.), *SFPE handbook of fire protection engineering*. National Fire Protection Association (pp. 2-200–202-210).

Ohlemiller, T.J., & Luca, D.A. (1983). An experimental comparison of forward and reverse smolder propagation in permeable fuel beds. *Combustion and Flame, 54*(1-3)*,* 131-147. doi: 10.1016/0010-2180(83)90027-5

Pabon, M., & Corpart J.M. (2002). Fluorinated surfactants: synthesis, properties, effluent treatment. *Journal of Fluorine Chemistry, 114*(2), 149-156. doi: 10.1016/S0022-1139(02)00038-6

Pan, G., Jia, C., Zhao, D., You, C., Chen, H., & Jiang, G. (2009). Effect of cationic and anionic surfactants on the sorption and desorption of perfluorooctane sulfonate (PFOS) on natural sediments. *Environmental Pollution, 157*(1), 325–330. doi: 10.1016/j.envpol.2008.06.035

Pancras, T., Schrauwen, G., Held, T., Baker, K., Ross, I., & Slenders, H. (2016). Environmental fate and effects of poly- and perfluoroalkyl substances (PFAS).

Paul, A.G., Jones, K.C., & Sweetman, A.J. (2009). A First Global Production, Emissions, And Environmental Inventory for Perfluorooctane Sulfonate. *Environmental Science & Technology, 43*(2), 386-392. doi: 10.1021/es802216n

Pironi, P., Switzer, C., Gerhard, J.I., Rein, G., & Torero, J.L. (2011). Self-Sustaining Smoldering Combustion for NAPL Remediation: Laboratory Evaluation of Process Sensitivity to Key Parameters. *Environmental Science & Technology, 45*(7), 2980-2986. doi: 10.1021/es102969z

Pironi, P., Switzer, C., Rein, G., Gerhard, J. I., & Torero, J. L. (2009). Small-Scale Forward Smouldering Experiments for Remediation of Coal Tar in Inert Media. *Proceedings of the Combustion Institute, 32*(2), 1957–1964. doi: 10.1016/j.proci.2008.06.184

Prevedouros, K., Cousins, I. T., Buck, R. C., & Korzeniowski, S. H. (2006). Sources, Fate and Transport of Perfluorocarboxylates. *Environmental Science & Technology, 40*(1), 32–44. doi:10.1021/es0512475

Rahman, M. F., Peldszus, S., & Anderson, W. B. (2014). Behaviour and fate of perfluoroalkyl and polyfluoroalkyl substances (PFASs) in drinking water treatment: A review. *Water Research, 50*, 318–340. doi: 10.1016/j.watres.2013.10.045

Rashwan, T. L., Gerhard, J. I., & Grant, G. P. (2016). Application of self-sustaining smouldering combustion for the destruction of wastewater biosolids. *Waste Management, 50*, 201–212. doi: 10.1016/j.wasman.2016.01.037

Rein, G. (2009). Smouldering Combustion Phenomena in Science and Technology. *International Review of Chemical Engineering*, 1, 3–18.

Ohlemiller, T.J. (2002). Smoldering Combustion. In P.J. DiNenno, D. Drysdale, W.D. Walton, R.L.P. Custer, J.R. Hall Jr., & J.M. Watts Jr. (Eds.), *SFPE Handbook of Fire Protection Engineering (3rd ed.)* (pp. 200-210). Quincy, Massachusetts: National Fire Protection Association

Rein, G. (2016). Smoldering Combustion. In M.J. Hurley, D. Gottuk, J.R. Hall Jr., K. Harada, E. Kuligowski, M. Puchovsky, J. Torero, J.M. Watts Jr., C. Wieczorek (Eds.), *SFPE Handbook of Fire Protection Engineering* (pp. 581–603). New York, New York: Springer

Rein, G., Cohen, S., & Simeoni, A. (2009). Carbon emissions from smouldering peat in shallow and strong fronts. *Proceedings of the Combustion Institute, 32*(2), 2489–2496. doi: 10.1016/j.proci.2008.07.008

Rein, G., Fernandez-Pello, A. C., & Urban, D. L. (2007). Computational model of forward and opposed smoldering combustion in microgravity. *Proceedings of the Combustion Institute, 31*(2), 2677–2684. doi: 10.1016/j.proci.2006.08.047

Ross, I., McDonough, J., Miles, J., Storch, P., Kochunarayanan, P.T., Kalve, E., Hurst, J., Dasgupta, S.S., & Burdick, J. (2018). A review of emerging technologies for remediation of PFASs. *Remediation Journal, 28*(2), 101-126. doi: 10.1002/rem.21553

Salman, M., Gerhard, J.I., Major, D.W., Pironi, P., & Hadden, R. (2015). Remediation of trichloroethylene-contaminated soils by star technology using vegetable oil smoldering. *Journal of Hazardous Materials, 285*, 346-355. doi: 10.1016/j.jhazmat.2014.11.042

Schaefer, C.E., Andaya, C., Urtiaga, A., McKenzie, E.R., & Higgins, C.P. (2015). Electrochemical treatment of perfluorooctanoic acid (PFOA) and perfluorooctane sulfonic acid (PFOS) in groundwater impacted by aqueous film forming foams (AFFFs). *Journal of Hazardous Materials, 295*, 170-175. doi: 10.1016/j.jhazmat.2015.04.024

Scholes, G.C., Gerhard, J.I., Grant, G.P., Major, D.W., Vidumsky, J.E., Switzer, C., & Torero, J.L. (2015). Smoldering Remediation of Coal-Tar-Contaminated Soil: Pilot Field Tests of STAR. *Environmental Science & Technology, 49*(24), 14334-14342. doi: 10.1021/acs.est.5b03177

Schultz, M. M., Barofsky, D. F., & Field, J. A. (2004). Quantitative Determination of Fluorotelomer Sulfonates in Groundwater by LC MS/MS. *Environmental Science & Technology, 38*(6), 1828–1835. doi:10.1021/es035031j

SGS. (2018, September). *Physical and Chemical Properties of PFAS Compounds.* Retrieved May 31, 2019, from https://www.sgs-ehsusa.com/wp-content/uploads/2018/09/Physical-and-Chemical-Properties-of-PFAS-compounds_vKFMH.pdf

Solinger, R., Grant, G.P., Scholes, G.C., Murray, C., & Gerhard, J.I. (2020). STARx Hottpad for smoldering treatment of waste oil sludge: Proof of concept and sensitivity to key design parameters. *Journal of Waste Management & Research.* doi: 10.1177/0734242X20904430

Sorengard, M., Kleja, D.B., Ahrens, L. (2019). Stabilization of per- and polyfluoroalkyl substances (PFASs) with colloidal activated carbon (PlumeStop®) as a function of soil clay and organic matter content. *Journal of Environmental Management, 249,* 109345. doi: 10.1016/j.jenvman.2019.109345

Stynar, M.J., Lindstrom, A.B., Nakayama, S.F., Egeghy, P.P., & Helfant, L.J. (2012). Pilot scale application of a method for the analysis of Perfluorinated compounds in surface soils. *Chemosphere, 86*(3)*,* 252-257. doi: 10.1016/j.chemosphere.2011.09.036

Switzer, C., Pironi, P., Gerhard, J.I., Rein, G., & Torero, J.L. (2009). Self-Sustaining Smoldering Combustion: A Novel Remediation Process for Non-Aqueous-Phase Liquids in Porous Media. *Environmental Science & Technology, 43*, 5871-5877. doi: 10.1021/es803483s

Switzer, C., Pironi, P., Gerhard, J.I., Rein, G., & Torero, J.L. (2014). Volumetric scale-up of smouldering remediation of contaminated materials. *Journal of Hazardous Materials, 268*, 51-60. doi: 10.1016/j.jhazmat.2013.11.053

Su, Y., Rao, U., Khor, C.M., Jensen, M.G., Teesch, L.M., Wong, B.M., Cwiertny, D.M., & Jassby, D. (2019). Potential-Driven Electron Transfer Lowers the Dissociation Energy of the C-F Bond and Facilitates Reductive Defluorination of Perfluorooctane Sulfonate (PFOS). *Applied Materials & Interfaces, 11,* 33913-33922. doi: 10.1021/acsami.9b10449

Taylor, P., & Yamada, T. (2003). Laboratory Scale Thermal Degradation of Perfluoro-Octanyl Sulfonate and Related Precursors.

ThermoFisher Scientific. (2018, January). *Safety Data Sheet (Pentafluoropropionic acid).* Retrieved April 5, 2020, from https://www.fishersci.com/store/msds?partNumber=AC416920500&productDescription=PENTAFLUOROPROPIONIC+ACI+50GR&vendorId=VN00032119&countryCode=US&language=en

Torero, J. L., & Fernandez-Pello, A. C. (1995). Natural Convection Smolder of Polyurethane Foam, Upward Propagation. *Fire Safety Journal, 24*(1), 35–52. doi: 10.1016/0379-7112(94)00030-J

Torero, J. L., & Fernandez-Pello, A. C. (1996). Forward Smolder of Polyurethane Foam in a Forced Air Flow. *Combustion and Flame, 106*(1-2), 89–109. doi: 10.1016/0010-2180(95)00245-6

Trojanowicz, M., Bojanowska-Czajka, A., Bartosiewicz, I., & Kulisa, K. (2018). Advanced Oxidation/Reduction Processes treatment for aqueous perfluorooctanoate (PFOA) and perfluorooctanesulfonate (PFOS) – A review of recent advances. *Chemical Engineering Journal, 336*, 170-199. doi: 10.1016/j.cej.2017.10.153

U.S. Centers for Disease Control and Prevention. (2019, January). Fourth National Report on Human Exposure to Environmental Chemicals.

U.S. EPA. (2009). Soil screening levels for perfluorooctanoic (PFOA) and perfluorooctyl sulfonate (PFOS). Retrieved January 7, 2020, from https://archive.epa.gov/pesticides/region4/water/documents/web/pdf/d_final_pfc_soil_screening_values_11_20_09.pdf

U.S. EPA. (2016). Fact Sheet PFOA & PFOS Drinking Water Health Advisories (EPA 800-F- 12-003). Retrieved January 7, 2020, from https://www.epa.gov/ground-water-and-drinking-water/drinking-water-health-advisories-pfoa-and-pfos

Vecitis, C. D., Park, H., Cheng, J., Mader, B. T., & Hoffmann, M. R. (2009). Treatment technologies for aqueous perfluorooctanesulfonate (PFOS) and perfluorooctanoate (PFOA). *Frontiers of Environmental Science & Engineering in China, 3*(2), 129–151. doi: 10.1007/s11783-009-0022-7

Wang, F., Lu, X., Shih, K., & Liu, C. (2011). Influence of calcium hydroxide on the fate of perfluorooctanesulfonate under thermal conditions. *Journal of Hazardous Materials, 192*(3), 1067–1071. doi: 10.1016/j.jhazmat.2011.06.009

Wang, F., Shih, K., Lu, X., & Liu, C. (2013). Mineralization Behavior of Fluorine in Perfluorooctanesulfonate (PFOS) during Thermal Treatment of Lime-Conditioned Sludge. *Environmental Science & Technology, 47*(6), 2621–2627. doi: 10.1021/es305352p

Wang, Z., Cousins, I. T., Scheringer, M., & Hungerbuehler, K. (2015). Hazard assessment of fluorinated alternatives to long-chain perfluoroalkyl acids (PFAAs) and their precursors: Status quo, ongoing challenges and possible solutions. *Environment International, 75*, 172–179. doi: 10.1016/j.envint.2014.11.013

Watanabe, N., Takata, M., Takemine, S., & Yamamoto, K. (2018). Thermal mineralization behavior of PFOA, PFHxA, and PFOS during reactivation of granular activated carbon (GAC) in nitrogen atmosphere. *Advances in Environmental Chemistry of Pollutants, 25*(8), 7200–7205. doi: 10.1007/s11356-015-5353-2

Watanabe, N., Takata, M., Takemine, S., & Yamamoto, K. (2016). Residual organic fluorinated compounds from thermal treatment of PFOA, PFHxA and PFOS adsorbed onto granular activated carbon (GAC). *Journal of Material Cycles and Waste Management, 18*, 625-630. doi: 10.1007/s10163-016-0532-x

Wei, C., Song, X., Wang, Q., & Hu, Z. (2017). Sorption kinetics, isotherms and mechanisms of PFOS on soils with different physicochemical properties. *Ecotoxicology and Environmental Safety, 142*, 40–50. doi: 10.1016/j.ecoenv.2017.03.040

Xiao, F., Simcik, M. F., Halbach, T. R., & Gulliver, J. S. (2015). Perfluorooctane sulfonate (PFOS) and perfluorooctanoate (PFOA) in soils and groundwater of a U.S. metropolitan area: Migration and implications for human exposure. *Water Research, 72*, 64–74. doi: 10.1016/j.watres.2014.09.052

Yamada, T., Taylor, P.H., Buck, R.C., Kaiser, M.A., Giraud, R.J. (2005). Thermal degradation of fluorotelomer treated articles and related materials. *Chemosphere, 61*, 974-984. doi: 10.1016/j.chemosphere.2005.03.025

Yermán, L., Cormier, D., Fabris, I., Carrascal, J., Torero, J.L., Gerhard, J.I., & Cheng, Y.-L. (2017). Potential Bio-oil Production from Souldering Combustion of Faeces. *Waste Biomass Valorization, 8*(2), 329-338. doi: 10.1007/s12649-016-9586-1

Yermán, L., Hadden, R.M., Carrascal, J., Fabris, I., Cormier, D., Torero, J.L., Gerhard, J.I., Krajcovic, M., Pironi, P., & Cheng, Y.-L. (2015). Smouldering combustion as a treatment technology for faeces: Exploring the parameter space. *Fuel, 147*, 108-116. doi: 10.1016/j.fuel.2015.01.055

Yeung, L. W. Y., Silva, A. O. De, Loi, E. I. H., Marvin, C. H., Taniyasu, S., Yamashita, N., Mabury, S.A., Muir, D.C.G., & Lam, P. K. S. (2013). Perfluoroalkyl substances and extractable organic fluorine in surface sediments and cores from

Lake Ontario. *Environment International, 59*, 389–397. doi: 10.1016/j.envint.2013.06.026

Zhang, K., Huang, J., Yu, G., Zhang, Q., Deng, S., & Wang, B. (2013). Destruction of Perfluorooctane Sulfonate (PFOS) and Perfluorooctanoic Acid (PFOA) by Ball Milling. *Environmental Science & Technology, 47*(12), 6471–6477. doi: 10.1021/es400346n

Chapter 3

Smouldering Combustion Treatment of Soils and Granular Activated Carbon

Contaminated with Per- and Polyfluoroalkyl Substances

3.1. Introduction

Per- and polyfluoroalkyl substances (PFAS) are a group of compounds extensively used in commercial, industrial, and military applications since the 1950's (Cousins et al., 2016). Water-proof clothing, stain-resistant furniture, fast-food containers, and aqueous film forming foam (AFFF) are examples of PFAS-containing products (Paul et al., 2009; Schaider et al., 2017). Significant PFAS-contamination has been reported at manufacturing facilities and sites which have used AFFF, such as military bases, airports, and fire training facilities (Cousins et al., 2016; Hu et al., 2016; Milley et al., 2018; Rayne & Forest, 2009).

PFAS are amphipathic compounds that consist of a fluorocarbon chain of a specific length and a functional group (for example, sulfonic, carboxylic, or phosphonic) (Buck et al., 2011; Pabon et al., 2002). The strong carbon-fluorine bonds make PFAS highly stable and thus are resistant to thermal and chemical degradation (3M Corporation, 1999; Buck et al., 2011; Kissa, 2001). There is evidence suggesting some PFAS will degrade to perfluoroalkyl acids (PFAA) under certain conditions (O'Carroll et al., 2020). However, PFAA have shown resistance to biological degradation (Buck et al., 2011; Pabon et al., 2002; Kuroda et al., 2014;). Overall, PFAS are a long-term source of contamination to groundwater, surface water, drinking water, and soil (Wang et al., 2015; Espana et al., 2015; Kuroda et al., 2014). The extent of PFAS-contamination is widespread; for example, quantifiable PFAS concentrations have been measured in biota in both the Arctic and

Antarctica and in humans worldwide (Cai et al., 2012; Inoue et al., 2004; Young et al., 2007).

Numerous industrialized countries, including Australia, Canada, and the United States, have placed increasingly stringent limits on PFAS. Many countries have drinking water guidelines set for perfluorooctanesulfonic acid (PFOS) and perfluorooctanoic acid (PFOA), which are the two PFAS compounds that have received the most attention in research (Crone et al., 2019; Milley et al., 2018). Health Canada (HC), Environment and Climate Change Canada (ECCC), and the Department of Health (DoH) in Australia have also set guidelines for surface water, groundwater, and soil (DoH, 2019; HC, 2019; ECCC, 2017). Soil contamination is increasing in concern due to its potential role as a continuous source of groundwater PFAS contamination (Aly et al., 2019). The adoption of more stringent regulatory limitations has spurred interest in the development of remediation options for both contaminated water and soils (Trojanowicz et al., 2018).

With respect to water, granular activated carbon (GAC) is one of the most common treatment options, removing >90% of PFAS (Hale et al., 2017; Espana et al., 2015; Kucharzyk et al., 2017; Crownover et al., 2019). However, once saturated, management and disposal of the PFAS-loaded GAC is necessary. With respect to soils, traditional remediation techniques for organic contaminants are insufficient or ineffective (Brusseau, 2018; Schaefer et al., 2015). The strength of the carbon-fluorine bonds and the high electronegativity of the fluorine create challenges for biological and chemical-based remediation techniques (Jin & Zhang, 2015). The most common methods used to manage PFAS-contaminated soils are excavation and landfill, incineration, and soil washing (Crownover et al., 2019; Dorrance et al., 2017; Ross et al., 2018). Landfilling PFAS-

contaminated media is becoming more unfavourable due to increasingly restrictive regulations, increasing costs, and the long-term liability (Ross et al., 2018; Hale et al. 2017). Soil washing can be expensive and does not eliminate the PFAS, making these options unsuitable for large-scale treatment of PFAS-contaminated soils (Dorrance et al., 2017; Mahinroosta & Seneviranthna, 2020). There are a number of new concepts in early stages of development for treating PFAS-contaminated soil and water including physical, chemical, and irradiation techniques (Mahinroosta & Seneviranthna, 2020; Ross et al., 2018).

In particular, thermal treatment of PFAS in both GAC and soil has generated significant interest. Heating PFAS in an oven to 400-500°C can achieve volatilization but is not expected to destroy the compounds (Ross et al., 2018). Incomplete destruction of PFAS compounds could result in the production of shorter-chain PFAS compounds and other volatile organic fluorine (VOF) by-products (such as CF_4 and C_2F_6) which are harmful greenhouse gases (Wang et al., 2015; Ross et al., 2018; Watanabe et al., 2016). Studies have demonstrated 700°C is sufficient to mineralize some PFAS during GAC regeneration; however, temperatures of 900-1100°C are likely necessary for a high degree of PFAS destruction and to minimize the production of undesired by-products (Watanabe et al., 2016; Ross et al., 2018; Yamanda et al., 2005; Wang et al., 2015). When mineralization of PFAS occurs, hydrofluoric acid (HF) will be produced (Trautmann et al., 2015; Ross et al., 2018). Destruction of PFAS by high temperature incineration or desorption plus thermal oxidation is therefore an option. However, such facilities are not yet widely proven or permitted for PFAS, existing facilities are typically not designed or operated for PFAS destruction, and they are expensive and carbon-intensive to operate due to the need for

continual fuel input (Dorrance et al., 2017; Espana et al., 2015). GAC destruction is particularly problematic for incinerators since, although it is energy dense (Higher Heating Value of 30.82 MJ/kg), it does not gasify, which is a key requirement of incinerator fuels.

Smouldering combustion is here proposed as a new thermal PFAS remediation technique. Smouldering is flameless oxidation reaction that occurs on the surface of a solid fuel when penetrated by gaseous oxygen (Ohlemiller, 1985). Smouldering can be self-sustaining after ignition, meaning no external energy input is needed to convert the carbonaceous fuel to primarily heat, water, and carbon dioxide (Ohlemiller, 2002); conversion of charcoal to ash in a traditional barbeque is a well-known example. Smouldering combustion is an emerging remediation technique available commercially as STAR (Self-Sustaining Treatment for Active Remediation). STAR has been demonstrated to effectively treat organic-contaminated soils at laboratory and field (commercial) scales applied as both an in situ and ex situ technique (Grant et al., 2016; Sabadell et al., 2019; Scholes et al., 2015; Solinger et al., 2020; Switzer et al., 2014). The smouldering reaction propagates as a hot, thin front through the soil in the direction of air injection, oxidizing the contaminant and leaving clean soil behind. STAR is regularly applied to soils contaminated with hydrocarbons such as coal tar and crude oil, where the contaminant is the fuel for the smouldering reaction (Switzer et al., 2009; Pironi et al., 2011). When the contaminant cannot act as the fuel, because it is too volatile or its concentration in soil is too low, the soil can be impregnated with a surrogate fuel such as vegetable oil or wood chips to permit remediation by self-sustained smouldering (Gianfelice et al., 2019; Kinsman et al., 2017; Salman et al., 2015). Smouldering temperatures range from 600 to

1200˚C depending primarily on the energy content of the fuel (contaminant or surrogate) and its concentration in soil (Zanoni et al., 2019).

The potential for smouldering to treat PFAS-contaminated soils has never been examined. As the typical concentrations of PFAS in soils, ng/kg to µg/kg, are too low to be a fuel for self-sustaining smouldering, a surrogate fuel would be needed. In combustion literature, carbon particles added in small concentrations to inert porous media (3.1 – 3.6% by mass) have been shown to generate self-sustaining smouldering reactions of approximately 1050 ˚C (Baud et al., 2015; Martins et al., 2020). A motivating hypothesis for this study is that GAC added to soil could provide a mixture that would support self-sustaining smoldering at temperatures that could eliminate PFAS from the GAC and the soil while mineralizing a significant fraction of the PFAS.

This study explored, for the first time, the ability of smouldering to remediate PFAS-contaminated soils and PFAS-impacted GAC. First, the relationship between GAC concentration and smouldering temperature was evaluated without PFAS. Then, smouldering experiments were conducted with both surrogate soil and GAC contaminated with PFAS in the laboratory. Additional smouldering experiments were then conducted with PFAS-contaminated soil from a field site. A comprehensive suite of targeted and non-targeted analytical techniques were employed to quantify PFAS, mineralized fluorine, and total organic fluorine in the soils and emissions associated with smouldering treatment. In this work, targeted analysis provided quantitative results while non-targeted analysis provided qualitative results on emission products. This work provides the basis for a new approach to remediation of PFAS that has the potential to be destructive while also cost effective due to minimal energy requirements of smouldering.

3.2. Experimental Procedure

3.2.1. Experimental Phases

Experiments were conducted in four phases (Table 3.1). Phase I explored the effect of

GAC concentration and injected air flux on the behaviour of smouldering soil. In Phase I,

the GAC and soil did not contain any PFAS. Conditions that would achieve self-sustained

smouldering above 1000°C were established and then carried forward to subsequent

phases that did include PFAS. Phase II evaluated the ability of smouldering combustion

to remediate PFOS-contaminated GAC, Phase III evaluated PFAS-spiked soil mixed with

clean GAC, and Phase IV considered a PFAS-contaminated field soil mixed with clean

GAC (Table 3.1).

Table 3.1: Experimental Conditions and Summary of Results

Experimental Conditions				Results	
Experiment	GAC Concentration (mg GAC/kg soil)	Air Flux (cm/s)	Number of PFAS$_{13}$	Average Peak Temperature (˚C)	Smouldering Velocity (cm/min)
Phase I: No PFAS					
I-1	60	5.0	0	1257 ± 63	0.64 ± 0.13
I-2	40	5.0	0	1003 ± 50	0.66 ± 0.13
I-3	20	5.0	0	707 ± 35	0.49 ± 0.10
I-4	40	2.5	0	1024 ± 51	0.47 ± 0.09
I-5	40	7.5	0	1056 ± 53	0.70 ± 0.14
I-6	60	2.5	0	1184 ± 59	0.37 ± 0.07
I-7	20	2.5	0	662 ± 33	0.33 ± 0.07
Phase II: PFOS-Contaminated GAC					
II-1	44	5.0	1[a]	1048 ± 52	0.45 ± 0.09
II-2	46	5.0	1[a]	1011 ± 51	0.40 ± 0.08
Phase III: PFAS-Spiked Soil					
III-1 (blank)	50	5.0	0	1085 ± 54	0.69 ± 0.14
III-2	50	5.0	6[b]	1093 ± 55	0.64 ± 0.13
III-3	50	5.0	6[b]	1145 ± 57	0.71 ± 0.14
III-4	50	5.0	6[b]	1143 ± 57	0.48 ± 0.10
III-5	15	5.0	6[b]	642 ± 32	0.24 ± 0.05
Phase IV: PFAS-Contaminated Field Soil					
IV-1	51	5.0	3[c]	1040 ± 52	0.38 ± 0.08
IV-2	51	5.0	3[c]	1012 ± 51	0.47 ± 0.10

[a] PFOS.
[b] Perfluorobutanesulfonic acid (PFBS), perfluorohexanesulfonic acid (PFHxS), perfluoroheptanoic acid (PFHpA), PFOA, PFOS, and perfluorononanoic acid (PFNA).
[c] Number of PFAS found at concentrations above the detection limit.

3.2.2. Smouldering Column Setup

All experiments followed a standard smouldering setup and procedure documented elsewhere (Switzer et al., 2009; Pironi et al., 2011; Yermán et al., 2015), hence only a summary is presented here. A contaminated porous media mixture was packed to a known height (21 to 28 cm) in a stainless-steel reactor of 16 cm inner diameter (Figure 3.1a). Thermocouples (TCs) (KQIN-18U-6, Omega Ltd.) placed at 3.5 cm intervals measured temperatures at the centerline of the column. Clean coarse sand (12ST, mean grain diameter = 0.88mm, Bell & Mackenzie Co.) was packed on top of the porous media mixture ($\approx$12

cm) and the column was insulated with 5 cm thick mineral wool pipe insulation (McMaster-Carr) to minimize the heat losses. The emissions were continuously analyzed for volume fractions of oxygen, carbon monoxide, and carbon dioxide using a multi-gas analyzer (MGA-3000 Series, ADC). TC and gas emissions data were recorded in two-second intervals using a data logger (Multifunction Switch/Measure Unit 34980A, Agilent Technologies) which was connected to a computer. Three emissions trains were implemented simultaneously to supply cumulative (integrated) samples for targeted and non-targeted PFAS, HF, and total organic fluorine (TOF) as well as snapshot emission samples for non-targeted volatile organic fluorine compounds (VOFs) (Figure 3.1b); these are described in Sections 2.7 – 2.10.
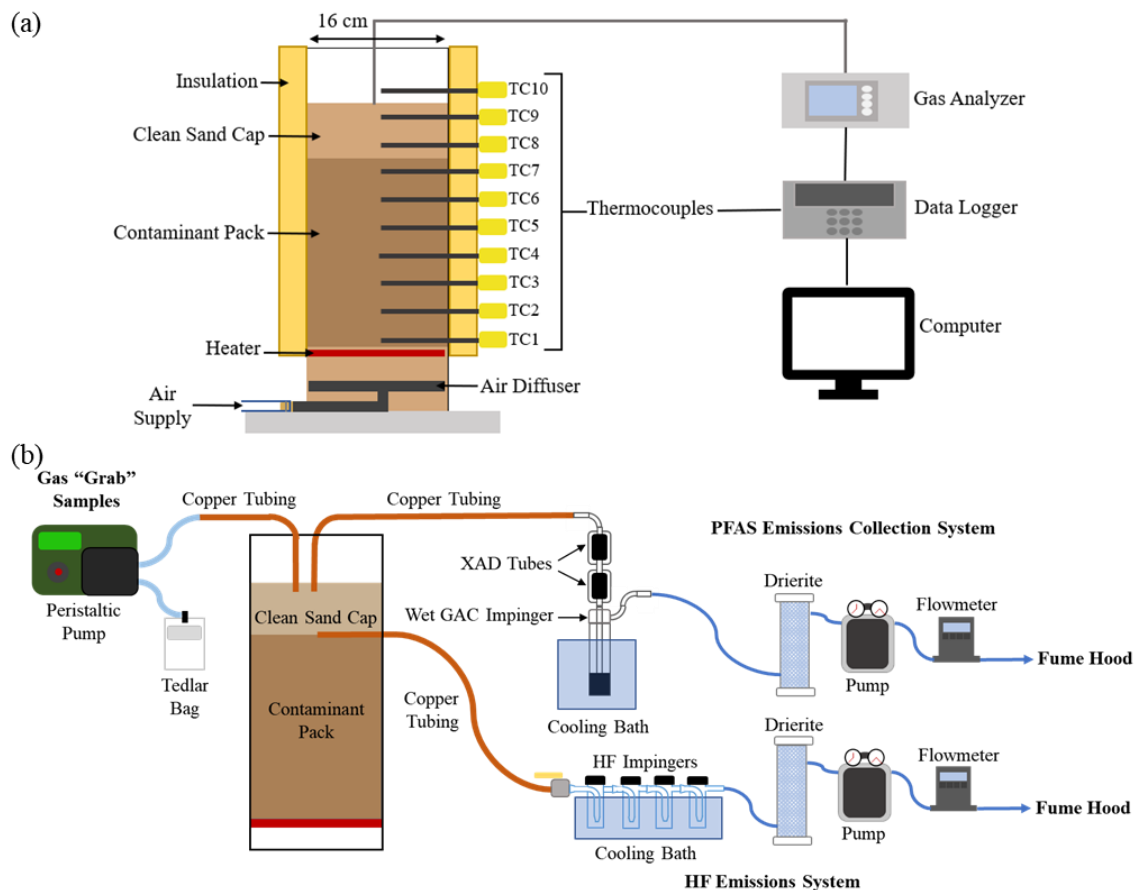
Figure 3.1: (a) Schematic of smouldering experimental setup including reactor and all data smouldering data collection equipment; (b) Emissions collection systems: HF, targeted and non-targeted PFAS, non-targeted volatile organic fluorine compounds (VOFs), and total organic fluorine (TOF).

3.2.3. Preparing the Porous Media Mixtures

The porous media mixture comprised GAC and sand (Phases I and II) or GAC and soil (Phases III and IV). First, intentional loading with PFAS occurred as described in Sections 3.2.3.1 and 3.2.3.2 for the GAC and the soil, respectively. Subsequently, the desired amounts of GAC and sand/soil were placed in a stainless-steel bowl and mechanically mixed (Model KSM7581CA0, KitchenAid) until uniform. Once prepared, the porous media mixture was carefully placed in the column in short lifts and gently tamped to maximize homogeneity. GAC (CAS # 7440-44-0, McMaster Carr) was used for all Table

3.1 experiments. Phase I and II experiments mixed the GAC with coarse sand at the concentrations provided in Table 3.1. Phase III experiments used a laboratory-spiked soil designed to imitate a field soil with a controlled grain size distribution ($\sigma = 1.16$, poorly sorted soil) and organic fraction (1%). The spiked soil comprised 28% (dry wt %) black topsoil (Fisher's Landscaping, London, Ontario), 47% medium sand (1240S, mean grain diameter = 0.50 mm, Bell & Mackenzie Co.), and 25% coarse sand (further details in Appendix A). In Phase IV experiments, a PFAS-contaminated field soil was obtained from a former airfield (Naval Air Station Joint Reserve Base, Willow Grove, United States). Note that, subsequent to the three 18.9 L pails of contaminated soil acquired for this study, the rest of the PFAS-contaminated soil at this site was removed and treated. The soil was homogenized and grains larger than 12.5 mm were removed prior to mixing with GAC (no sand or spiked soil was used). During packing of the reactor, three representative samples of the "pre-treatment" contaminated porous media mixtures were collected for analysis.

3.2.3.1.   Preparation of the PFAS-Contaminated GAC

The Phase II experiments utilized GAC contaminated with PFOS. A stock solution was prepared for each experiment in which 0.1972-0.1980 g of PFOS (CAS # 2795-39-3, purity = 98%, Sigma-Aldrich) and 950 mL of deionized water were added to each of 12 one litre polypropylene bottles. The mass added represents approximately 13% of the solubility of PFOS, which was taken as 1.52 g/L (SGS, 2018). These were placed on a shaker table for 48 hours at 170 RPM. Then 40 g of GAC was added to each stock solution bottle and placed back on the shaker table at 170 RPM for 96 hours. To separate the GAC and stock solution, a laboratory vacuum filtration system was used with 12.5 cm filter paper (Cat # 09-790-12E, coarse porosity, Fisher Scientific). The contents of each one litre bottle was

poured into the vacuum system. The GAC was removed from the vacuum when the free water was removed. The PFOS-contaminated GAC was then stored in a polypropylene container. PFOS concentration on the GAC was determined by measuring the difference in the stock solution concentration prior to adding the GAC and after removing the GAC. This method was chosen after direct extractions of PFOS from GAC at such high concentrations proved to be less reliable (Appendix B). Though the GAC grains appeared dry, they had an average moisture content of 32% (ASTM D2974-14) from water bound by the intragranular porosity.

3.2.3.2. Preparation of the PFAS-Spiked Soil

The Phase III experiments used spiked soil intentionally contaminated with known amounts of six common PFAS: PFOA, PFOS, perfluorohexanesulfonic acid (PFHxS), perfluoroheptanoic acid (PFHpA), perfluorobutanesulfonic acid (PFBS), and perfluorononanoic acid (PFNA). Of the three components of the spiked soil, only the black topsoil was loaded with PFAS. Since the topsoil contained all the organic carbon, it had the highest sorption capacity of the components in the spiked soil. First, the topsoil was dried, crushed, and sieved (ASTM C136 C126M-14); particles ≥ 2 mm were removed. Note that Expt III-1 is a blank, following the same methodology but omitting the PFAS addition.

For each experiment, 15 L of stock solution was created in a 20 L polypropylene carboy (Life Technologies). Each PFAS was added: 0.4445 g PFOA (CAS # 335-67-1, purity = 95%, ThermoFisher Scientific), 0.0117 g PFOS, 0.0291 g PFHxS (CAS # 3871-99-6, purity = 98%, Sigma-Aldrich), 0.0525 g PFHpA (CAS # 375-85-9, purity = 99%, Sigma-Aldrich), 0.0362 g PFBS (CAS # 375-73-5, purity = 97%, Sigma-Aldrich), and 0.0202 g

PFNA (CAS # 375-95-1, purity = 97%, Sigma-Aldrich) was added to 15 L of deionized water. Masses used represented approximately 13% of the solubility for PFOA and <1.3% of the solubility for the other five PFAS (SGS, 2018) (see Appendix B for PFAS solubilities); note: in Expt III-2 0.1270 g of PFBS was used (full details in Appendix B). The carboy was shaken regularly over a 48-hour period to allow the PFAS to dissolve. 9.2 kg of the dried, sieved topsoil was added (note: for Expt III-2, 2.3 kg was added) and the carboy was agitated regularly over a 96-hour period. Individual batches of contaminated spiked soil were created for Expts III-1 and III-2, while a single batch was created, homogenized, and subdivided for Expts III-3, III-4, and III-5. Masses of PFAS added to stock solution were chosen in order to target 2-3 mg PFOA/kg and 0.1-0.4 mg/kg of the other five PFAS on the porous media mixture. PFAS concentrations were chosen to reflect typical concentrations at PFAS-contaminated sites.

To separate the soil from the solution, silicone tubing (Part # 96410-25, Masterflex) and a peristaltic pump (Model 520S, Watson Marlow) were used to pump the carboy contents into the laboratory vacuum filtration system described above. The spiked topsoil remained the in vacuum system until all free water was removed. The drained, contaminated topsoil appeared moist and an average moisture content of 14.3% was measured (ASTM D2974-14), which translated into a moisture content of 4.2% for the spiked soil once all three components were mixed. Once drained, the PFAS-contaminated topsoil was stored in a polypropylene container. Spiked soil samples were analyzed on a wet mass basis because both the spiked soil and the remaining moisture were contaminated with PFAS, and both contributed to the PFAS loading in these experiments.

3.2.4. Smouldering Experiments

A well-established procedure was followed for smouldering treatment of contaminated soil (Pironi et al., 2011; Switzer et al., 2009; Yermán et al., 2015). The heater at the base of the reactor (Figure 3.1a) was turned on until the first TC (TC1) above the heater reached 260°C, at which time a set air flux was introduced through the air diffuser at the base (Figure 3.1a) using a mass flow controller (FMA5541, Omega Ltd.). This started a smouldering reaction, which then propagated upwards. When the reaction reached TC2, the heater was turned off. However, the airflow remained on for the duration of the experiment, such that the self-sustained smouldering reaction travelled upwards until no fuel (i.e., GAC) remained and the reactor cooled to ambient temperature. The average smouldering velocity and average peak temperature for each experiment (Table 3.1) were calculated using standard procedures (Pironi et al., 2011). Appendix C outlines parameters used for additional experiments.

3.2.5. Post-treatment Sampling

Following each experiment containing PFAS, the reactor was excavated carefully to provide representative "post-treatment" samples. All sample bottles were cleaned using methanol, isopropyl alcohol, and deionized water wash method (details in Appendix D). The clean sand cap was first removed; for select experiments (III-1, III-5, and IV-2) samples of the clean sand cap were collected. A 250 mL sample was then collected from the centre of the treatment zone. The treatment zone for these experiments was considered to be between TCs 5-7 and excluded sand within 2 cm of the smouldering column wall. Due to heat losses around the wall of the smouldering column, there is a radial decreased in temperature outwards, therefore post-treatment samples from the center of the column

will correlate with the temperatures measured by the TCs. Triplicates of pre- and post-treatment samples were analyzed and averaged for each experiment.

3.2.6. PFAS Analysis of Soil, Condensates, Washes, and XAD Absorbent

All PFAS analyses were conducted by the Environmental Sciences Group at the Royal Military College of Canada. Targeted PFAS analysis of solid and liquid samples was completed following EPA 8327 using liquid chromatography with tandem mass spectrometry (LC-MS/MS). Solid samples were extracted by adding 5 mL of basic methanol (0.1% ammonium hydroxide v/v) to 0.5 g of soil and glass wool or 1.0 g GAC in a 15 mL c-tube. While typical extractions of PFAS from GAC have shown poor recovery (Du et al., 2014), protocols were adjusted such that extraction achieved 95% PFAS recovery efficiency. Protocol adjustments included using a larger sample/solvent ratio and extracting the filter paper used to filter the GAC; the latter was necessary to extract PFAS sorbed to the fine particulate GAC trapped in the filter matrix.

Samples were vortexed for 30 seconds, then placed on an end-over-end shaker rotating at 30 RPM for 48 hours. Samples were then centrifuged at 4000x RPM for 20 minutes and a sub-sample was taken and put into an HPLC vial for analysis. Liquid samples were directly sub-sampled into HPLC vials for analysis or further diluted with basic methanol. Mass-labelled internal standards of PFOA, PFOS, PFHxS were added to solid samples before extraction to examine matrix effects. Concentrations of 13 PFAS were calculated using an eight-point calibration curve across 0.01 ppb to 200 ppb. See Appendix E for the list of the 13 PFAS analyzed. Internal standard recoveries were found to be between 70-120% and no correction was applied. Two double injection blanks (basic methanol) were run before each method blank, reagent blank, calibration curve, post-treatment sample, and

experimental blanks to eliminate contamination and carry-over from other samples. Sample duplicates within 30% relative percent difference (RPD) was considered acceptable according to EPA Method 531.1. The instrumental detection limit was 0.0004 ppm PFAS and the quantitation limit was 0.001 ppm PFAS (see Appendix E for full analysis procedure). The results using this method are hereafter referred to as "PFAS$_{13}$" to indicate that the results represent the quantifiable mass within the 13 analytical suite.

For Expt II-2, an additional targeted and non-targeted PFAS analysis was conducted. Trifluoroacetic acid (TFA) and perfluoropropanoic acid (PFPA) were added to the targeted PFAS analysis. Screening for H/F exchange PFAS compounds was accomplished using the same elution profile as for the PFAS$_{13}$ suite, except with a longer profile C18 column (150 mm). The LC-MS/MS was run first in mass scan mode to identify the presence of the suspected compounds, then run again using SIM mode to allow for better peak area determination relative to the PFAS$_{13}$ compounds.

3.2.7. Emissions Collection: HF

A hydrogen fluoride (HF) collection system was used to measure the fraction of PFAS mineralization that occurred (Figure 3.1b). In the series of four impingers (Part # 7544-35, Ace Glass Inc.), the first and fourth were used as a knock-out and the second and third contained 15 mL of 0.1 N sulfuric acid (H_2SO_4) (modified EPA Method 26). All glassware used was cleaned using the rigorous procedure outlined in Appendix D and the copper tubing was replaced for every experiment. Prior to each experiment, a leak test was completed by injecting pure nitrogen and measuring for oxygen (details included in Appendix F). This method ensured that any leakage, representing the fraction of sample drawn by the pump that came from outside the reactor, was known and never exceeded

10%. This value was minimized by iterative testing and adjusting of piping/impinger connections for each experiment. The emissions were sampled from directly above the contaminant pack (Figure 3.1b). A vacuum pump and flow totalizer (FMA 4000, Omega Ltd.) were started at the same time as the injected airflow in the experiment. The flowrate through the HF collection system was quantified for each experiment, ranging from 2-3 L/min (EPA Method 26), representing 2.5-4.2% of the injected air during the experiment (calculated using the known leakage factor for each experiment). The fraction of emissions captured was used to back-calculate the HF production for each entire experiment. Once the smouldering had eliminated all the GAC in the contaminant pack, the vacuum pump was turned off. One integrated sample was collected for each experiment and analyzed using Ion Chromatography (US EPA Method 26A, ALS).

3.2.8. Emissions Collection: PFAS

A PFAS collection system was employed to trap PFAS compounds in the emissions during smouldering (Figure 3.1b). This system was designed using the best practice from literature and a series of tests (see Appendix G). An emissions subsample was collected through copper tubing submerged in the clean sand cap to prevent dilution with fumehood air. The emissions subsample then flowed through two XAD-2 tubes (ALS) and one impinger (Greenburg-Smith Modified 7536-16, Ace Glass Inc.) placed in series. Each XAD tube contained 50 g of clean GAC and the impinger contained 50g of GAC and enough deionized water to fill the pore spaces. Glass wool (CAS # 65997-17-3, Sigma-Aldrich) was added above the GAC in the XAD tubes to hold it in place. All glass components were cleaned prior to each experiment using the procedure in Appendix D and the copper tubing was replaced for each experiment. Before each experiment, the PFAS

collection system was leak tested as described above (details in Appendix F). Sampling began when the airflow injection started and continued until the GAC in the reactor was eliminated and the clean sand cap began to cool. The flowrate for the PFAS collection system was regulated at 2-3 L/min using a pump and flow totalizer (FMA6616, Omega Ltd.). 3.2-4.3% of the total injected air was sampled; the determined fraction was used to back calculate the total mass of PFAS emitted during each experiment. Following the experiments, the glass wool, the GAC from each XAD tube (homogenized but not combined), and the GAC and water from the impinger was analyzed individually for $PFAS_{13}$ as described in Section 2.6. The copper tubing and each piece of glassware was rinsed prior to the experiment and following each experiment with basic methanol (1% w/w using sodium hydroxide), and these samples were reserved for $PFAS_{13}$ testing.

3.2.9. Emissions Collection: VOFs

Non-targeted, qualitatively analysis for VOF compounds emitted during smouldering was conducted via emissions grab samples. Gas samples were collected in a Tedlar bag though sampling from the sand cap using a peristaltic pump (Figure 3.1b). The compounds collected in the VOF grab samples are expected to be the same as those collected in the PFAS emissions collection system. Triplicate samples of approximately 5 mL were collected at two individual times during the smouldering period for each experiment; these represent a snapshot of emissions as opposed to a continuous integral of emissions collected by the other emissions trains. Qualitative analysis was completed using gas chromatography – mass spectrometry (GC-MS).

3.2.10. Total Organic Fluorine (TOF) Samples

Total organic fluorine analysis was completed on the PFAS-contaminated porous media mixture samples, both pre-treatment and post-treatment, as well as on samples from the PFAS collection system (glass wool and GAC from both XAD tubes and from the impinger). Samples were taken from the top and bottom of each XAD tube to monitor for breakthrough. This analysis aimed to quantify the totality of fluorinated compounds being released during smouldering both within and outside the $PFAS_{13}$ analytical suite. Under ideal circumstances, quantifying the additional fluorinated species being produced during smouldering should help complete the fluorine mass balance. The method involves taking 3-6 g subsample from the homogenized sample after each experiment, from which a 0.2 g subsample is analyzed via Combustion Ion Chromatography (CIC) (Eurofins Environmental Testing Australia).

Soluble fluoride analysis was completed by analyzing 0.5 g subsamples. An aqueous solution was used to extract the soluble fluoride from solid samples and was analyzed using a fluoride ion-selective electrode (ISE) (Eurofins Environmental Testing Australia).

3.3. Results

3.3.1. Smouldering

Seven experiments using a mixture of GAC and coarse sand examined the influence of GAC concentration and air flux on the smouldering reaction (Table 3.1). Figure 3.2 illustrates typical results for a smouldering experiment, in this case for Expt III-3 (50 g GAC/kg sand, 5 cm/s air flux). The sharp rise in temperature at TC1 coinciding with the onset of air flow indicates the smouldering of GAC at this location (Figure 3.2a). The succession of crossing TC profiles and steady peak temperatures reveals a self-sustaining

smouldering reaction propagating along the contaminated pack (Switzer et al., 2009). The average peak temperature for Expt III-3 was $1145 \pm 57°C$ and the average smouldering velocity was 0.71 ± 0.14 cm/min. The reported uncertainty is $\pm$ 5% for temperature and $\pm$ 20% for velocity, which is based upon an analysis of repeatability in smouldering experiments and represents a conservative estimate of the inherent random variability (further details in Appendix H). As expected, decreased oxygen and increased carbon dioxide concentrations in the emissions coincide with the duration of smouldering (Figure 3.2b). All experiments in this work show similar behaviour; thermocouple and gas emission profiles for all experiments are included in Appendix I. Table 3.1 summarizes the average peak temperatures and average smouldering velocities for all experiments.
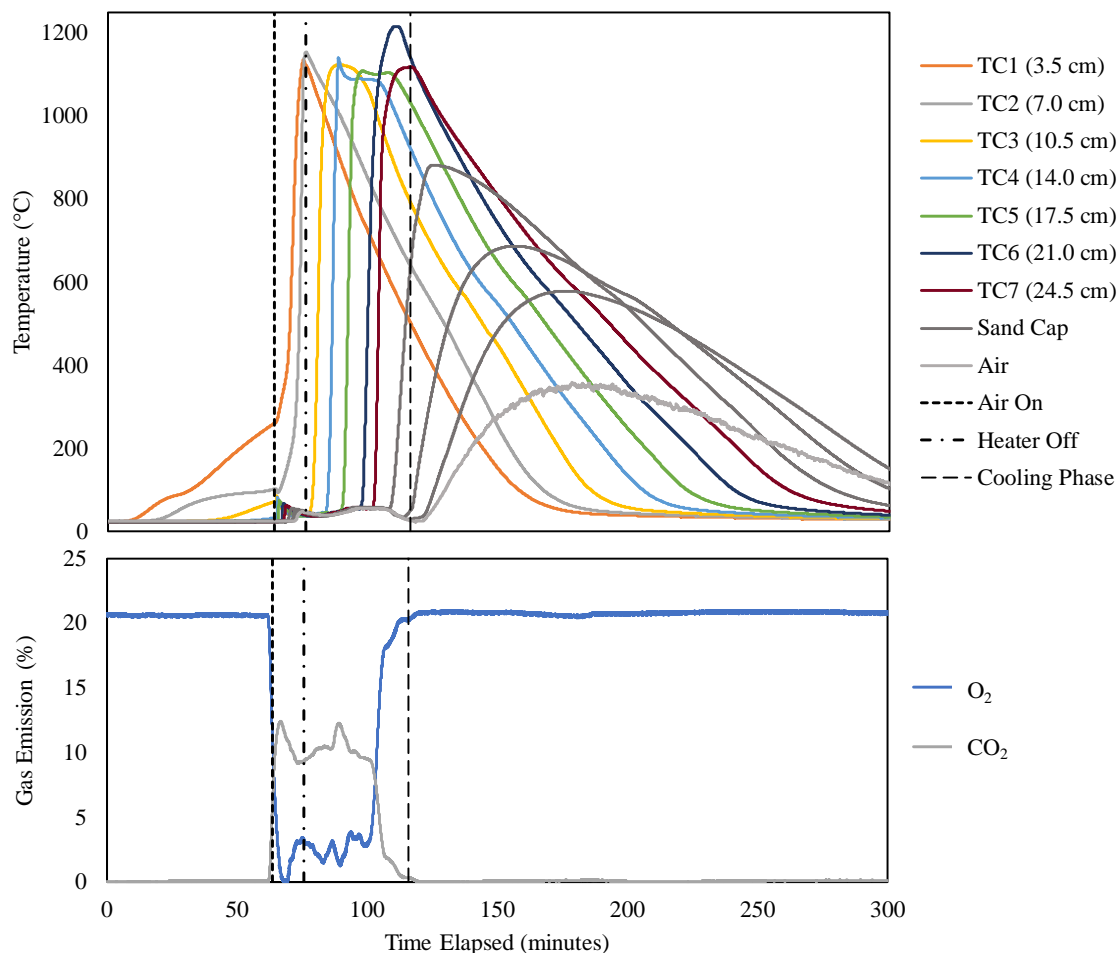
Figure 3.2: Smouldering data for Expt III-3 (50 g GAC/kg soil, 5 cm/s air flux). (a) Thermocouple profiles, and (b) combustion gas emission profiles. The first vertical dashed line indicates when the air flow was turned on, the second when the heater was turned off and the third when the reaction reached the top of the porous media mixture, ending the smoldering phase.

Figure 3.3 illustrates a key finding: the linear dependence of average peak temperature on GAC concentration. This is due to an increase in the rate at which net energy is released at higher fuel concentrations (Zanoni et al., 2019). Similar trends were observed for soils contaminated with organic liquids, such as coal tar and crude oil (Pironi et al., 2011), but have not been previously demonstrated for smouldering GAC. This indicates that the operator can control the peak smouldering temperature by selecting the GAC concentration. Importantly, for this work, these results reveal that exceeding 40 g GAC/kg

sand will generate temperatures exceeding 900˚C, the threshold considered necessary for significant mineralization of PFAS. Therefore, the rest of the experiments were conducted at concentrations in the range 44 – 51 g GAC/kg soil (Table 3.1); the exception was Expt III-5, which intentionally examined the influence of lower peak temperatures on PFAS fate by using 15 g GAC/kg soil. Figure 3.3 also shows that the field soil experiments (IV-1 and IV-2) exhibited a slightly lower average peak temperature (1012 – 1040 ˚C) than the experiments using the spiked soil (1085 – 1145˚C) despite similar GAC concentrations. This is likely due to different properties of the soils, including organic content, heat capacity, and moisture content.
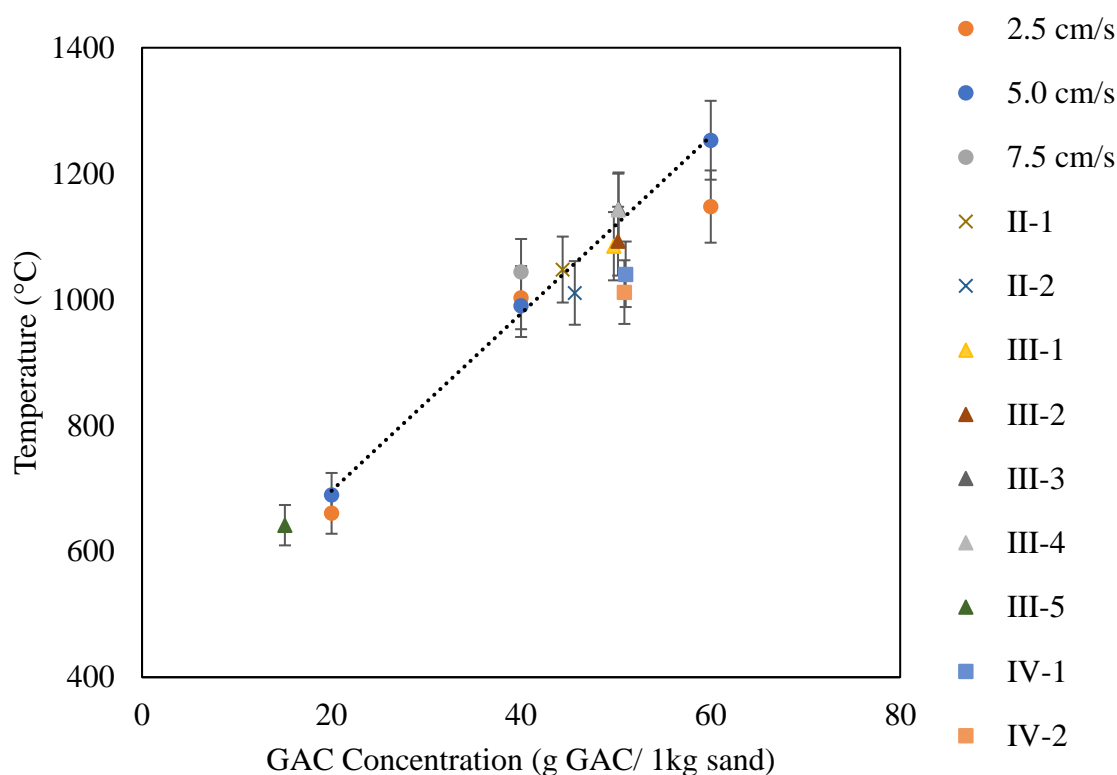
Figure 3.3: Experimental GAC concentration compared to the resulting average peak temperature. Linear trendline shown for Phase I experiments with 5 cm/s air flux.

Figure 3.4 reveals the positive correlation found between air flux and smouldering velocity. A similar relationship was observed for organic-liquid contaminated soils (Pironi

et al., 2011; Switzer et al., 2014). This occurs because excess oxygen is available (e.g., Figure 3.2b) and therefore the reaction propagation rate is primarily controlled by forward convective heat transfer (Zanoni et al., 2019). The air flow transfers heat forward from (i) the reaction and (ii) heat stored in the clean sand behind the reaction, thereby preheating the GAC and sand ahead of the front to ignition temperatures. This dependence of velocity on air flux indicates that the STAR operator can control the rate of mass destruction and the time required to treat a batch of contaminated soil by adjusting the air flow rate. The relationship between air flux and front velocity for all experiments is included in Appendix J.
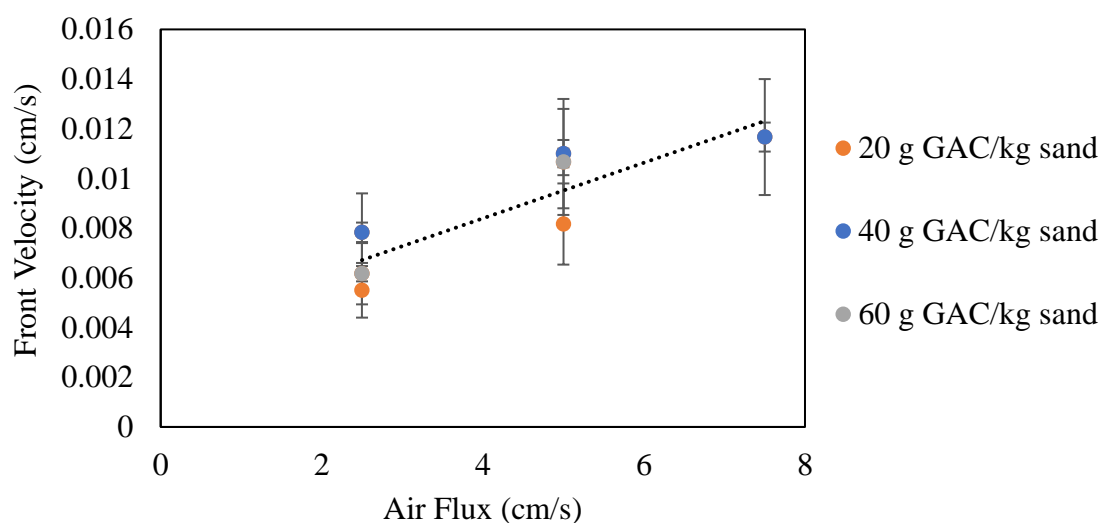
Figure 3.4: Relationship between the air flux and front velocity in Phase I experiments.

It is further noted that the experiments demonstrated good repeatability with respect to average peak temperatures and smouldering velocities. For example, Expts II-1 and II-2 agree on these two measures within uncertainty, as do Expts III-2, III-3, and III-4 for

average peak temperature. The smouldering velocity for Expt III-4 was lower than the other two experiments, which may be due to uneven distribution of GAC in this case.

3.3.2. Fluorinated Compounds

3.3.2.1. PFAS in Porous Media Mixtures

Phase II: PFOS-Contaminated GAC

Expts II-1 and II-2 are replicates in which GAC was intentionally loaded with high amounts of PFOS; this is akin to spent GAC requiring disposal after having been used to treat contaminated water. Due to the high sorption capacity of GAC, virtually all of the PFOS added to the stock solution adsorbed to the GAC (Appendix K). Prior to smouldering treatment, the PFOS concentrations of the GAC/sand mixture was 182 and 198 mg/kg for Expts II-1 and II-2, respectively (Figure 3.5a). Following smouldering treatment, the soil pack (sand and ash only since GAC is eliminated) measured B.D.L. for PFOS for Expt II-1 and 0.4 mg/kg for Expt II-2 (average of triplicate samples) (Figure 3.5a). This represents 100% and 99.8% reduction of PFOS, respectively. Quantities for all of the PFAS compounds in the analytical suite for all pre- and post-treatment porous media mixtures are in Appendix L.

Phase III: PFAS-Spiked Soil

Pre-treatment $PFAS_{13}$ concentrations for the spiked soil experiments in the range 3-5 mg/kg (Figure 3.5b). Expt III-1 (blank), which excluded the PFAS contamination step, exhibited 0.003 mg/kg of PFBS and 0.009 mg/kg of PFHxS illustrating some pre-existing contamination of the purchased topsoil, however the quantity is negligible in relation to the spiked PFAS concentrations. Note the difference in the concentration axis scale from Figure 3.5a, since the pre-treatment concentrations were less than in Phase II, despite the

same spiking procedure, due to the soil having a lower sorption capacity in water relative to the GAC. Adsorption of PFAS to soil media has been shown to increase with increasing fraction organic carbon, which aligns with higher adsorption of PFAS to GAC versus soil (Higgins & Luthy, 2006). While a single spiked soil batch was used for Expts III-3, III-4, and III-5, the pre-treatment PFAS concentrations in Figure 3.5b were determined individually for each experiment. The PFAS concentrations generated in the spiked soil are representative of typical PFAS concentrations observed in field-contaminated soils (Hale et al., 2017; Houtz, Higgins, Field, & Sedlak, 2013; Sorengard, Niarchos, Jensen, & Ahrens, 2019).

In the post-treatment soils, all PFAS concentrations were B.D.L. for all experiments, except for Expt III-2 with an average PFOA concentration of 0.0003 mg/kg (Figure 3.5b). This represents 100% reduction in all six PFAS in all five experiments except for a 99.99% reduction in PFOA in Expt III-2. Note that Expt III-5 intentionally used a lower GAC concentration (15 g GAC/kg sand) in order to investigate the influence of a lower smouldering temperature (642 $\pm$ 32˚C). As indicated in Figure 3.5b, the lower peak temperature did not impact the degree of PFAS removal from the soil. Crownover et al. (2019) also found that when PFAS-contaminated soil was heated for 10 or 14 days at 350-400˚C, the PFAS removal was 98.63% to >99.999%. This is not surprising since the boiling temperatures of these six PFAS are all $\leq$ 350˚C. Additional experiments completed in this work using a small cell subjected to hot air injection (no smouldering) found that temperatures of $\approx$350˚C removed all PFAS from contaminated spiked soil (results in Appendix G).

Phase IV: PFAS-Contaminated Field Soil

Pre-treatment $PFAS_{13}$ concentrations in the field soil were lower than the artificially contaminated experiments (Figure 3.5c) but are consistent with contaminated field sites (Hale et al., 2017; Houtz et al., 2013; Sorengard et al., 2019). The same field soil was used for both experiments, thus the variability in pre-treatment $PFAS_{13}$ concentrations reveal heterogeneity within the soil (despite best attempts at homogenization). After smouldering treatment, $PFAS_{13}$ concentrations in the soil were B.Q.L. or B.D.L. for both experiments (Figure 3.5c).
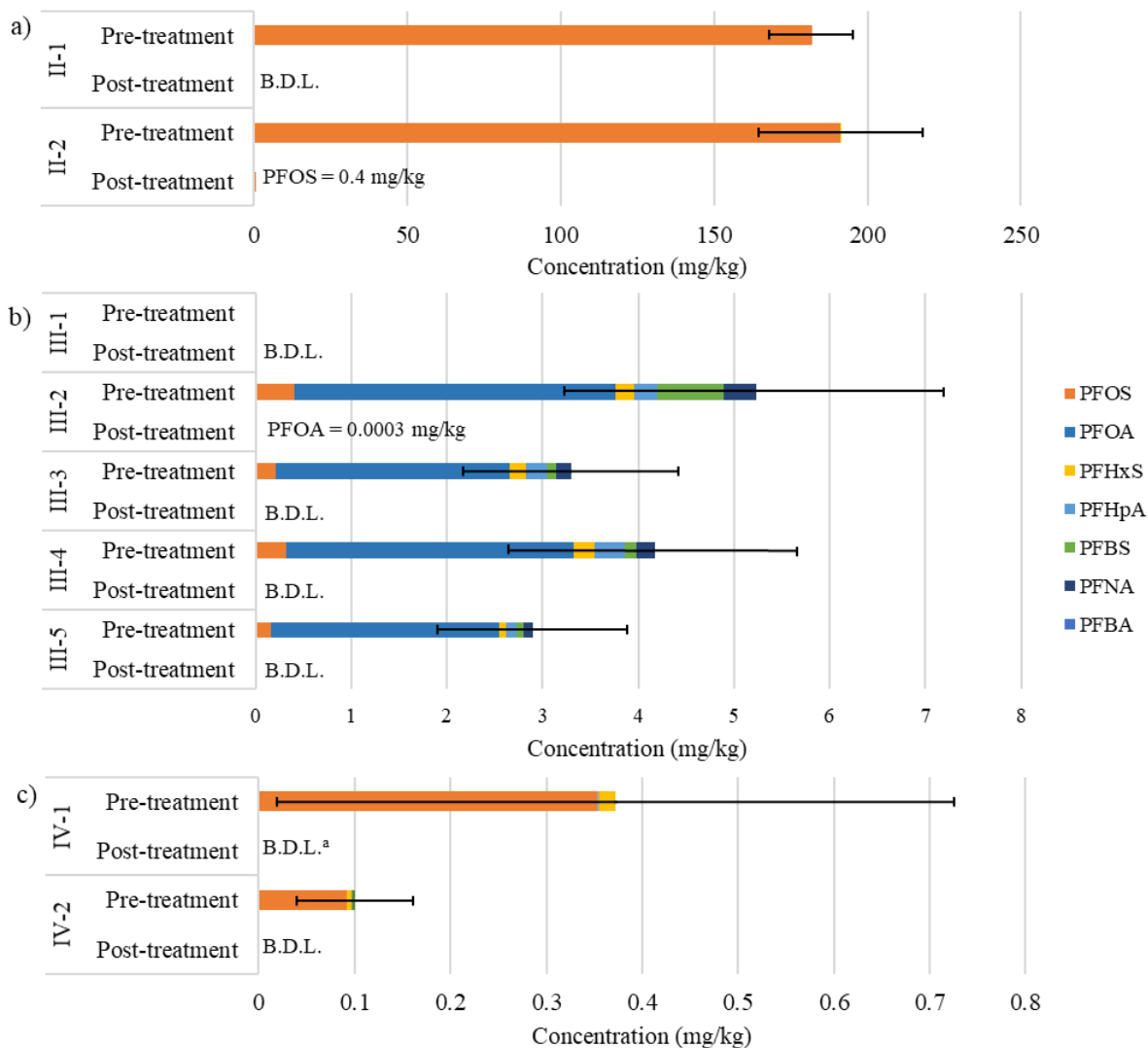
Figure 3.5: Porous media mixture pre- and post-treatment PFAS$_{13}$ concentrations for (a) Phase II: PFOS-contaminated GAC) (b) Phase III: PFAS-spiked soil, (c) Phase IV: PFAS-contaminated field soil. B.D.L. = 0.0004 mg/kg (III-2 B.D.L. = 0.0002 mg/kg), B.Q.L. = 0.001 mg/kg. Error bars represented uncertainty in cumulative PFAS concentration associated with the analytical method.

3.3.2.2. PFAS and VOFs in Emissions

For all experiments, regardless of the contaminated media used, there was very little PFAS$_{13}$ found in the emissions (Appendix N). Table 3.2 outlines that 0.81% of the fluorine originally in the smouldering column was the maximum quantified in the PFAS emissions train as PFAS within the analytical suite, for the controlled PFAS experiments (II-1 to III-

5). PFAS was predominantly found in the first XAD tube GAC and glass wool; in only a few experiments was PFAS was found in the second XAD tube and glass wool, and in those cases it was on the order of 1% of that found in the first XAD tube. No PFAS were detected in the third stage of the train (impinger containing GAC and deionized water) in any experiment, providing confidence that no PFAS breakthrough from the train occurred. All glassware used to capture emissions were rinsed with a basic methanol solution (1 % w/w using sodium hydroxide) and analyzed in Expts II-1 and III-3, and no significant PFAS concentrations were measured in any rinse solution samples. See Appendix M for full results. While Expt IV-2 provides a higher fraction of fluorine captured in Table 3.2, this value is less reliable than the rest because (a) all of the PFAS was obtained from the glass wool in the XAD tube while none was found on the GAC, and (b) the pre-treatment PFAS concentrations were so low in the field soil that such quantification in the emissions becomes difficult.

Low PFAS concentrations captured in the PFAS emissions system lead to the hypothesis that the PFAS compounds are being altered during smouldering. Several studies suggest that heat and oxidation can cause volatile organic fluorine compounds to be produced (Watanabe et al., 2016; Ross et al., 2018). Bentel et al. (2019) determined that PFAS can be altered through H/F exchange and dissociation of the functional groups. Desulfonation of PFOS has been observed to occur more readily than defluorination when using ultraviolet irradiation (Su et al., 2019). That study also demonstrated PFOS can transform into PFOA and shorter-chain perfluorinated carboxylic acids (Su et al., 2019). Indeed, in most of the experiments in this work, shorter-chain PFAS compounds with carboxyl functional groups that were not present in the pre-treatment porous media mixture

were observed in the emissions (see red items in Table 3.2). To investigate this further, GAC from the first XAD tube in Expt II-2 was re-analyzed with an expanded targeted PFAS method to include the shorter-chained compounds TFA and PFPA. Concentrations of TFA and PFPA were then found to be greater than all other PFAS in the emissions, increasing the fraction captured from 0.25% to 0.49%. This demonstrates that smouldering can breakdown the C4-C9 compounds added to the soil in this study to C2 and C3 chain lengths. Additional non-targeted, qualitative analysis using LC-MS/MS performed for Expt II-2 confirmed the occurrence of H/F exchanges occurring on PFPA, PFBA, and PFPeA. 6:2 fluoroteomer sulfonate (FTS) was also found, which could be produced by PFOS undergoing four consecutive H/F exchanges.

Those results, which used extractions from the emissions XAD GAC, are further supported with the non-targeted, qualitative analysis of emissions grab samples performed with GC-MS. 46 different fluorinated compounds, the majority of which were short-chain, were captured in the emissions samples. It is worth noting that a heating region precedes the arrival of the smouldering front throughout the reactor, since air travelling through the reaction carries heat that is deposited ahead of the front (Kinsman et al., 2017). Production of short-chain fluorinated compounds has been observed at temperatures below 900°C (Watanabe et al., 2016), and thus PFAS could be subjected to such breakdown processes in this pre-heating region. Altogether, these results support the hypothesis that the majority of the original PFAS compounds in the porous media mixture are being removed from the soil and substantially altered in the emissions during smouldering.

Table 3.2: PFAS₁₃ Compounds Pre-Treatment and Observed in PFAS Emissions Collection System

Experiment	Percent of F Captured (%)[a,b]	Blue = PFAS₁₃ in Pre-Treatment Media Red = PFAS₁₃ Observed in PFAS Emissions Collection System *(Column indicates chain length)*							
		2C	3C	4C	5C	6C	7C	8C	9C
Contaminated GAC									
Pre-treatment								PFOS	
II-1	0.25%			PFBA	PFPeA	PFHxA			
II-2	0.49 %	TFA	PFPA	PFBA	PFPeA	PFHxA	PFHpA	PFOA PFOS	
Spiked Soil									
Pre-treatment				PFBS		PFHxS	PFHpA	PFOA PFOS	PFNA
III-2	n/a[c]			PFBA	PFPeA	PFHxA	PFHpA	PFOA	
III-3	0.45%			PFBS	PFPeA		PFHpA	PFOA	
III-4	0.27%					PFHxA		PFOS	
III-5	0.81%			PFBA				PFOS	
Contaminated Field Soil									
Pre-treatment				PFBA PFBS		PFHxS		PFOS	
IV-1	n/a[c]					n/c[c]			
IV-2	19.89%			PFBA					PFNA

[a]Corrected for fraction of emissions collected during experiment.
[b]Fluorine mass balance completed considering the PFAS captured in the PFAS emissions system only.
[c]An alternative method was used to capture emissions which was found to be unreliable.

3.3.2.3.   PFAS Mineralization

Phase II: PFOS-Contaminated GAC and Phase III: PFAS-Spiked Soil

Experiments with PFOS-contaminated GAC (II-1, II-2) mineralized 41 – 46% of the

PFOS fluorine as shown by the amounts of HF captured from the emissions (Table 3.3),

demonstrating that smouldering can completely breakdown nearly half of the PFOS in the

reactor. Experiments using the PFAS-spiked soil (III-2, III-4) mineralized 16-17% of the

PFAS-derived fluorine (Table 3.3). Note that these HF values are considered to be

conservative because fluorine may be lost to mineral surfaces, reactor walls and tubing,

and other sinks which cannot be quantified. Moreover, current quantification limits of the

analytical methods required to measure fluorine on soil surfaces is greater than required for

this research. It is noted that Expt III-1 (blank) resulted in no HF generated, as expected

(Table 3.3).These results suggest that (1) the amount of PFAS volatilized in the pre-heating region, and the amount thermally decomposed into shorter-chain compounds, is less when the PFAS are sorbed to GAC than when PFAS are sorbed to soil; and (2) the fraction mineralized is higher when PFAS are sorbed to GAC than sorbed to soil. It is hypothesized that these effects are due to several causes. First, PFAS sorbs more strongly to GAC than to soil. Studies have demonstrated that PFAS is highly resistant to desorption from GAC (Du et al., 2014). This strong sorption would limit the amount of PFAS volatilized in the pre-heating region. Second, it is expected that PFAS compounds on the GAC would experience higher temperatures than those sorbed to soil. The temperatures recorded by the thermocouples ($\approx$1000°C, Table 3.1) are an average of the material near the thermocouple probe tip, and thus represent an average of the inert sand and soil (heat sinks) and oxidizing GAC (heat source) in the tip's vicinity. Recall that there is much more sand than GAC at any given location ($\approx$45 g GAC/kg sand). Thus the GAC, and the PFOS sorbed to it, are likely experiencing temperatures significantly exceeding 1000°C while the sand/soil adjacent are likely experiencing $\approx$1000°C.

This hypothesis is further supported by the result of Expt III-5, which repeated Expts III-2 to III-4 but had a peak temperature of 642°C instead of $\approx$1000°C (due to lower concentration of GAC). This experiment resulted in soil free from $PFAS_{13}$ (Figure 3.5b) but produced no HF in the emissions (Table 3.3). This suggests that such temperatures are sufficient for volatilizing and thermally degrading PFAS to smaller-chained compounds (Table 3.3) but not sufficient to mineralize any PFAS. Note that the high uncertainty in the fluorine captured as HF reported in Table 3.3 is due to the inherent uncertainty with the

pre-treatment PFAS concentrations. HF losses may also occur if HF adheres to the sand, the walls of the smouldering column, or the copper tubing used for the HF emissions train.

Phase IV: PFAS-Contaminated Field Soil

Table 3.3 reveals that for the field soil, more HF was produced than would be expected based on the $PFAS_{13}$ measured in the pre-treatment field soil. It is hypothesized that there are significant additional fluorinated compounds, including PFAS, in the soil which are beyond analytical coverage. Furthermore, the concentrations of PFAS quantified in this field soil are small compared to the spiked soil and impregnated GAC. As a result, minor amounts of other PFAS could cause large discrepancies in the fluorine mass balance. Nevertheless, it seems reasonable to conclude that a substantial degree of mineralization occurred in these samples.

Table 3.3: Summary of HF Captured

Experiment	Mass of HF Captured (mg HF)	F Captured as HF (%)[a]
Contaminated GAC		
II-1	17.2	45.7 ± 4.1
II-2	15.5	40.6 ± 5.9
Spiked Soil		
III-1 (Blank)	B.D.L.	0.0
III-2	0.0951	16.6 ± 14.7
III-3[b]	-	-
III-4	0.106	16.1 ± 14.2
III-5	B.D.L.	0.0
Contaminated Field Soil		
IV-1	0.195	577.0 ± 1403.8
IV-2	0.259	2438.1 ± 4069.2

[a]Corrected for fraction of emissions collected during experiment.
[b]HF was not measured during this experiment due to a malfunction in the emissions capture system.

3.3.2.4.   Total Organic Fluorine (TOF)

Phase II: PFOS-Contaminated GAC

TOF concentrations of the PFOS-contaminated GAC for Expts II-1 and II-2 were within 18% and 35%, respectively, of the determined PFOS concentrations (data in Table 3.4 and Figure 3.5). Note that in Table 3.4 the TOF and PFAS$_{13}$ subsample concentrations have been upscaled by the mass of material they represent to provide estimated the total mass of fluorine in each compartment. This is a reasonable mass balance and suggests that in simple systems such as PFOS-loaded GAC, TOF can be a useful metric. Table 3.4 further reveals that negligible organic fluorine remains in the post-treatment sand after smouldering. This confirms the earlier conclusions that the sand was free of PFAS following treatment (Figure 3.5).

There was high capture of organic fluorine in the emissions train relative to the starting PFOS concentration on the GAC. The majority of the TOF was located in the first XAD tube GAC with negligible amounts in the second XAD tube and the impinger. Thus, TOF results confirmed no breakthrough of fluorinated compounds occurred in the sample train. Overall, when back-calculated to adjust for the fraction of emissions sampled, an estimated 712 mg of total organic fluorine was observed in the emissions of Expt II-2 (Table 3.4). This is significantly greater than the 5.56 mg fluorine associated with the PFAS analytical suite. The TOF results confirm the presence of altered, likely shorter-chain, fluorinated organic compounds in the emissions.

Phase III: PFAS-Spiked Soil and Phase IV: PFAS-Contaminated Field Soil

Pre-treatment TOF results indicated the majority of fluorine existed in the spiked soil and field soil from sources other than PFAS (Table 3.4). Studies have shown that is it

common for uncontaminated soils to have concentrations of 133-617 mg fluorine per kg soil (Chavoshi et al., 2011; Loganathan, Gray, Hedley, & Roberts, 2006). These organic fluorine compounds were present in the topsoil (i.e., organic) fraction of the assembled spiked soil. Moreover, post-treatment soil samples indicated that the majority of this organic fluorine remained after smouldering (Table 3.4). It is further noted that Expt III-1 (blank) also exhibited a similarly large pre-treatment TOF concentration, and this TOF was unaffected by treatment. As discussed above, no HF was produced in either Expt III-1 (blank) or Expt III-5 (low temperature); therefore, the organic fluorine naturally present in the soil was not mineralized and did not contribute to the HF captured in the Phase III experiments. Altogether, these results demonstrate that the spiked soil contains organic fluorine which is not PFAS and which mostly remains in the soil despite smouldering. However, the small change in total organic fluorine due to smouldering was nevertheless greater than the fluorine mass associated with the PFAS eliminated from the soil, indicating that either (1) some of the naturally occurring organic fluorine in the soil may be reacting during the experiment, or (2) there were additional PFAS present beyond what was intentionally added and beyond analytical coverage that were removed. Moreover, it suggests the surprising conclusion that the TOF analytical method, which is based on combustion, can remove organic fluorine compounds at $\approx 1000°C$ that smouldering at that temperature does not. This may be related to the complete combustion of 0.2 g sample that is achieved in TOF compared to the incomplete combustion in a heterogeneous porous media mixture that occurs in a smouldering reactor. Further methods are being explored to measure any fluorine, which may remain on the soil, that would not be measured during TOF analysis.

Less total organic fluorine was captured in the emissions for the spiked soil and field soil experiments than the PFAS-loaded GAC experiments (Table 3.4), which correlates to the reduced amount of PFAS present in the soil before treatment. The organic fluorine captured was primarily in the first XAD tube GAC, with smaller amounts in the second XAD tube, and negligible amounts in the impinger; this agrees with the PFAS analytical results and supports the conclusion that no fluorinated compounds achieved breakthrough of the emissions capture system. TOF results quantified considerably more fluorine in emissions than in the PFAS analysis (Table 3.4), which supports the hypothesis that the fraction of PFAS in the porous media mixture that was not mineralized were predominantly emitted as shorter-chained fluorinated compounds that are beyond current analytical capabilities.

Table 3.4: TOF-Determined Fluorine Masses in Soil and Emissions

Experiment[a]	Pre-Treatment		Post-Treatment		Captured in Emissions System[b]	
	TOF (mg F)	PFAS$_{13}$ (mg F)	TOF (mg F)	PFAS$_{13}$ (mg F)	TOF (mg F)	PFAS$_{13}$ (mg F)
Contaminated GAC						
II-1	1021.3	845.8	17.2	0.0	n/a[c]	0.959
II-2	689.9	971.5	8.0	1.8	712	5.56
Spiked Soil						
III-1 (blank)	119.8	0.03	130.4	0.0	8.64	n/a[d]
III-4	146.5	16.5	99.2	0.0	21.6	0.044
III-5	188.6	12.8	106.4	0.0	12.2	0.107
Contaminated Field Soil						
IV-2	1295.8	0.3	941.4	0.0	27.8	0.065

[a]TOF samples were not collected for III-2, III-3, and IV-1.
[b]Corrected for fraction of emissions collected during experiment.
[c]Emissions samples were not analyzed using same procedure as other experiments.
[d]XAD and impinger GAC were not analyzed for this experiment.

Challenges with Using TOF for Fluorine Mass Balance

Numerous challenges were noted while attempting to complete a fluorine mass balance using the TOF results. First, there was considerable variability in the TOF concentrations:

a 30% difference was not unusual in replicate TOF subsamples from the same experimental (homogenized) subsample (porous media mixture or XAD GAC). This is likely related to the small (0.2 g) sample size used in TOF, which may quantify a level of heterogeneity that is not representative of the bulk sample. While this could be overcome by either (1) submitting many more subsamples for analysis, or (2) developing a TOF method that uses larger samples, the cost and capabilities of TOF at a commercial laboratory prevented either of these options for this study. As a result, the quantitative values of TOF presented are associated with large degree of uncertainty.

A second challenge was the high background organic fluorine concentrations in the spiked and field soils. These concentrations far exceed the organic fluorine from the laboratory-spiked or field-contaminated PFAS contamination, creating a small signal to noise ratio. For the field soil, it was particularly challenging to discern between the organic fluorine that was naturally occurring and that contributed from the PFAS contamination.

Note that no soluble fluorine was found in the pre-treatment or post-treatment samples for Expts III-4, III-5, IV-1, and IV-2 (Appendix O). Further research is required to identify the naturally occurring organic fluorine compounds in the soil.

3.4. Environmental Significance

New remediation technologies are needed for treating PFAS-contaminated water and soil. GAC is frequently used to treat water, however, there are challenges with disposal once it is saturated. Landfilling PFAS-contaminated soils has become restricted due to increasingly stringent regulations. Meanwhile, incineration is energy/carbon/cost intensive, since it requires continuous additions of fuel (e.g., diesel), and GAC is problematic for incinerators. This study reveals that smouldering of PFAS-contaminated

soil mixed with fresh or PFAS-loaded GAC may be an effective treatment option. Smouldering at any temperature above approximately 350˚C is expected to remove the PFAS from the soil. Using GAC concentrations in the porous media mixture above 40 g/kg will ensure that smouldering temperatures exceed 900˚C and that some of the PFAS is mineralized, captured as HF in the emissions. Moreover, the fraction of PFAS mineralized is close to 50% if the PFAS is sorbed on the GAC instead of the soil. The PFAS that is not mineralized is predominantly transformed into shorter-chained PFAS and a variety of fluorinated compounds that are effectively captured on GAC in the emissions scrubbing system. Once the GAC from the emissions scrubbing system is saturated, it could then be used as the surrogate fuel to treat more PFAS-contaminated soil.

It is reasonable to suspect that the fraction of PFAS mineralized can be improved with efforts to optimize the system, such as higher GAC concentrations to achieve higher temperatures in the soil or lower air fluxes to minimize volatilization in the pre-heating region. This work suggests that an effective approach might be a sequential process of (1) low temperature smouldering to drive all PFAS out of the soil and concentrate it as a variety of fluorinated compounds on GAC in the emissions scrubbing system, followed by (2) high temperature smouldering treatment of this GAC to mineralize the fluorine. Because smouldering uses no external energy after ignition, a large ex situ batch treatment system or a smaller continuous treatment reactor could be a very economical way to destroy the PFAS present in large volumes of soil or water. While transforming PFAS in soil and GAC into HF emissions represent success, it is acknowledged that HF needs to be carefully managed; however, numerous approaches are available for removing HF from incinerator emissions.

3.5. References

3M. The Science of organic fluorochemistry. AR226-0527; 1999.

Aly, Y.H., McInnis, D.P., Lombardo, S.M., Arnold, W.A., Pennell, K.D., Hatton, J., & Simcik, M.F. (2019). Enhanced adsorption of perfluoro alkyl substances for in situ remediation. *Environmental Science: Water Research & Technology, 5,* 1867-1875. doi: 10.1039/c9ew00426b

Baud, G., Salvador, S., Debenest, G., & Thovert, J.-F. New Granular Model Medium to Investigate Smouldering Fronts Propagation – Experiments. *Energy & Fuels, 29*(10), 6780-6792. doi: 10.1021/acs.energyfuels.5b01325

Bentel, M.J., Yu, Y., Xu, L., Li, Z., Wong, B.M., Men, Y., & Liu, J. (2019). Defluorination of Per- and Polyfluoroalkyl Substances (PFASs) with Hydrated Electrons: Structural Dependence and Implications to PFAS Remediation and Management. *Environmental Science & Technology, 53*(7), 3718-3728. doi: 10.1021/acs.est.8b06648

Brusseau, M.L. (2018). Assessing the potential contributions of additional retention processes to PFAS retardation in the subsurface. *Science of the Total Environment, 613-614,* 176-185. doi: 10.1016/j.scitotenv.2017.09.065

Buck, R.C., Franklin, J., Berger, U., Conder, J.M., Cousins, I.T., de Voogt, P., Jensen, A.A., Kannan, K., Mabury, S.A., & van Leeuwen, S.P. (2011). Perfluoroalkyl and Polyfluoroalkyl Substances in the Environment: Terminology, Classification, and Origins. *Integrated Environmental Assessment and Management, 7*(4), 513-541. doi: 10.1002/ieam.258

Cai, M., Yang, H., Xie, Z., Zhao, Z., Wang, F., Lu, Z., Sturm, R., & Ebinghaus, R. (2012). Per- and polyfluoroalkyl substances in snow, lake, surface runoff water and coastal seawater in Fildes Peninsula, King George Island, Antarctica. *Journal of Hazardous Materials, 209-210,* 335-342. doi: 10.1016/j.jhazmat.2012.01.030

Chavoshi, E., Afyuni, M., Hajabbasi, M.A., Khoshgoftarmanesh, A.H., Abbaspour, K.C., Shariatmadari, H., & Mirghafari, N. (2011). Health Risk Assessment of Fluoride Exposure in Soil, Plants, and Water at Isfahan, Iran. *Human and Ecological Risk Assessment, 17*(2), 414-430. doi: 10.1080/10807039.2011.552397

Cousins, I.T., Vestergren, R., Wang, Z., Scheringer, M., & McLachlan, M.S. (2016). The precautionary principle and chemicals management: The example of perfluoroalkyl acids in groundwater. *Environment International, 94,* 331-340. doi: 10.1016/j.envint.2016.04.044

Crone, B.C., Speth, T.F., Wahman, D.G., Smith, S.J., Abulikemu, G., Kleiner, E.J., Pressman, J.G. (2019). Occurance of per- and polyfluoroalkyl substances (PFAS) in source water and their treatment in drinking water. *Critical Reviews in Environmental Science and Technology, 49*(24), 2359-2396. doi: 10.1080/10643389.2019.1614848

Crownover, E., Oberle, D., Kluger, M., & Heron, G. (2019). Perfluoroalkyl and polyfluoroalkyl substances thermal desorption evaluation. *Remediation, 29*(4), 77-81. doi: 10.1002/rem.21623

Department of Health Australia. (16 September 2019). *Health Based Guidance Values for Per- and Polyfluoroalkyl Substances (PFAS).* https://www1.health.gov.au/internet/main/publishing.nsf/Content/ohp-pfas-hbgv.htm

Dorrance, L.R., Kellogg, S., Love, A.H. (2017). What You Should Know About Per- and Polyfluoroalkyl Substances (PFAS) for Environmental Claims. *Environmental Claims Journal, 29*(4), 290-304. doi: 10.1080/10406026.2017.1377015

Du, Z., Deng, S., Bei, Y., Huang, Q., Wang, B., Huang, J., & Yu, G. (2014). Adsorption behaviour and mechanism of perfluoinated compounds on various adsorbents – A review. *Journal of Hazardous Materials, 274,* 443-454. doi: 10.1016/j.jhazmat.2014.04.038

Environment and Climate Change Canada. (2017). *Federal Environmental Quality Guidelines: Perfluorooctane Sulfonate (PFOS).*

Espana V.A.A., Mallavarapu, M., & Naidu, R. (2015). Treatment technologies for aqueous perfluorooctanesulfonate (PFOS) and perfluorooctanoate (PFOA): A critical review with an emphasis on field testing. *Environmental Technology & Innovation,* 4, 168-181. doi: 10.1016/j.eti.2015.06.001

Gianfelice, G., Della Zassa, M., Biasin, A., & Canu B.P. (2019). Onset and propagation of smouldering in pine bark controlled by addition of inert solids. *Renewable Energy, 132,* 596-614. doi: 10.1016/j.renene.2018.08.028

Grant, G.P., Major, D., Scholes, G.C., Horst, J., Hill, S., Klemmer, M.R., & Couch, J.N. (2016). Smoldering Combustion (STAR) for the Treatment of Contaminated Soils: Examining Limitations and Defining Success. *Remediation Journal, 26*(3), 27-51. doi: 10.1002/rem.21468

Hale, S.E., Arp, H.P.H., Slinde, G.A., Wade, E.J., Bjørseth, Breedveld, G.D., Straith, B.F., Moe, K.G., Jartun, M., & Høisæter, Å. (2017). Sorbent amendment as a remediation strategy to reduce PFAS mobility and leaching in a contaminated sandy soil from a Norwegian firefighting training facility. *Chemosphere, 171,* 9-18. doi: 10.1016/j.chemosphere.2016.12.057

Health Canada. (2019, April). *Water Talk – Perfluoroalkylated substances in drinking water.* Retrieved January 7, 2020, form https://www.canada.ca/en/services/health/publications/healthy-living/water-talk-drinking-water-screening-values-perfluoroalkylated-substances.html

Higgins, C. P., & Luthy, R. G. (2006). Sorption of Perfluorinated Surfactants on Sediments. *Environmental Science & Technology, 40*(23), 7251–7256. doi: 10.1021/es061000n

Houtz, E.F., Higgins, C.P., Field, J.A., & Sedlak, D.L. (2013). Persistence of Perfluoroalkyl Acid   Precursors in AFFF-Impacted Groundwater and Soil. *Environmental Science & Technology, 47*(15), 8187-8195. doi: 10.1021/es4018877

Hu, X.C., Andrews, D.Q., Lindstrom, A.B., Bruton, T.A., Schaider, L.A., Grandjean, P., Lohmann, R., Carignan, C.C., Blum, A., Balan, S.A., Higgins, C.P., & Sunderland, E.M. (2016). Detection of Poly- and Perfluoroalkyl Substances

(PFASs) in U.S. Drinking Water Linked to Industrial Sites, Military Fire Training Areas, and Wastewater Treatment Plants. *Environmental Science & Technology Letters, 3*(10), 344-350. doi: 10.1021/acs.estlett.6b00260

Inoue, K., Okada, F., Ito, R., Kato, S., Sasaki, S., Nakajima, S., Uno, A., Saijo, Y., Sata, F., Yoshimura, Y., Kishi, R., & Nakazawa, N. (2004). Perfluorooctane Sulfonate (PFOS) and Related Perfluorinated Compounds in Human Maternal and Cord Blood Samples: Assessment of PFOS Exposure in Susceptible Population during Pregnancy. *Environmental Health Perspectives, 112*(11), 1204-1207. doi: 10.1289/ehp.6864

Jin, L., & Zhang, P. (2015). Photochemical decomposition of perfluorooctance sulfonate (PFOS) in an anoxic solution by 185 nm vacuum ultraviolet. *Chemical Engineering Journal, 280,* 241-247. doi: 10.1016/j.cej.2015.06.022

Kinsman, L., Torero, J.L., & Gerhard, J.I. (2017). Organic liquid mobility induced by smoldering remediation. *Journal of Hazardous Materials, 325,* 101-112. doi: 10.1016/j.jhazmat.2016.11.049

Kissa, E. (2001). *Fluorinated Surfactants and Repellants* (2nd ed.). New York, NY: Marcel Dekker, Inc.

Kucharzyk, K.H., Darlington, R., Benotti, M., Deeb, R., & Hawley, E. (2017). Novel treatment technologies for PFAS compounds: A critical review. *Journal of Environmental Management, 204,* 757-764. doi: 10.1016/j.jenvman.2017.08.016

Kuroda, K., Murakami, M., Oguma, K., Takada, H., & Takizawa, S. (2014). Investigating sources and pathways of perfluoroalkyl acid (PFAAs) in aquifers in Tokyo using multiple tracers. *Science of the Total Environment, 488-489,* 51-60. doi: 10.1016/j.scitotenv.2014.04.066

Loganathan, P., Gray, C.W., Hedley, M.J., & Roberts, A.H.C. (2006). Total and soluble fluorine concentrations in relation to properties of soils in New Zealand. *European Journal of Soil Science, 57*(3)*,* 411-421. doi: 10.1111/j.1365-2389.2005.00751.x

Mahinroosta, R., & Senevirathna, L. (2020). A review of emerging treatment technologies for PFAS contaminated soils. *Journal of Environmental Management, 255,* 1-12. doi: 10.1016/j.jenvman.2019.109896

Martins, M.F., Salvador, S., Thovert, J.-F., & Debenest, G. (2010). Co-current combustion of oil shale – Part 2: Structure of the combustion front. *Fuel, 89*(1), 133-143. doi: 10.1016/j.fuel.2009.06.040

Milley, S.A., Koch, I., Fortin, P., Archer, J., Reynolds, D., Weber, K.P. (2018). Estimating the number of airports potentially contaminated with perfluoroalkyl and polyfluoroalkyl substances from aqueous film forming foam: A Canadian example. *Journal of Environmental Management, 222,* 122-131. doi: 10.1016/j.jenvman.2018.05.028

Ohlemiller, T.J. (1985). Modeling of smoldering combustion propagation. *Progress in Energy and Combustion Science, 11*(4), 277-310. doi: 10.1016/0360-1285(85)90004-8

Ohlemiller, T.J. (2002). Smoldering Combustion. In P.J. DiNenno, D. Drysdale, W.D. Walton, R.L.P. Custer, J.R. Hall Jr., & J.M. Watts Jr. (Eds.), *SFPE Handbook of Fire Protection Engineering (3rd ed.)* (pp. 200-210). Quincy, Massachusetts: National Fire Protection Association

Pabon, M., & Corpart J.M. (2002). Fluorinated surfactants: synthesis, properties, effluent treatment. *Journal of Fluorine Chemistry, 114*(2)*,* 149-156. doi: 10.1016/S0022-1139(02)00038-6

Paul, A.G., Jones, K.C., & Sweetman, A.J. (2009). A First Global Production, Emissions, and Environmental Inventory For Perfluorooctane Sulfonate. *Environmental Science & Technology, 43*(2), 386-392. doi: 10.1021/es802216n

Pironi, P., Switzer, C., Gerhard, J.I., Rein, G., & Torero, J.L. (2011). Self-Sustaining Smoldering Combustion for NAPL Remediation: Laboratory Evaluation of Process Sensitivity to Key Parameters. *Environmental Science & Technology, 45*(7), 2980-2986. doi: 10.1021/es102969z

Rayne, S., & Forest, K. (2009). Perfluoroalkyl sulfonic and carboxylic acids: A critical review of physiochemical properties, levels and patterns in waters and wastewaters, and treatment methods. *Journal of Environmental Science and Health Part A, 44*(12), 1145-1199. doi: 10.1080/10934520903139811

Ross, I., McDonough, J., Miles, J., Storch, P., Kochunarayanan, P.T., Kalve, E., Hurst, J., Dasgupta, S.S., & Burdick, J. (2018). A review of emerging technologies for remediation of PFASs. *Remediation Journal, 28*(2), 101-126. doi: 10.1002/rem.21553

Sabadell, G., Scholes, G., Thomas, D., Murray, C., Bireta, P., Grant, G., & Major, D. Ex Situ Treatment of Organic Wastes or Oil-Impacted Soil using a Smoldering Process. *Waste Management and the Environment IX, 231*(10), 367-376. doi: 10.2495/WM180341

Salman, M., Gerhard, J.I., Major, D.W., Pironi, P., & Hadden, R. (2015). Remediation of trichloroethylene-contaminated soils by star technology using vegetable oil smoldering. *Journal of Hazardous Materials, 285,* 346-355. doi: 10.1016/j.jhazmat.2014.11.042

Schaefer, C.E., Andaya, C., Urtiaga, A., McKenzie, E.R., & Higgins, C.P. (2015). Electrochemical treatment of perfluorooctanoic acid (PFOA) and perfluorooctane sulfonic acid (PFOS) in groundwater impacted by aqueous film forming foams (AFFFs). *Journal of Hazardous Materials, 295,* 170-175. doi: 10.1016/j.jhazmat.2015.04.024

Schaider, L.A., Balan, S.A., Blum, A., Andrews, D.Q., Strynar, M.J., Dickinson, M.E., Lunderberg, D.M., Lang, J.R., & Peaslee, G.F. (2017). Fluroinated Compounds in U.S. Fast Food Packaging. *Environmental Science & Technology Letters, 4*(3), 105-111. doi: 10.1021/acs.estlett.6b00435

Scholes, G.C., Gerhard, J.I., Grant, G.P., Major, D.W., Vidumsky, J.E., Switzer, C., & Torero, J.L. (2015). Smoldering Remediation of Coal-Tar-Contaminated Soil: Pilot Field Tests of STAR. *Environmental Science & Technology, 49*(24), 14334-14342. doi: 10.1021/acs.est.5b03177

SGS. (2018, September). *Physical and Chemical Properties of PFAS Compounds.* Retrieved May 31, 2019, from https://www.sgs-ehsusa.com/wp-content/uploads/2018/09/Physical-and-Chemical-Properties-of-PFAS-compounds_vKFMH.pdf

Solinger, R., Grant, G.P., Scholes, G.C., Murray, C., & Gerhard, J.I. (2020). STARx Hottpad for smoldering treatment of waste oil sludge: Proof of concept and sensitivity to key design parameters. *Journal of Waste Management & Research.* doi: 10.1177/0734242X20904430

Sörengård, M., Niarchos, G., Jensen, P.E., & Ahrens, L. (2019). Electrodialytic per- and polyfluoroalkyl substances (PFASs) removal mechanism for contaminated soil. *Chemosphere, 232,* 224-231. doi: 10.1016/j.chemosphere.2019.05.088

Su, Y., Rao, U., Khor, C.M., Jensen, M.G., Teesch, L.M., Wong, B.M., Cwiertny, D.M., & Jassby, D. (2019). Potential-Driven Electron Transfer Lowers the Dissociation Energy of the C-F Bond and Facilitates Reductive Defluorination of Perfluorooctane Sulfonate (PFOS). *Applied Materials & Interfaces, 11,* 33913-33922. doi: 10.1021/acsami.9b10449

Switzer, C., Pironi, P., Gerhard, J.I., Rein, G., & Torero, J.L. (2009). Self-Sustaining Smoldering Combustion: A Novel Remediation Process for Non-Aqueous-Phase Liquids in Porous Media. *Environmental Science & Technology, 43,* 5871-5877. doi: 10.1021/es803483s

Switzer, C., Pironi, P., Gerhard, J.I., Rein, G., & Torero, J.L. (2014). Volumetric scale-up of smouldering remediation of contaminated materials. *Journal of Hazardous Materials, 268,* 51-60. doi: 10.1016/j.jhazmat.2013.11.053

Trautmann, A.M., Schell, H., Schmidt, K.R., Mangold, K.M. & Tiehm, A. (2015). Electrochemical degradation of perfluoroalkyl and polyfluoroalkyl substances (PFASs) in groundwater. *Water Science & Technology, 71*(10), 1569-1575. doi: 10.2166/wst.2015.143

Trojanowicz, M., Bojanowska-Czajka, A., Bartosiewicz, I., & Kulisa, K. (2018). Advanced Oxidation/Reduction Processes treatment for aqueous perfluorooctanoate (PFOA) and perfluorooctanesulfonate (PFOS) – A review of recent advances. *Chemical Engineering Journal, 336,* 170-199. doi: 10.1016/j.cej.2017.10.153

Wang, F., Lu, X., Li, X., & Shih, K. (2015). Effectiveness and Mechanisms of Defluorination of Perfluorinated Alkyl Substances by Calcium Compounds during Waste Thermal Treatment. *Environmental Science & Technology, 45 (9),* 5672-5680. doi: 10.1021/es506234b

Watanabe, N., Takata, M., Takemine, S., & Yamamoto, K. (2016). Residual organic fluorinated compounds from thermal treatment of PFOA, PFHxA and PFOS adsorbed onto granular activated carbon (GAC). *Journal of Material Cycles and Waste Management, 18,* 625-630. doi: 10.1007/s10163-016-0532-x

Yamada, T., Taylor, P.H., Buck, R.C., Kaiser, M.A., Giraud, R.J. (2005). Thermal degradation of fluorotelomer treated articles and related materials. *Chemosphere, 61,* 974-984. doi: 10.1016/j.chemosphere.2005.03.025

Yermán, L., Hadden, R.M., Carrascal, J., Fabris, I., Cormier, D., Torero, J.L., Gerhard, J.I., Krajcovic, M., Pironi, P., & Cheng, Y.-L. (2015). Smouldering combustion as a treatment technology for faeces: Exploring the parameter space. *Fuel, 147,* 108-116. doi: 10.1016/j.fuel.2015.01.055

Young, C.J., Furdui, V.I., Franklin, J., Koerner, R.M., Muir, D.C.G., & Mabury, S.A. (2007). Perfluorinated Acids in Arctic Snow: New Evidence for Atmospheric Formation. *Environmental Science & Technology, 41*(10)*,* 3455-3461. doi: 10.1021/es0626234

Zanoni, M.A.B., Torero, J.L., & Gerhard, J.I. (2019). Delineating and explaining the limits of self-sustained smouldering combustion. *Combustion and Flame, 201,* 78-92. doi: 10.1016/j.combustflame.2018.12.00

Chapter 4

Conclusions and Recommendations

4.1. Conclusions

This thesis focused on the application of STAR as a remediation technique for soil and GAC contaminated with PFAS. A series of laboratory experiments were first conducted to understand the influence of the GAC concentration and air flux on the smouldering temperatures and velocities. Laboratory experiments were then completed with three types of contaminated media; (i) PFAS-saturated GAC and sand, (ii) PFAS-contaminated topsoil with sand and GAC, and (iii) PFAS-contaminated field soil and GAC. Post-treatment sampling from these experiments were used to the assess the ability of smouldering combustion to remediate the contaminated media used. There are limited options available for quantifying and identifying PFAS compounds in soil or liquid samples and there are no accepted methods for identifying or quantifying compounds released in emissions. New methods were developed for this research to identify and quantify, when possible, the compounds in the emissions. This research presents, to date, one of the most comprehensive studies for fluorine mass balance of PFAS undergoing thermal remediation.

Smouldering temperatures can be controlled by selecting the corresponding GAC concentration. GAC concentrations greater than 50g GAC/kg sand will achieve temperatures above 900˚C. Air flux and smouldering velocity were found to be linearly related, allowing the operator to control the rate of mass destruction by adjusting the air flux. Smouldering remediation achieved ≥99.9% reduction of PFAS, this applied to contaminated GAC, spiked soil, or field soil, covering a wide range of PFAS

concentrations. Post-treatment results demonstrated STAR's potential as a remediation option for PFAS-contaminated soil and GAC.

PFAS mineralization will occur when smouldering temperatures exceed 900°C. A higher degree of mineralization occurred when PFAS is sorbed to GAC than soil. No mineralization occurred when peak temperatures were below 700°C, proving that lower temperatures can remove PFAS from the soils but temperatures greater than 900°C are required to thermally degrade PFAS. Hydrofluoric acid captured in the field soil experiments suggested there are additional PFAS in the soil that cannot be identified using current analytical methods.

PFAS emissions results indicated PFAS are being altered during smouldering. Chain shortening and hydrogen/fluorine exchanges both occurred during smouldering remediation. Non-targeted analysis demonstrated a wide variety of shorter-chain fluorinated products are formed during smouldering. Total Organic Fluorine analysis was shown to be valuable for analyzing the fate of PFOS on GAC but was demonstrated to be problematic when used for PFAS-contaminated soil due to interferences from other sources of fluorine.

In summary, experiments demonstrated GAC is an excellent smouldering fuel because temperatures greater than 900°C could be easily reached. PFAS were removed from the three types of contaminated media with a fraction of the PFAS being completely mineralized. Overall, STAR is a promising remediation option for soils and GAC, which have been contaminated by PFAS.

4.2. Recommendations

This research was an initial investigation on the ability for smouldering to treat PFAS-contaminated soils and PFAS-impacted GAC. All research for this work was completed in controlled laboratory experiments, which is only the beginning for full-scale remediation efforts. As a result, there are numerous questions which require additional research.

The following is recommended:

- Improving the HF capture system by replacing copper tubing with Inconel. This change would confirm that no HF is being lost due to corrosion.

- Continue analysis to quantify and identify the shorter-chain fluorinated compounds that are produced during smouldering. Quantifying the concentrations of the compounds will help provide a more complete understanding of the fluorine mass balance.

- Identify the natural fluorine in the topsoil and field soil. This would assist with the understanding TOF results and the influence the naturally occurring fluorine may have on the fluorine mass balance.

- Explore options to increase the mineralization of PFAS compounds. Research suggests increasing the temperature of the emissions or condition the porous media mixture could promote PFAS mineralization. This would minimize the production of undesirable fluorinated by-products.

- Explore the ability for STAR to treat contaminated soils and GAC at larger scales. Completing a series of experiments at a pilot-scale would help to better

understand the ability for STAR to be used as a full-scale remediation option for

PFAS-contaminated soils and GAC.

Appendices
Appendix A: Spiked Soil Grain Size Distribution
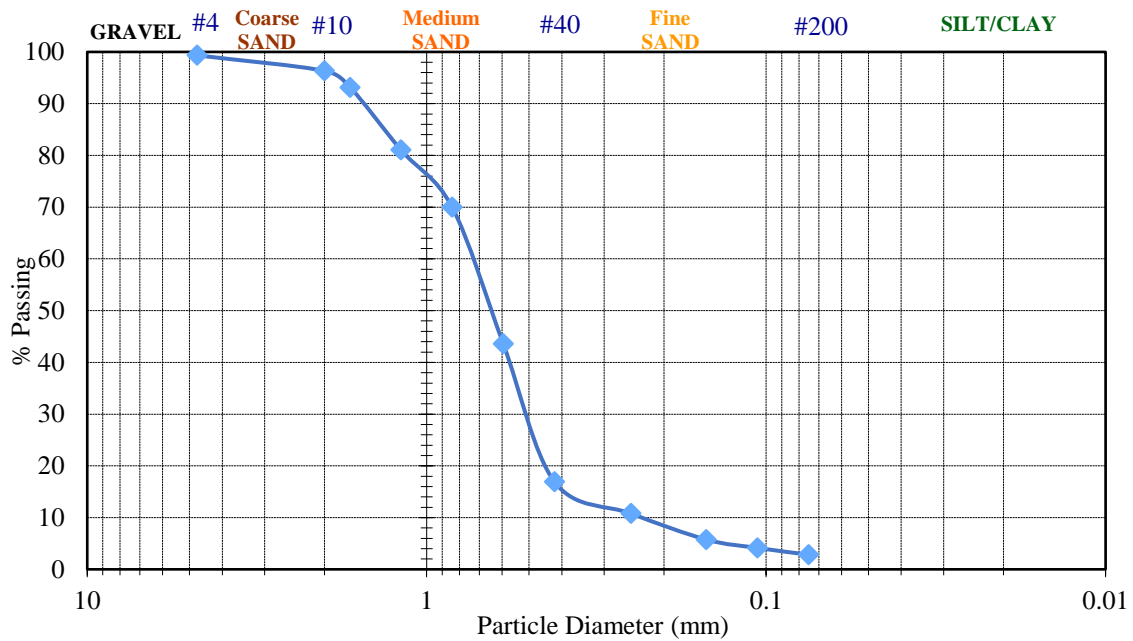
Figure A.1: Approximate grain size distribution curve for soil and sand mixture used for spiked soil smouldering experiments.

Appendix B: PFAS Stock Solution

Stock solution and GAC PFOS concentrations were measured for Expts II-1 and II-2. To compare the samples, stock solution and GAC samples were collected from one bottle (Table B.1). The PFOS concentration measured for II-2 on the GAC was greater than the mass of PFOS added to the stock solution bottles and therefore was determined to be unreliable. As a result, the stock solution samples were used to calculate the pre-treatment PFOS concentrations for II-1 and II-2.

Table B.1: Comparison of PFOS Concentrations Using Stock Solution and GAC Extraction

Experiment	Stock Solution Concentration (mg PFOS/bottle)	GAC Extraction Concentration (mg PFOS/bottle)
II-1	170.6	187.3
II-2	144.7	201.6

Three PFAS (PFOS, PFOA, and PFHxS) were used for the stock solution in experiments S-1 and S-2. PFAS masses were determined initially by using masses below the solubility values (Table B.2). In each bottle, approximately 0.6460 g PFOA, 0.0988 g PFOS, and 0.2660 g of PFHxS were added to each 1L polypropylene bottle (Table B.3). 950 mL of deionized water was added to each bottle. The remainder of the procedure complied with Section 3.2.3.1.

For experiment S-3, PFOA, PFOS, and PFHxS were used to create the stock solution and were added in concentrations of 20% of their solubility. All other PFAS-contaminated soil experiments used the three initial PFAS and Table B.3 outlines the amounts of each PFAS compound used to create the stock solutions for experiments PFAS-contaminated soil experiments. After the addition of PFAS, deionized water was added to create 15 L of stock solution for each experiment. The carboy was agitated periodically over a 48-hour

period to ensure the PFAS had dissolved. For experiments S-3 and S-4, 2.3 kg of the dried, sieved topsoil was then added to the carboy and was agitated periodically over an additional 96-hour period.

Table B.2: PFAS Solubility Values

	PFBS (g/L)	PFHpA (g/L)	PFHxS (g/L)	PFOA (g/L)	PFNA (g/L)	PFOS (g/L)
Solubility	51.4	4.2	2.3	3.4	9.5	1.52

Table B.3: Amount of Each PFAS Used to Create the Stock Solutions for Experiments Using PFAS-Contaminated Soil

Experiment Number	PFBS (g)	PFHpA (g)	PFHxS (g)	PFOA (g)	PFNA (g)	PFOS (g)
S-3	-	-	4.2	10.2	-	1.56
S-4	0.516	5.1	2.1	5.1	5.1	0.78
III-2	0.127	0.0523	0.0291	0.4440	0.0199	0.0117
Batch Spiked Soil (III-3, III-4, & III-5)	0.0362	0.0525	0.0291	0.4445	0.0202	0.0117

Appendix C: Parameters for Supplemental Experiments

Table C.1: Experimental Parameters for Additional Experiments

Experiment Number	Fuel	Ratio (g fuel/kg sand)	Air Flux (cm/s)
Phase II			
S-1	GAC (with PFAS)	43	5.0
S-2	GAC (with PFAS)	39	5.0
Phase III			
S-3	GAC	50	5.0
S-4	GAC	51	5.0

Appendix D: Cleaning Procedure

All sample bottles and glassware for experiments S-1 – S-4, III-2, and PE1 were rinsed twice with deionized water, followed with two rinses with methanol (Sigma-Aldrich, 179957-4L, purity ≥99.6%).

Sample bottles and glassware used for PE2-PE4 and experiments III-1, III-3 – III-5, and IV-1 were rinsed three times with deionized water, three times with methanol, and three times with isopropyl alcohol (Ward's Science, 99% purity, CAS#67-63-0, part # 470301-474). The cleaning protocol was adjusted to ensure there was no contamination during the experiments and when collecting samples.

Appendix E: PFAS Analysis Procedure

Solid samples were extracted by adding 5 mL of basic methanol (0.1% ammonium hydroxide v/v) to 0.1 grams of solid in a 15 mL c-tube. Samples were then vortexed for 30 seconds, then placed on an end-over-end shaker rotating at 30 RPM for 48 hours. Samples were then centrifuged at 4000x RPM for 20 minutes, and a sub-sample was taken and put into an HPLC vial for analysis. Samples that had an individual PFAS concentration above 200 ppb were diluted down with basic methanol to below 200 ppb. Liquid samples were directly sub-sampled into HPLC vials for analysis.

All samples were analyzed on an Agilent 6460 LC-MS/MS running in MRM mode. Separation was performed using a 150mm x 2.1mm x 3.0 um Zorbax C18 Eclipse Column coupled with guard column. Samples were eluted over a 10-minute period, starting at 95% water (10 mM ammonium acetate) and 5% acetonitrile, transitioning to 100% acetonitrile over 8 minutes, then holding at 100% acetonitrile for the last 2 minutes. The column was then re-equilibrated at original elution conditions for 4 minutes before the next sample analysis.

Mass-labelled internal standards of PFOA, PFOS, PFHxS were added to solid samples before extraction to examine matrix effects. Internal standard recoveries were found to be between 80-115% and no correction was applied for internal standard. Concentrations were calculated using an eight-point calibration curve across 0.01 ppb to 200 ppb (0.01, 0.1, 1, 5, 10, 50, 100, 200). Two double injection blanks (methanol) were run before each method blank, reagent blank, calibration curve, post-treatment sample, and experimental blanks to eliminate contamination and carry-over from other samples.

Sample duplicates within 30% relative percent difference (RPD) was considered acceptable according to EPA Method 531.1. The average detection limit was 0.0004 mg/kg and the average quantification limit was 0.001 mg/kg.

Standard PFAS Suite:

- PFBA
- PFBS
- PFPeA
- PFHxA
- PFHxS
- PFHpA
- PFOA
- PFOS
- PFNA
- PFDA
- PFUnA
- PFDoA
- PFOSA

Expanded PFAS Suite (only used for II-2 PFAS emissions collection system):

- TFA
- PFPA
- 6:2 FTS
- Qualitative H/F exchange

Appendix F: Leak Testing Procedure

Leak tests were completed to quantify the dilution in the sampling trains which may be occurring during smouldering experiments. For smouldering experiments, the HF emissions collection and PFAS emissions collection trains were tested prior to running the experiment. Once the trains were setup, nitrogen gas was blown through and the gas analyzer measured the percent of oxygen that was still in the emissions at the end of the train. Adjustments were made to the setup in to minimize the leak. The final leak value was assumed to be constant throughout the experiment.

For the PFAS emissions experiments, leak tests were completed prior to beginning the experiment to minimize the leak. For this leak test, nitrogen gas was blown through the cell and through the emissions train at the same flowrate that was going to be used for the experiment. The emissions train was adjusted to reduce the leak during the experiment. For the PFAS emissions experiments, the leak was monitored throughout the experiment because nitrogen gas was used for the airflow. Therefore, any oxygen registered by the gas analyzer would be the dilution occurring in the emissions train. The values recorded for the dilution would then be incorporated into the calculated total flow measured by the flow totalizer. See Table F.1 for recorded leak values for the HF impingers and PFAS collection system in each experiment.

Table F.1: Tested Leak Values for the HF Impinger System and the PFAS Emissions System

Experiment	HF Impingers Leak (%)	PFAS Emissions Leak (%)
PFOS-Contaminated GAC		
II-1	5.0	9.5
II-2	4.8	3.3
PFAS-Spiked Soil		
III-1	6.9	2.6
III-2	31.9	n/a[a]
III-3	8.8	3.0
III-4	3.6	2.4
III-5	5.2	4.1
PFAS-Contaminated Field Soil		
IV-1	2.32	n/a[a]
IV-2	0.72	3.1
Average	8.9	4.0

[a]These experiments used an alternative method for PFAS emissions capture.

Appendix G: PFAS Emissions Experiments

A series of experiments were completed to explore the efficiency of the PFAS emissions collection train. For these experiments, an aluminum permeability cell was wrapped with a coiled resistive heater. The intention with the smaller cell was to allow all of the emissions from the experiment to travel through the PFAS collection train. Collecting all of the emissions should minimize the possible losses of PFAS during the experiment and allow the system itself to be tested to understand its ability to collect the PFAS.

The air supply in the cell was connected through the bottom. The airflow for these experiments was 100% nitrogen gas (Praxair Canada Inc., Ultra High Purity 5.0). Nitrogen gas was selected as the air source to prevent any oxidation reactions from occurring during the experiment. A layer of clean, coarse sand was placed above the air supply to ensure the nitrogen gas was dispersed evenly throughout the cross-section of the cell. For all four experiments conducted, the soil was prepared using the method described in Section 3.2.3.1. Approximately 100g of soil was placed in the cell. Experiment PE1, used only the PFAS-contaminated soil, however, experiments PE2 onward used a mixture of PFAS-contaminated soil with medium and coarse sand, in the same ratios as the Phase II experiments. A screen was placed above the soil in the cell to prevent it from being blown through the PFAS emissions collection train.

One thermocouple couple was placed next to the heater and another was placed in the cell at the center. The heater was then turned on and the cell was heated until the interior temperature of the cell was over 350°C. By heating the interior of the cell to 350-400˚C, this was believed to provide sufficient heat to volatilize the PFAS but not mineralize them

(Watanabe, Takemine, & Yamamoto, 2016). Once the desired temperature was reached, the nitrogen gas would be turned on. The duration and flowrate for each experiment is outlined in Table G.1. The flowrates and durations of the experiment were adjusted with the intention of improving the collection.

Table G.1: Flowrates and Duration of Nitrogen Gas Used for PFAS Emissions Experiments

Experiment Name	Flowrate (cm/s)	Duration (min)
PE1	5.0	50
PE2	2.0	15
PE3	3.5	30
PE4	2.0	30

For experiments PE1 and PE2, impingers containing 450 mL of KOH solution. Four impingers were used in PE1 and five impingers were used in PE2. Experiments PE3 and PE4, used two XAD tubes containing GAC and impinger with GAC and water. In experiment PE3, the HF collection system was used in parallel to the PFAS collection system to ensure no HF was being produced during the experiment. For this experiment, the total airflow rate of 4.1 L/min was divided evenly between the two collection systems.

Pre-treatment soil concentrations are shown in Table G.2. The soil used for PE1 and PE2, had high concentrations of PFHxS, PFOA and PFOS. PE1 demonstrated significant reduction in PFAS concentrations with removal of PFHxS, PFOS, and PFOA being 97.31%, 96.52%, 99.97%, respectively. Less PFAS were removed in PE2; the maximum reduction was 62.18% of PFOA. The difference in removal between PE1 and PE2 was likely due to the shorter period at maximum temperature with nitrogen flowing through the cell in PE2.

For PE3 and PE4, the PFAS concentrations were decreased to limit the possibility of breakthrough occurring in the PFAS emissions system. Following the experiment, all

PFAS had been removed from the soil with the exception of PFHxS in PE3. These experiments suggest temperatures of 350°C with a nitrogen flux of 2.4 cm/s can achieve a 99.97% reduction in PFAS when concentrations are 220-280 mg/kg or remove PFAS from soils when the concentrations are below 2.4 mg/kg.

Table G.2: PFAS Concentrations of the Soil Before and After Each PFAS Emissions Experiment

	Experiment	PFOS (mg/kg)	PFOA (mg/kg)	PFBS (mg/kg)	PFNA (mg/kg)	PFHpA (mg/kg)	PFHxS (mg/kg)
PE1	Pre-treatment	223	284	0.036	0.270	0.129	46.1
	Post-treatment	7.75	0.075	1.49×10^{-3}	2.34×10^{-3}	0.022	1.24
PE2	Pre-treatment	198	248	B.Q.L.	B.Q.L.	B.Q.L.	41.5
	Post-treatment	158.6	93.8	B.Q.L.	B.Q.L.	0.096	23.3
PE3	Pre-treatment	0.156	2.635	B.D.L.	0.135	0.211	0.128
	Post-treatment	B.D.L.	B.D.L.	B.D.L.	B.D.L.	B.D.L.	0.008
PE4	Pre-treatment	0.302	2.429	0.102	0.218	0.268	0.188
	Post-treatment	B.D.L.	B.D.L.	B.D.L.	B.D.L.	B.D.L.	B.D.L.

B.D.L. = 0.0004 mg/kg
B.Q.L. = 0.001 mg/kg

In PE1, PFAS concentrations were measured in all four impingers containing KOH solution. This suggested that breakthrough had occurred even with low concentrations of PFAS. Modifications to the PFAS emissions system resulted in a maximum of 10.7% of PFAS to be captured (Table G.3).

Results from these experiments indicate alternations to the PFAS compounds in the soils. Shorter-chain PFAS with carboxyl functional groups were captured in the PFAS emissions system which were not originally in the soil. It is hypothesized that in these low-temperature heating tests the PFAS was substantially volatilized without transformation and the rest underwent low-energy transformations (e.g., dissociation of the functional group) such that the resulting fluorinated compounds were outside the analytical suite. Overall, these tests suggest that the PFAS emissions capture system was working adequately.

Table G.3: Percent of Fluorine Captured in the PFAS Emissions System from PFAS in the Soil Prior to the Experiments and PFAS Compounds Captured in the Emissions System

Experiment	Percent of F Captured (%)	PFAS Captured in Emissions System
PE1	0.02%	PFBA, PFBS, PFPeA, PFHxA, PFHxS, PFHpA, PFOA, PFOS, PFNA, PFDA
PE2	0.00%	n/a
PE3	0.64%[a]	PFHxS, PFOS
PE4	10.69%	PFBA, PFPeA, PFBA, PFHxA, PFHpA, PFHxS, PFOA, PFNA, PFOS

[a]Estimated value. All PFAS was captured in the glass wool and exact mass is not known.

Appendix H: Uncertainty for Smouldering Results

Table H.1: Smouldering Results Used to Calculate the Uncertainty in the Smouldering Temperature

		Data Set 1	Data Set 2		Data Set 3	Data Set 4	Variability		
Test No.		**1**	**2**	**3**	**4**	**5**	*Mean*	*Median*	*Mode*
Smouldering Velocity (cm/min)		0.54	0.42	0.25	0.50	0.48			
Variability	± *cm/min*	0.10	0.05	0.05	0.07	0.04	0.06	0.05	0.05
	± *%*	18.5	12	19	13.1	8.3	14.2	13.1	N/A

Table H.2: Smouldering Results Used to Calculate the Uncertainty in the Smouldering Velocity

		Data Set 1	Data Set 2		Data Set 3	Data Set 4	Variability		
Test No.		**1**	**2**	**3**	**4**	**5**	*Mean*	*Median*	*Mode*
Peak Temperature (°C)		543	544	460	641	954			
Variability	± *°C*	15	15	23	11	20.2	16.8	15	15
	± *%*	2.8	2.8	5.1	1.7	2.1	2.9	2.8	2.8

Test No. Specifics:

1. 4 repeats of base case w/ 95% confidence intervals assuming a logarithmic distribution of random error. 280 mm high x 138 mm internal diameter quartz column; stainless steel diffuser at base; cable heater; base case = 40 g trichloroethlyene/ kg sand, 42 g canola oil/ kg sand; No. 12 silica sand (mean grain size = 0.88 mm; coefficient of uniformity = 1.6).

2. 3 repeats @ 73% MC biosolids at 4.7 g/g S/B with 95% confidence interval. Open system; 60cm tall & 15cm diameter stainless steel column w/ conductive base.

3. 3 repeats @ 79% MC biosolids at 4.4 g/g S/B with 95% confidence interval. Open system; 60cm tall & 15cm diameter stainless steel column w/ conductive base.

4. 3 repeats w/ 95% confidence interval; 70 L/min & 35 g bitumen/ g coarse sand. Open system; 60cm tall & 15cm diameter stainless steel column w/ conductive base.

5. 3 repeats w/ 95% confidence interval; 60 L/min, 10% O_2 & 30 g GAC/ g medium sand. Two open & one closed system; 60cm tall & 15cm diameter stainless steel column w/ conductive base.

Appendix I: Thermocouple & GAS Emission Profiles

<u>I-1</u>

GAC Concentration: 60 g GAC/1 kg sand
Air Flux: 5.0 cm/s
Average Peak Temperature: 1257 ± 63 ˚C
Smouldering velocity: 0.64 ± 0.13 cm/min

Note: no gas data is available for this experiment.
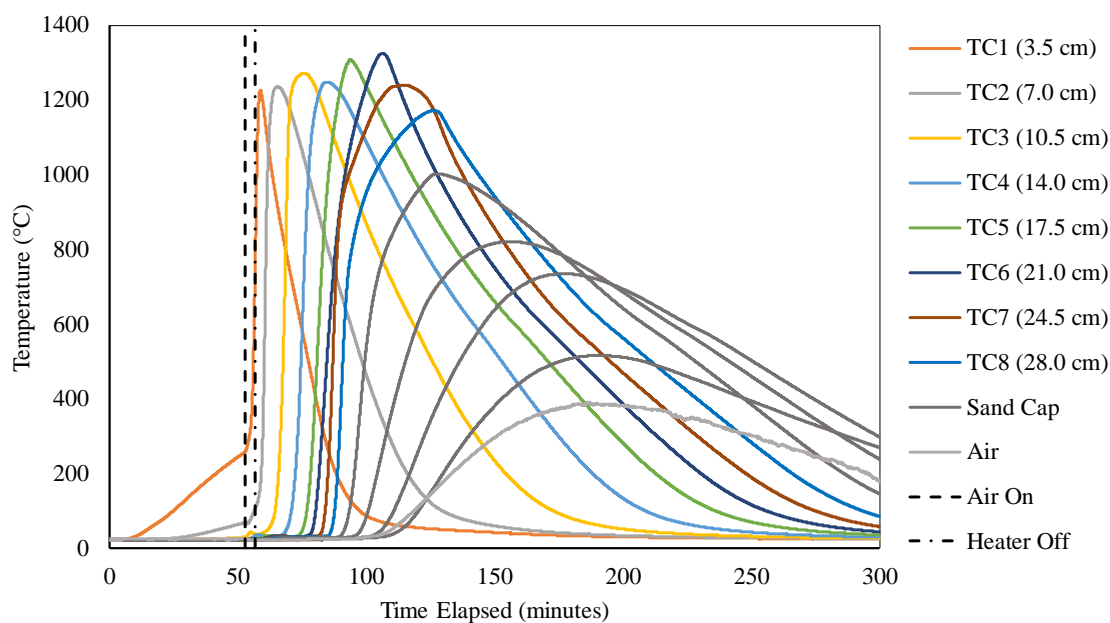
Figure I.1: Thermocouple profiles for I-1 using 60 g GAC/kg sand and an air flux of 5.0 cm/s.

I-2

GAC Concentration: 40 g GAC/1 kg sand
Air Flux: 5.0 cm/s
Average Peak Temperature: 1003 ± 50 ˚C
Smouldering velocity: 0.66 ± 0.13 cm/min
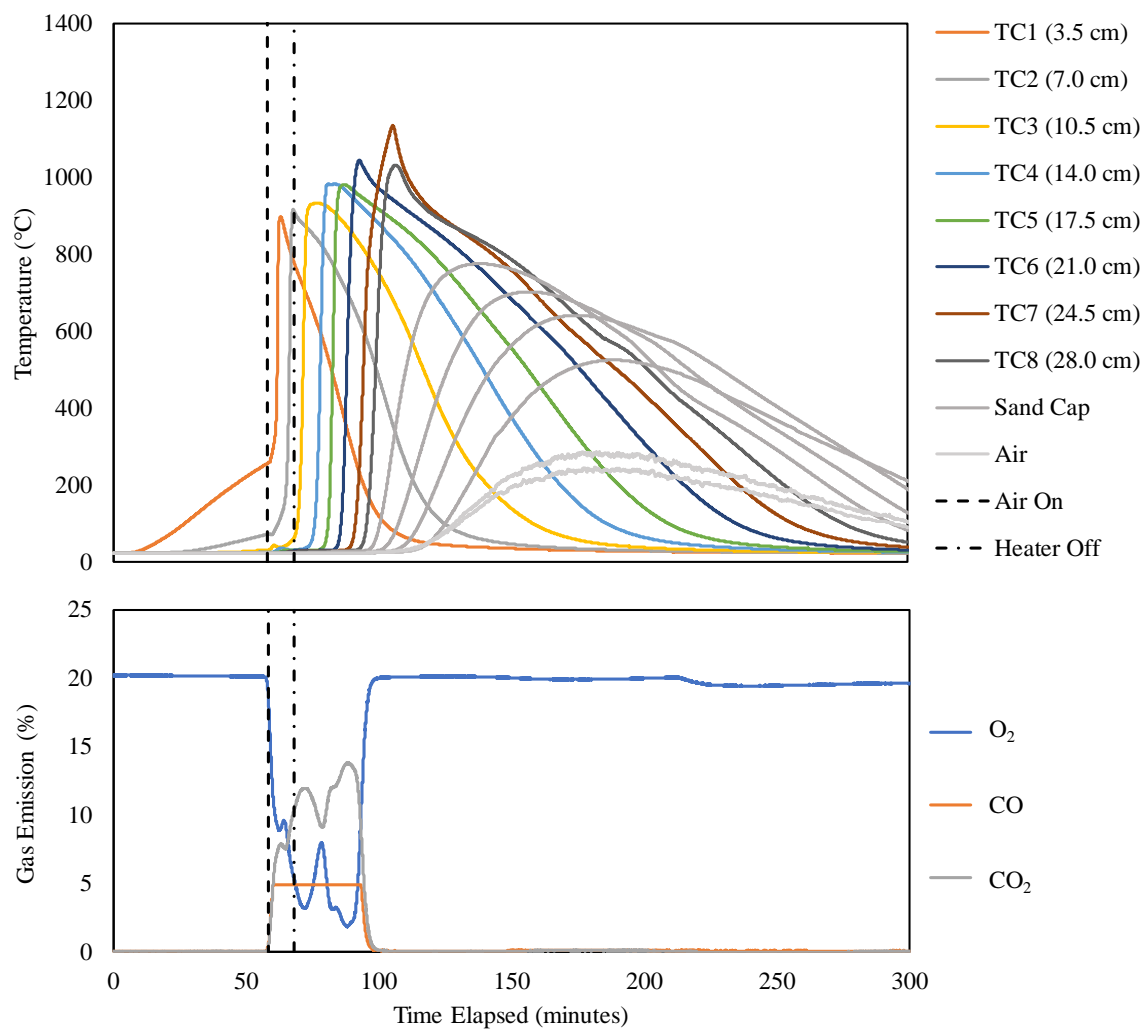
Figure I.2: Thermocouple and gas profiles for I-2 using 40 g GAC/kg sand and an air flux of 5.0 cm/s.

I-3

GAC Concentration: 20 g GAC/1 kg sand
Air Flux: 5.0 cm/s
Average Peak Temperature: 707 ± 35 ˚C
Smouldering velocity: 0.49 ± 0.10 cm/min
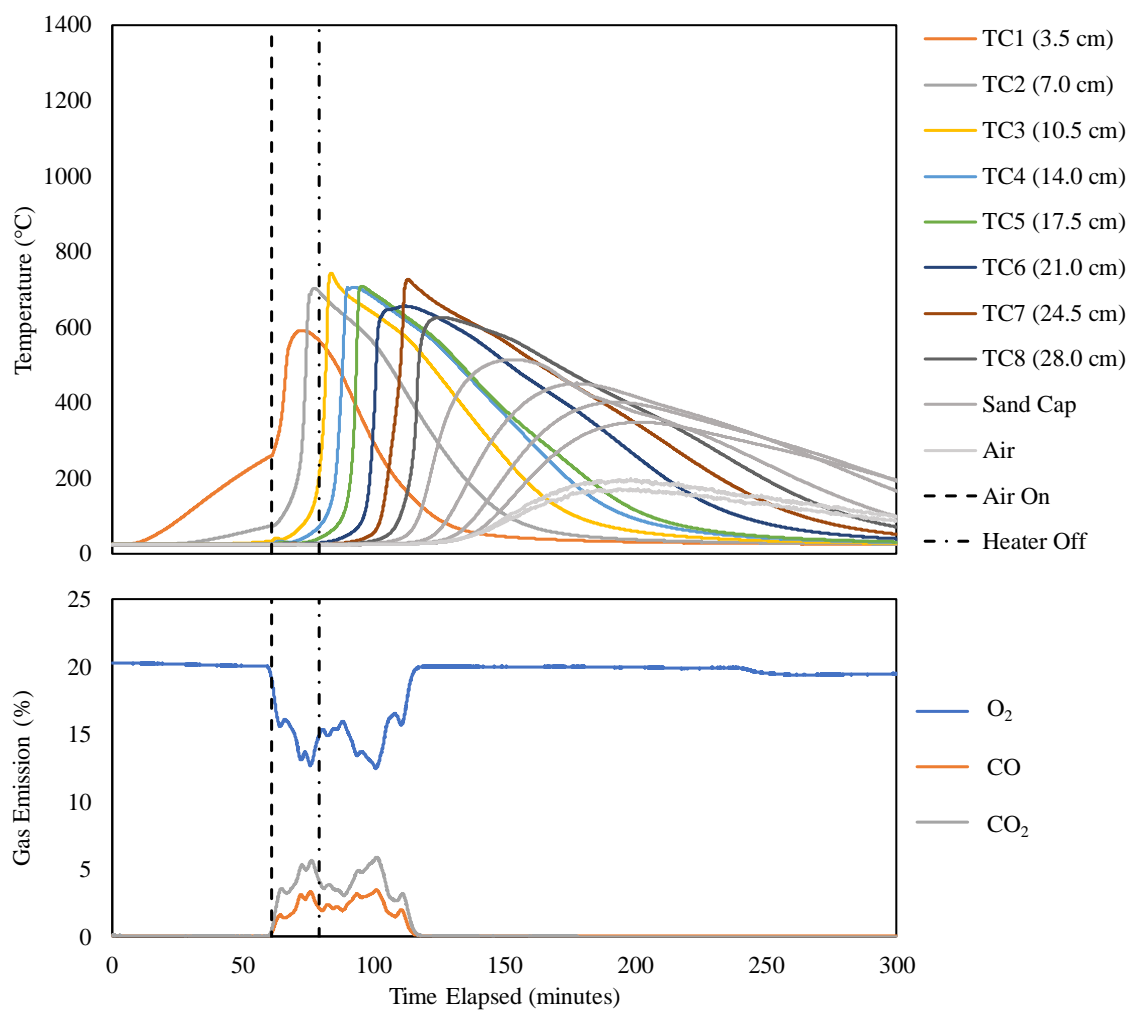
Figure I.3: Thermocouple and gas profiles for I-3 using 20 g GAC/kg sand and an air flux of 5.0 cm/s.

I-4

GAC Concentration: 40 g GAC/1 kg sand
Air Flux: 2.5 cm/s
Average Peak Temperature: 1024 ± 51 ˚C
Smouldering velocity: 0.47 ± 0.09 cm/min
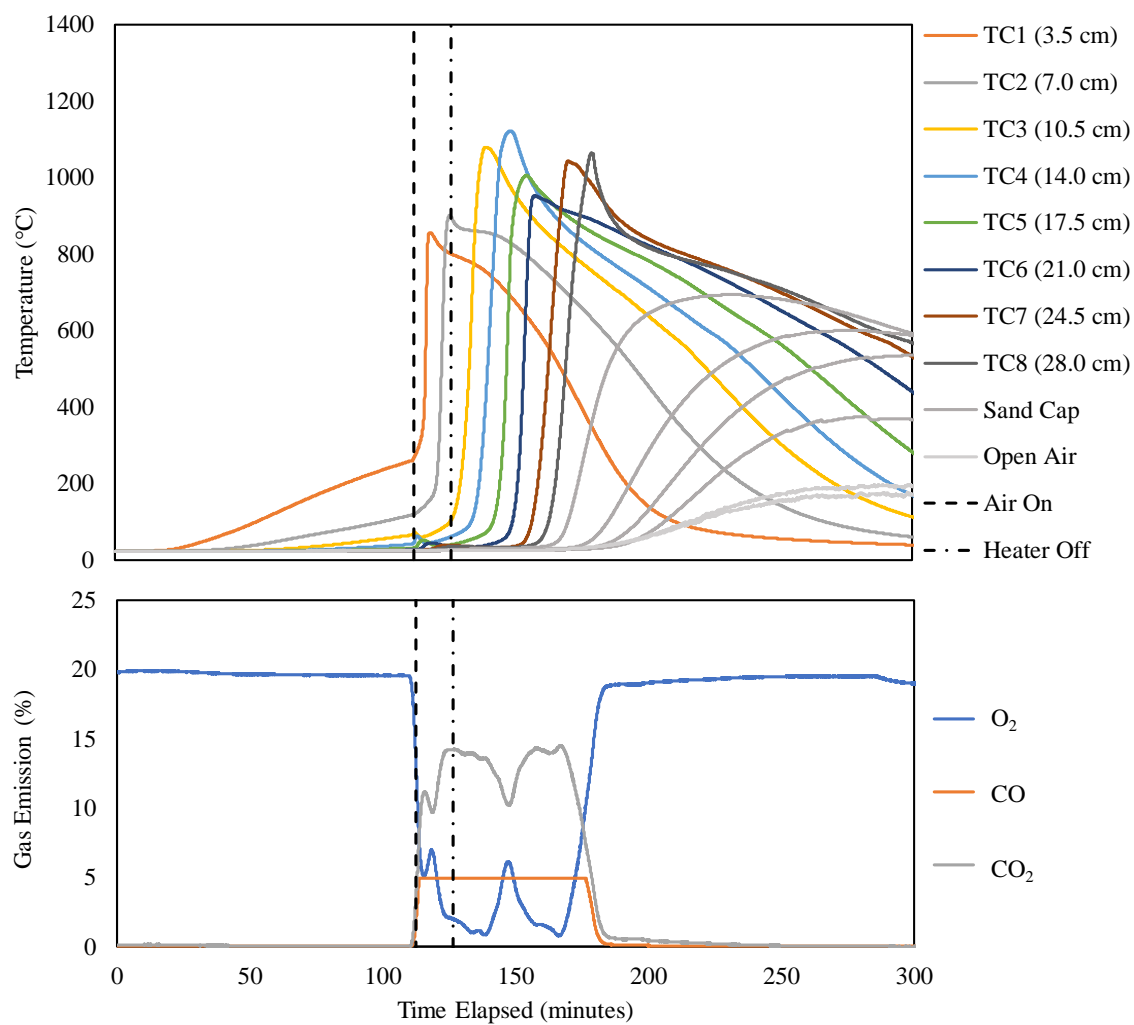
Figure I.4: Thermocouple and gas profiles for I-4 using 40 g GAC/kg sand and an air flux of 2.5 cm/s.

I-5

GAC Concentration: 40 g GAC/1 kg sand
Air Flux: 7.5 cm/s
Average Peak Temperature: 1056 ± 53 ˚C
Smouldering velocity: 0.70 ± 0.14 cm/min
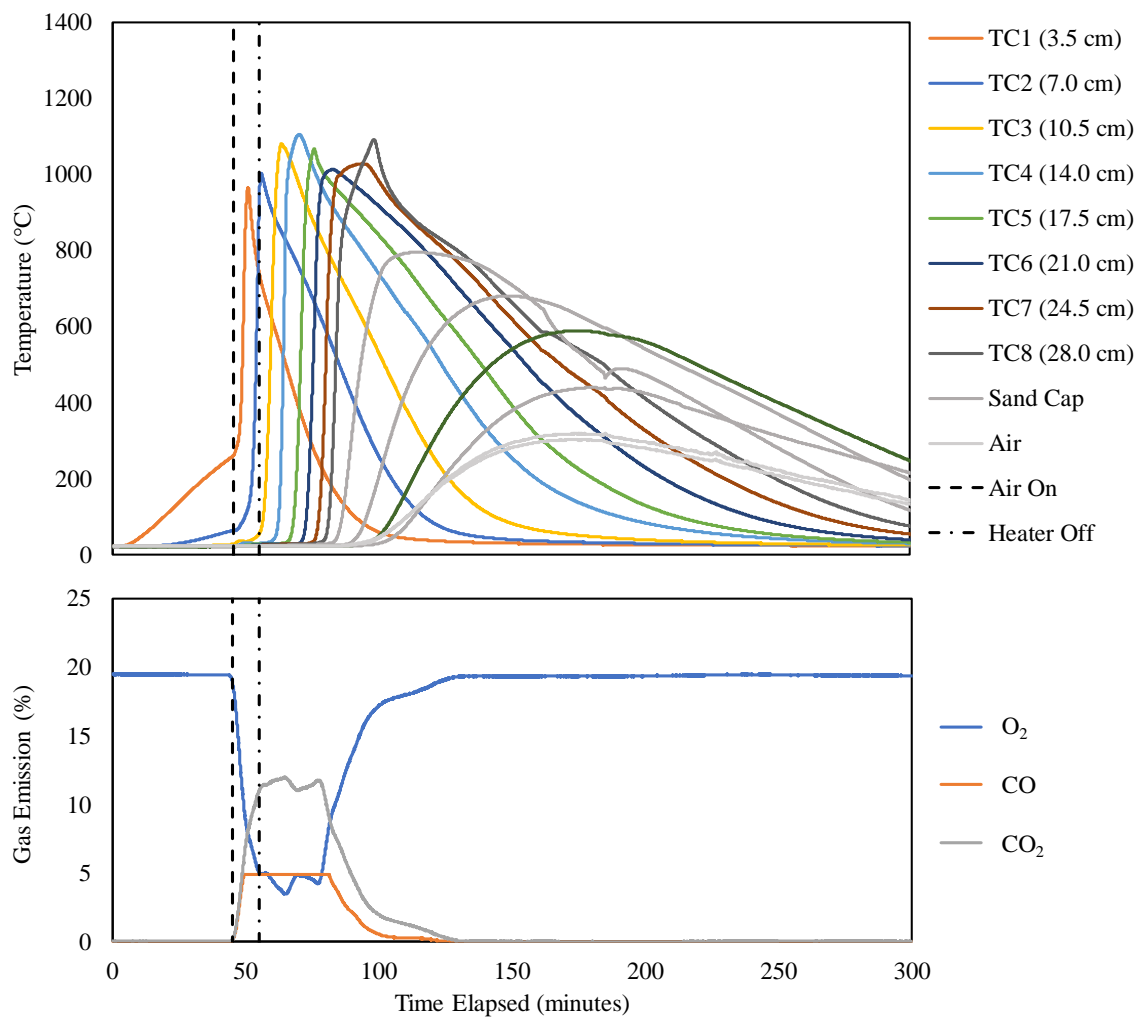
Figure 4.25: Thermocouple and gas profiles for I-5 using 40 g GAC/kg sand and an air flux of 7.5 cm/s.

I-6

GAC Concentration: 60 g GAC/1 kg sand
Air Flux: 2.5 cm/s
Average Peak Temperature: 1184 ± 59 ˚C
Smouldering velocity: 0.37 ± 0.07 cm/min
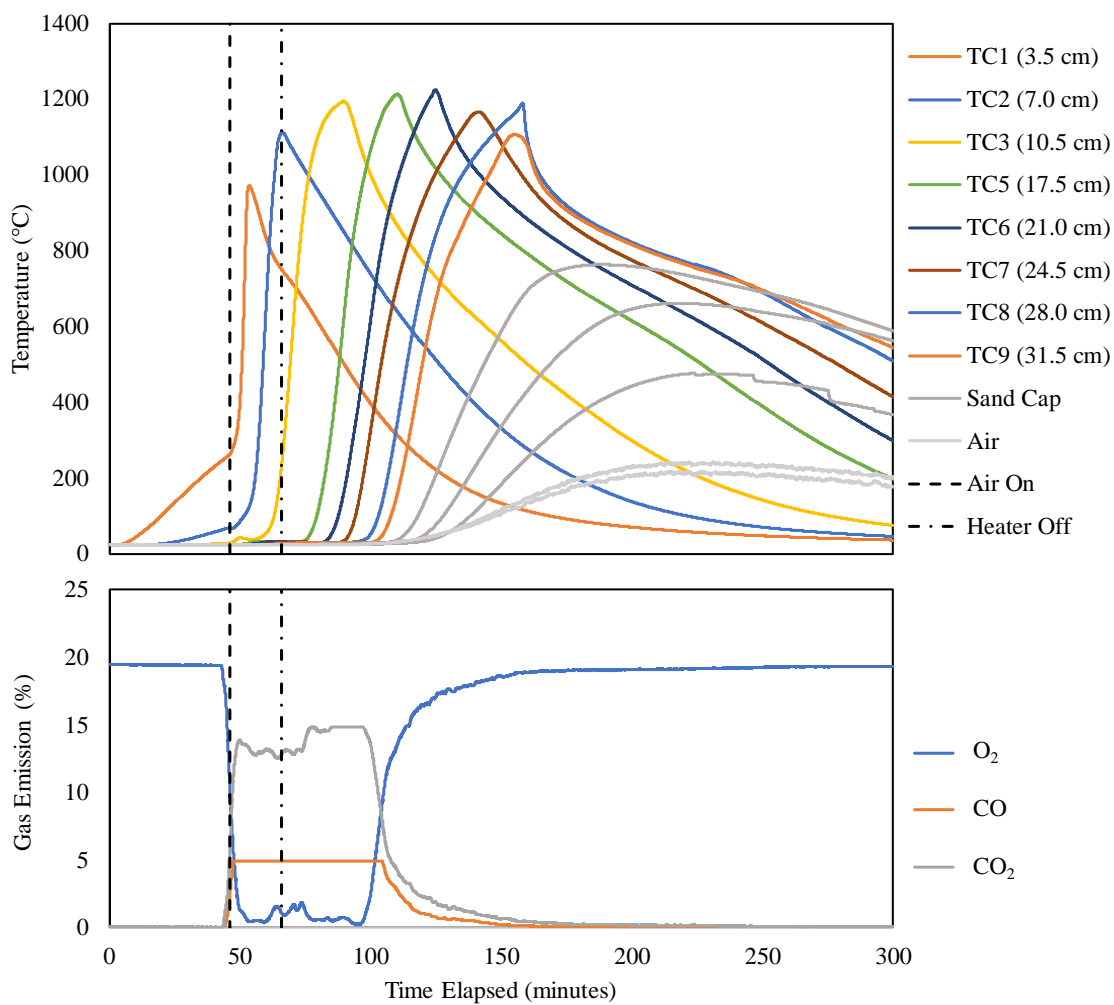
Figure I.6: Thermocouple and gas profiles for I-6 using 60 g GAC/kg sand and an air flux of 2.5 cm/s.

<u>I-7</u>

GAC Concentration: 20 g GAC/1 kg sand
Air Flux: 2.5 cm/s
Average Peak Temperature: 662 ± 33 ˚C
Smouldering velocity: 0.33 ± 0.07 cm/min
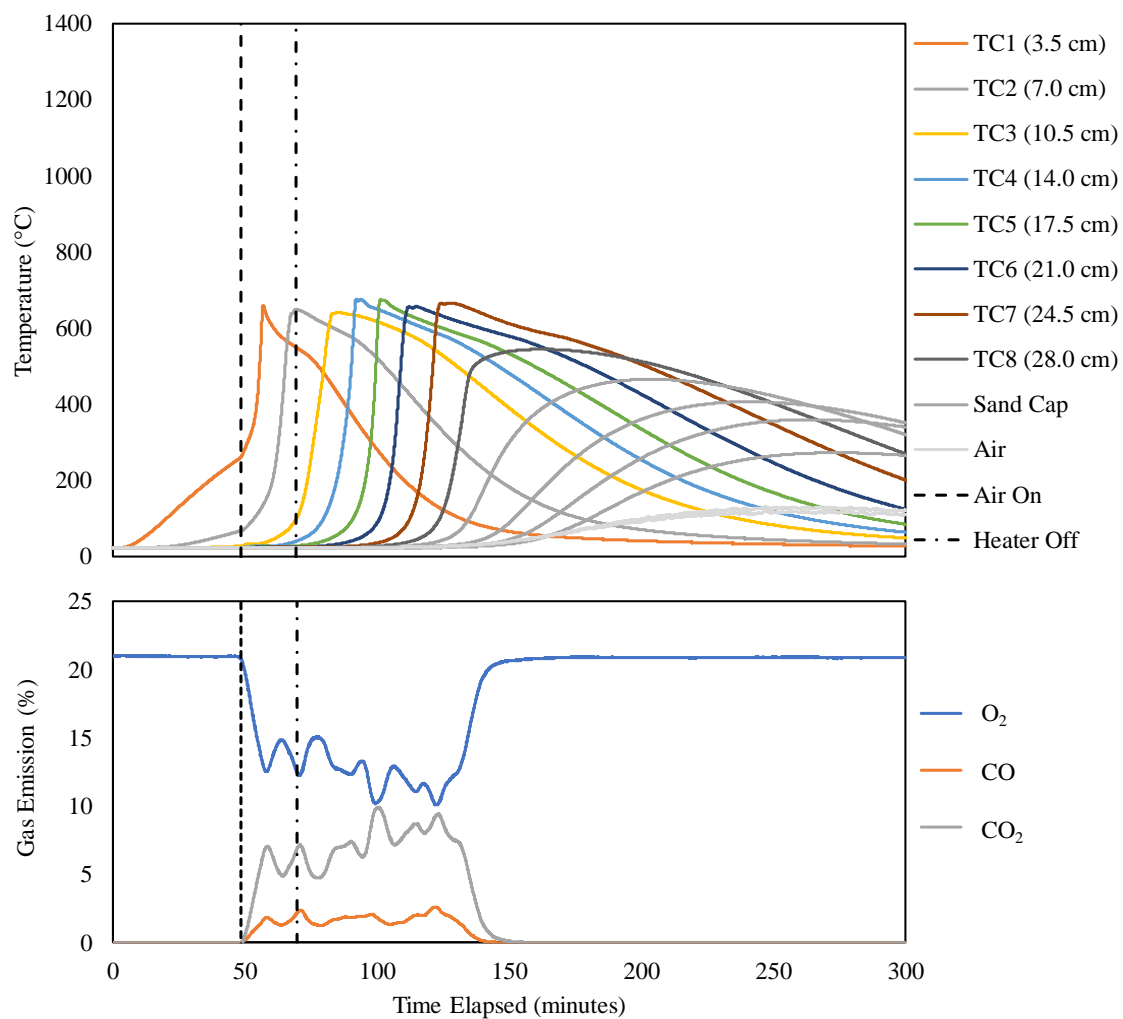
Figure I.7: Thermocouple and gas profiles for I-7 using 20 g GAC/kg sand and an air flux of 2.5 cm/s.

II-1

GAC Concentration: 44 g GAC/1 kg sand
Air Flux: 5.0 cm/s
Average Peak Temperature: 1048 ± 52˚C
Smouldering velocity: 0.45 ± 0.09 cm/min
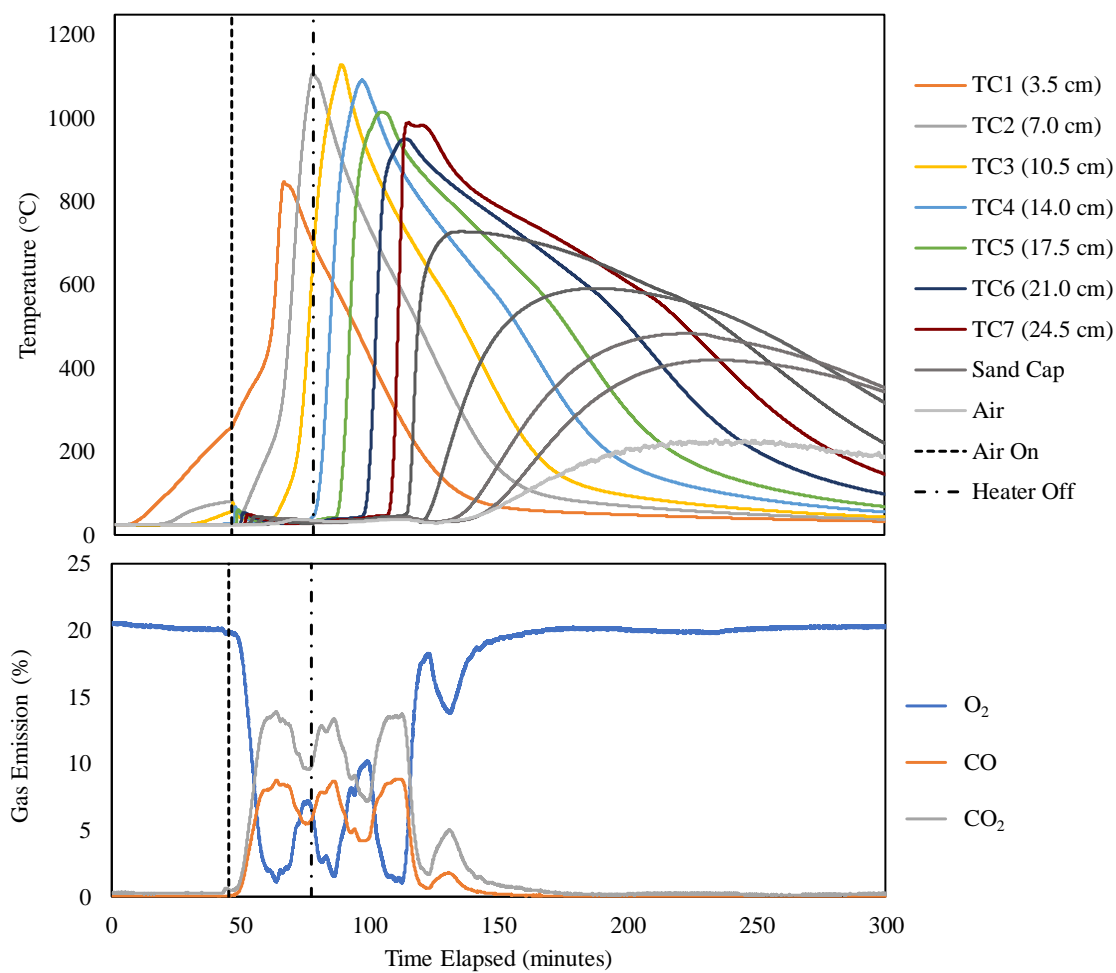
Figure I.8: Thermocouple and gas profiles for II-1 using 44 g GAC/kg sand and an air flux of 5.0 cm/s.

II-2

GAC Concentration: 46 g GAC/1 kg sand
Air Flux: 5.0 cm/s
Average Peak Temperature: $1011 \pm 51°C$
Smouldering velocity: 0.40 ± 0.08 cm/min
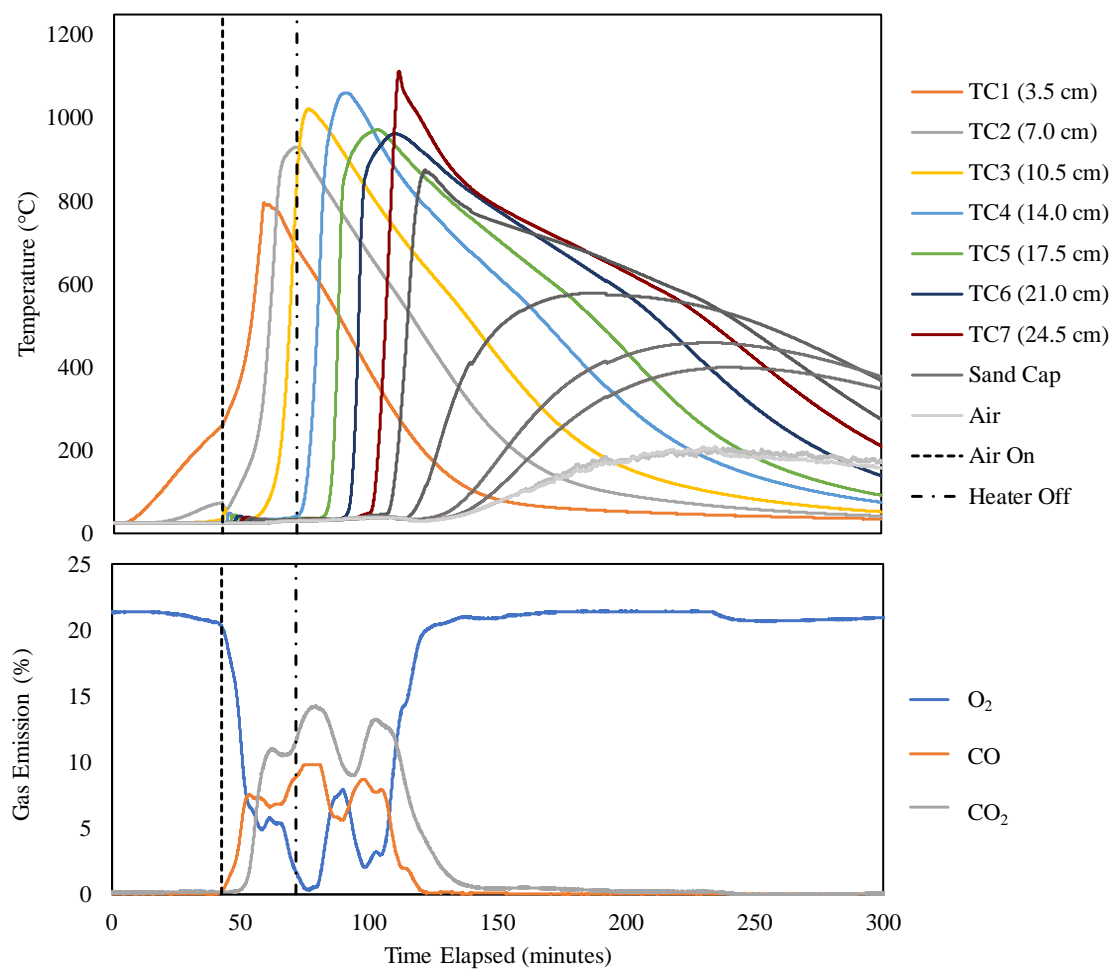
Figure I.9: Thermocouple and gas profiles for II-2 using 46 g GAC/kg sand and an air flux of 5.0 cm/s.

III-1

GAC Concentration: 50 g GAC/1 kg sand
Air Flux: 5.0 cm/s
Average Peak Temperature: 1085 ± 54˚C
Smouldering velocity: 0.69 ± 0.14 cm/min
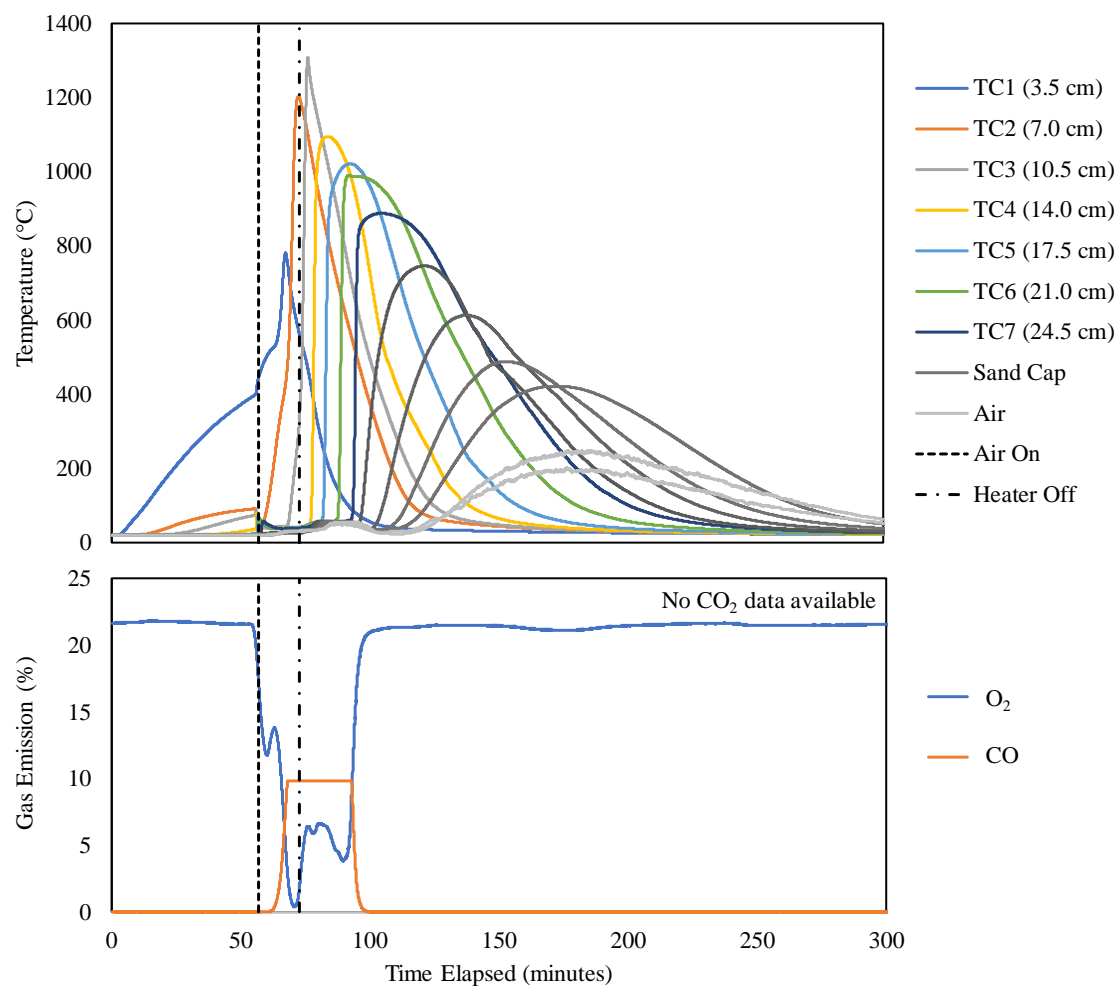
Figure I.10: Thermocouple and gas profiles for III-1 using 50 g GAC/kg sand and an air flux of 5.0 cm/s.

III-2

GAC Concentration: 50 g GAC/1 kg sand
Air Flux: 5.0 cm/s
Average Peak Temperature: 1093 ± 55˚C
Smouldering velocity: 0.64 ± 0.13 cm/min

Note: no gas data is available for this experiment.
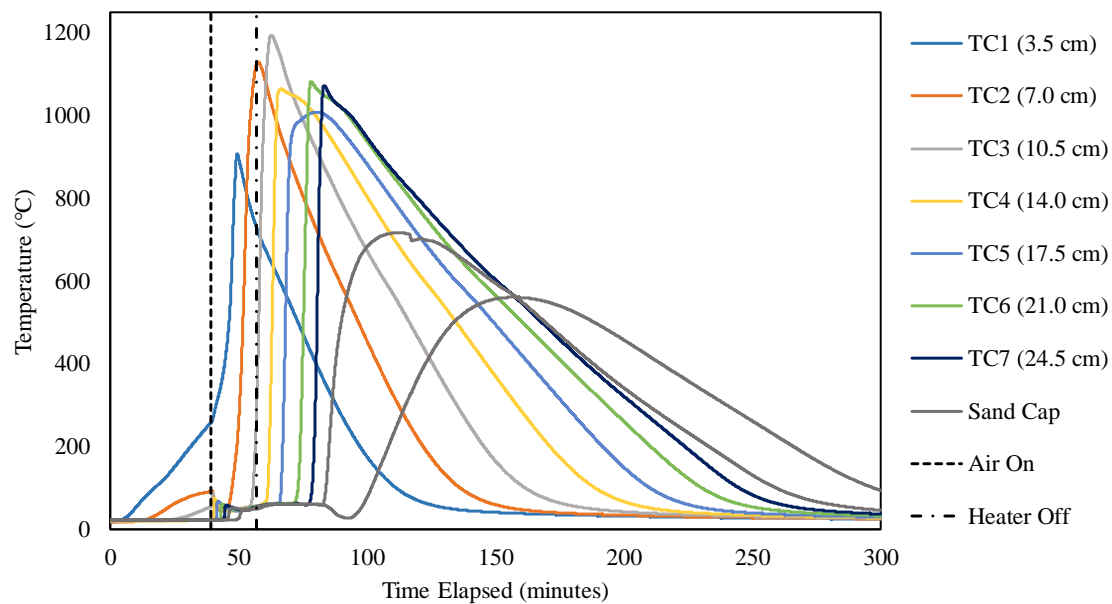
Figure I.11: Thermocouple for III-2 using 50 g GAC/kg sand and an air flux of 5.0 cm/s.

III-3

GAC Concentration: 50 g GAC/1 kg sand
Air Flux: 5.0 cm/s
Average Peak Temperature: 1145 ± 57˚C
Smouldering velocity: 0.71 ± 0.14 cm/min
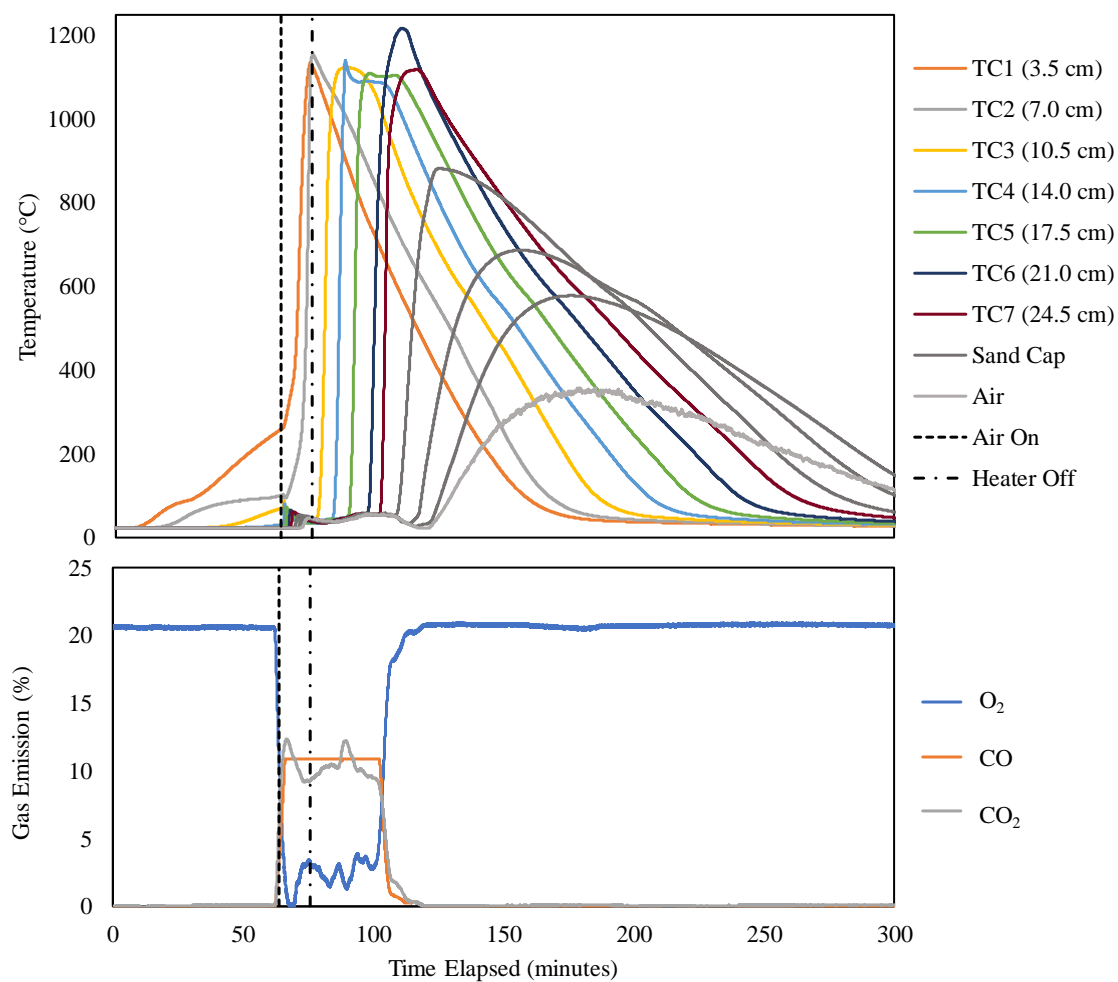
Figure I.12: Thermocouple and gas profiles for III-3 using 50 g GAC/kg sand and an air flux of 5.0 cm/s.

III-4

GAC Concentration: 50 g GAC/1 kg sand
Air Flux: 5.0 cm/s
Average Peak Temperature: 1143 ± 57˚C
Smouldering velocity: 0.48 ± 0.10 cm/min
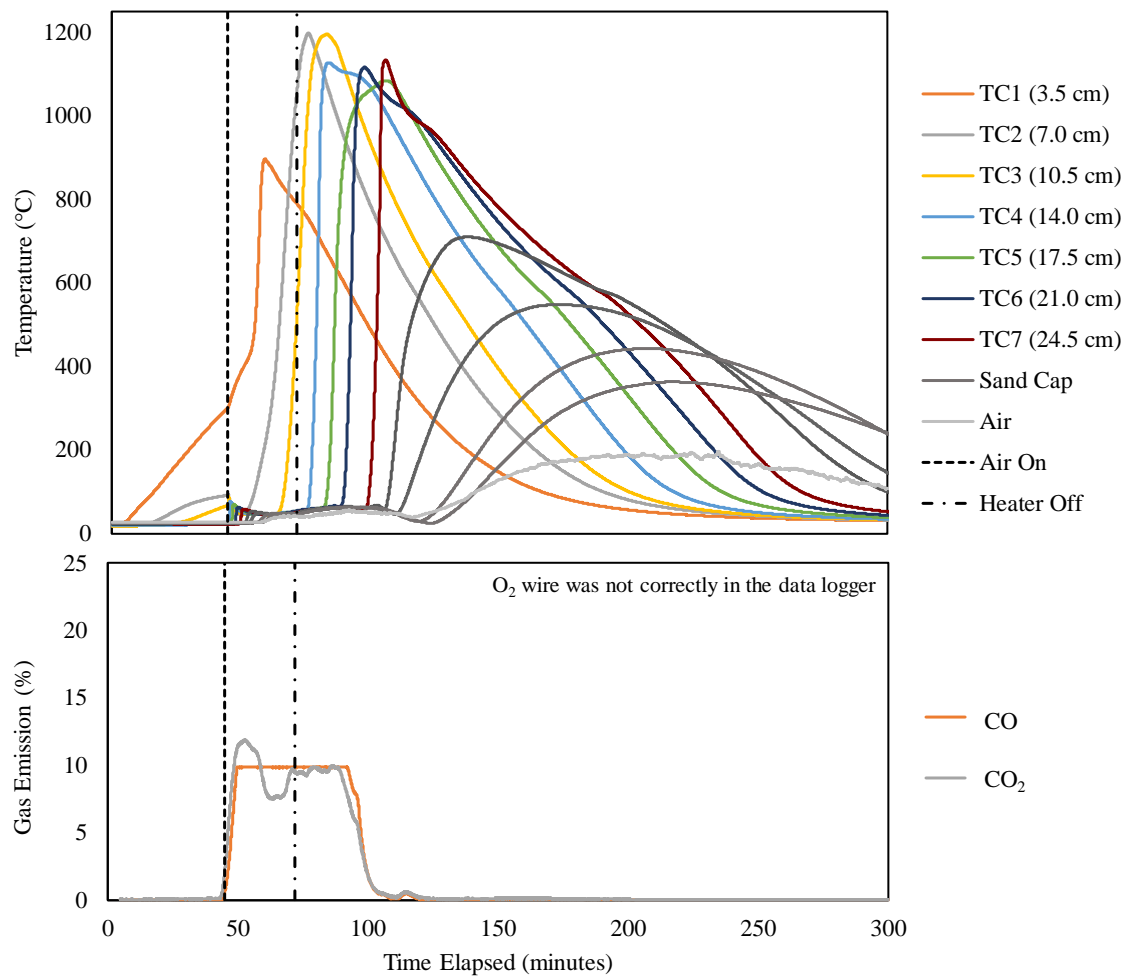
Figure I.13: Thermocouple and gas profiles for III-4 using 50 g GAC/kg sand and an air flux of 5.0 cm/s.

<u>III-5</u>

GAC Concentration: 15 g GAC/1 kg sand
Air Flux: 5.0 cm/s
Average Peak Temperature: 642 ± 32˚C
Smouldering velocity: 0.24 ± 0.05 cm/min
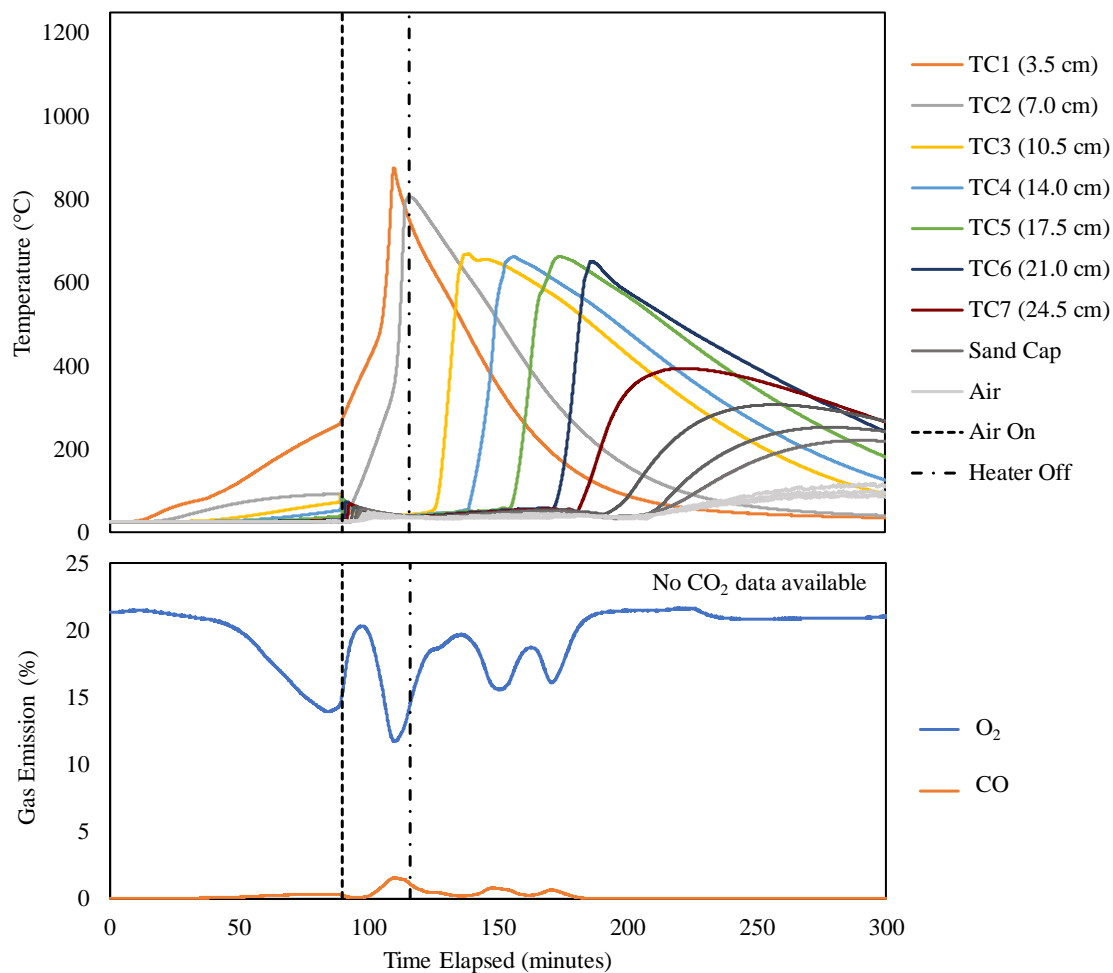
Figure I.14: Thermocouple and gas profiles for III-5 using 15 g GAC/kg sand and an air flux of 5.0 cm/s.

IV-1

GAC Concentration: 51 g GAC/1 kg sand
Air Flux: 5.0 cm/s
Average Peak Temperature: 1040 ± 52˚C
Smouldering velocity: 0.38 ± 0.08 cm/min
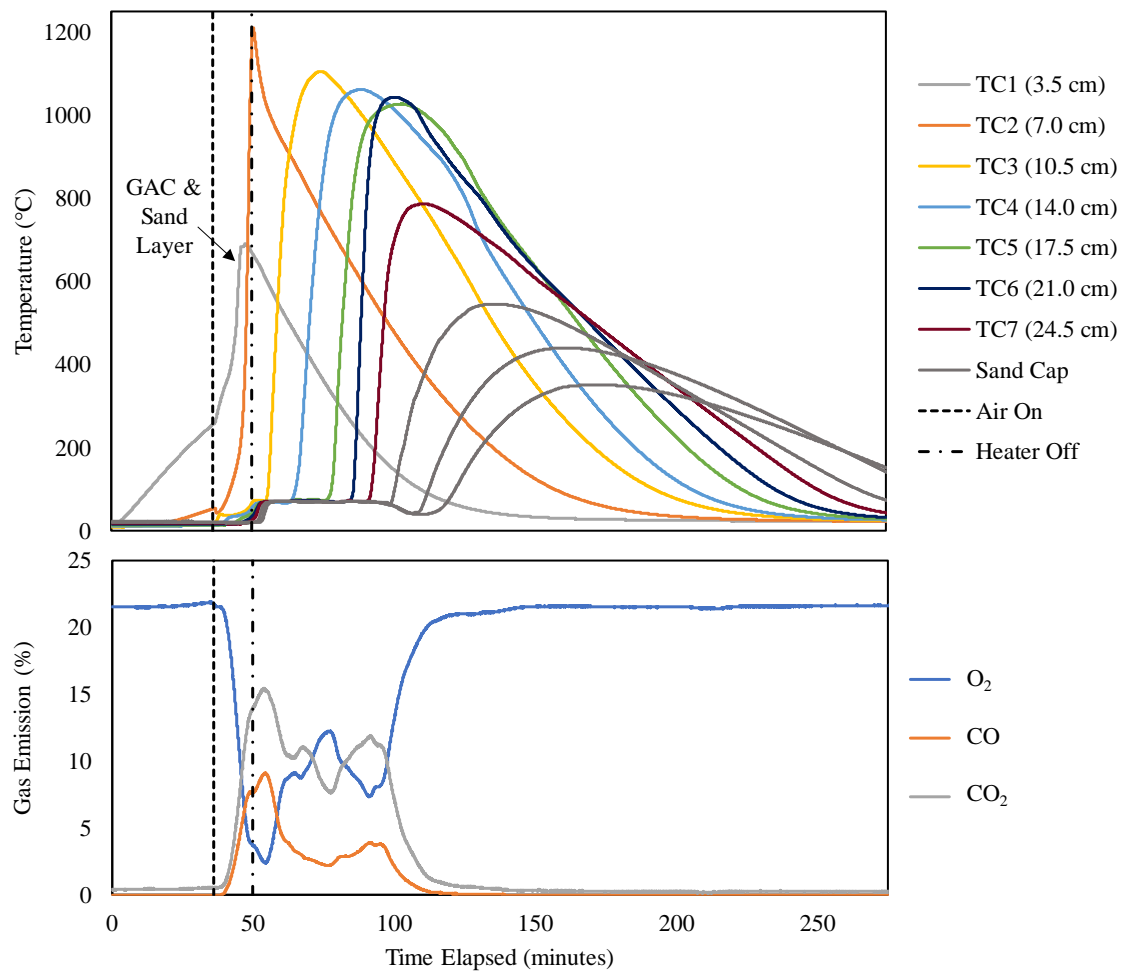
Figure I.15: Thermocouple and gas profiles for IV-1 using 51 g GAC/kg sand and an air flux of 5.0 cm/s. A clean sand and GAC layer was placed below the contaminated sand and GAC layer (TC1 to interface of TC2 and TC3).

IV-2

GAC Concentration: 51 g GAC/1 kg sand
Air Flux: 5.0 cm/s
Average Peak Temperature: $1012 \pm 51\,°C$
Smouldering velocity: 0.47 ± 0.01 cm/min
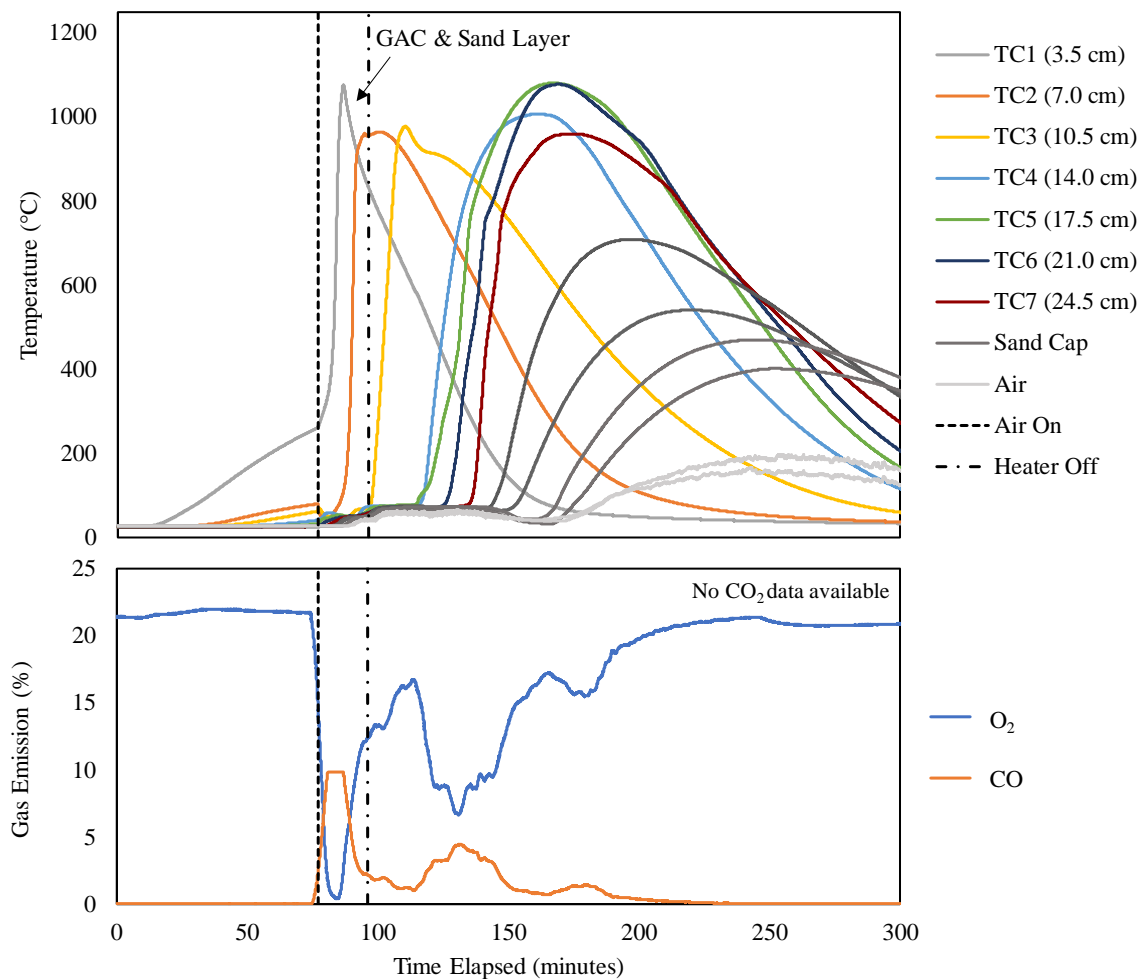
Figure I.16: Thermocouple and gas profiles for IV-2 using 51 g GAC/kg sand and an air flux of 5.0 cm/s. A clean sand and GAC layer was placed below the contaminated sand and GAC layer (TC1 to interface of TC2 and TC3).

S-1

GAC Concentration: 43 g GAC/1 kg sand
Air Flux: 5.0 cm/s
Average Peak Temperature: 928 ± 46˚C
Smouldering velocity: 0.69 ± 0.14 cm/min

Note: no gas data is available for this experiment.
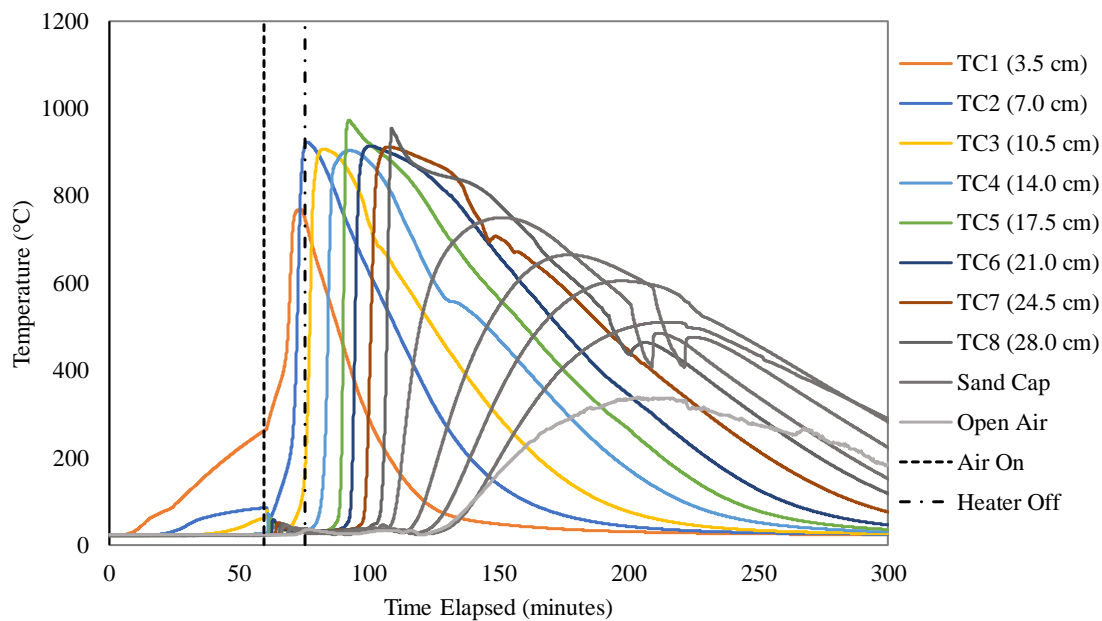
Figure I.17: Thermocouple profiles for S-1 using 43 g GAC/kg sand and an air flux of 5.0 cm/s.

S-2

GAC Concentration: 39 g GAC/1 kg sand
Air Flux: 5.0 cm/s
Average Peak Temperature: 960 ± 48°C
Smouldering velocity: 0.65 ± 0.13 cm/min
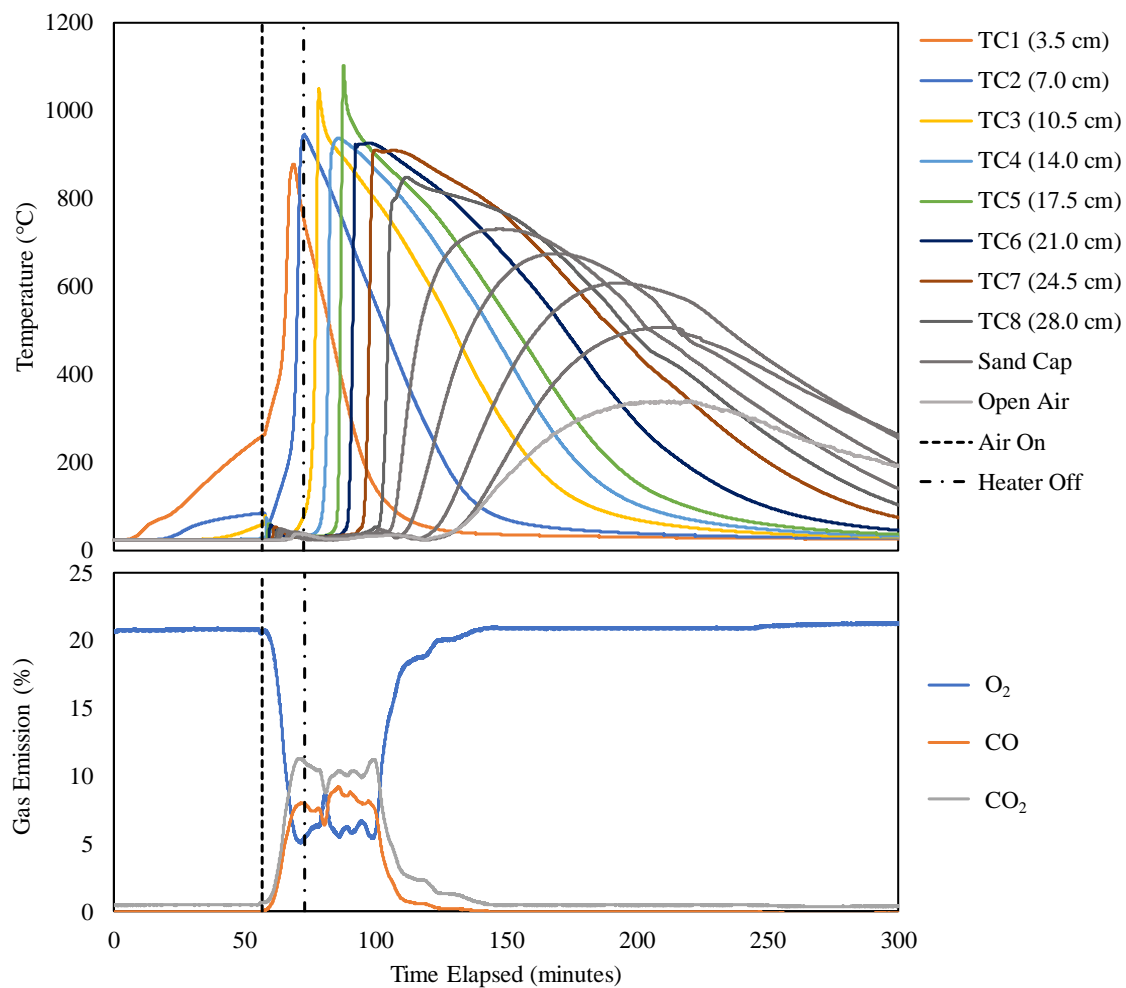
Figure I.18: Thermocouple and gas profiles for S-2 using 39 g GAC/kg sand and an air flux of 5.0 cm/s.

S-3

GAC Concentration: 50 g GAC/1 kg sand
Air Flux: 5.0 cm/s
Average Peak Temperature: 1070 ± 54˚C
Smouldering velocity: 0.63 ± 0.13 cm/min
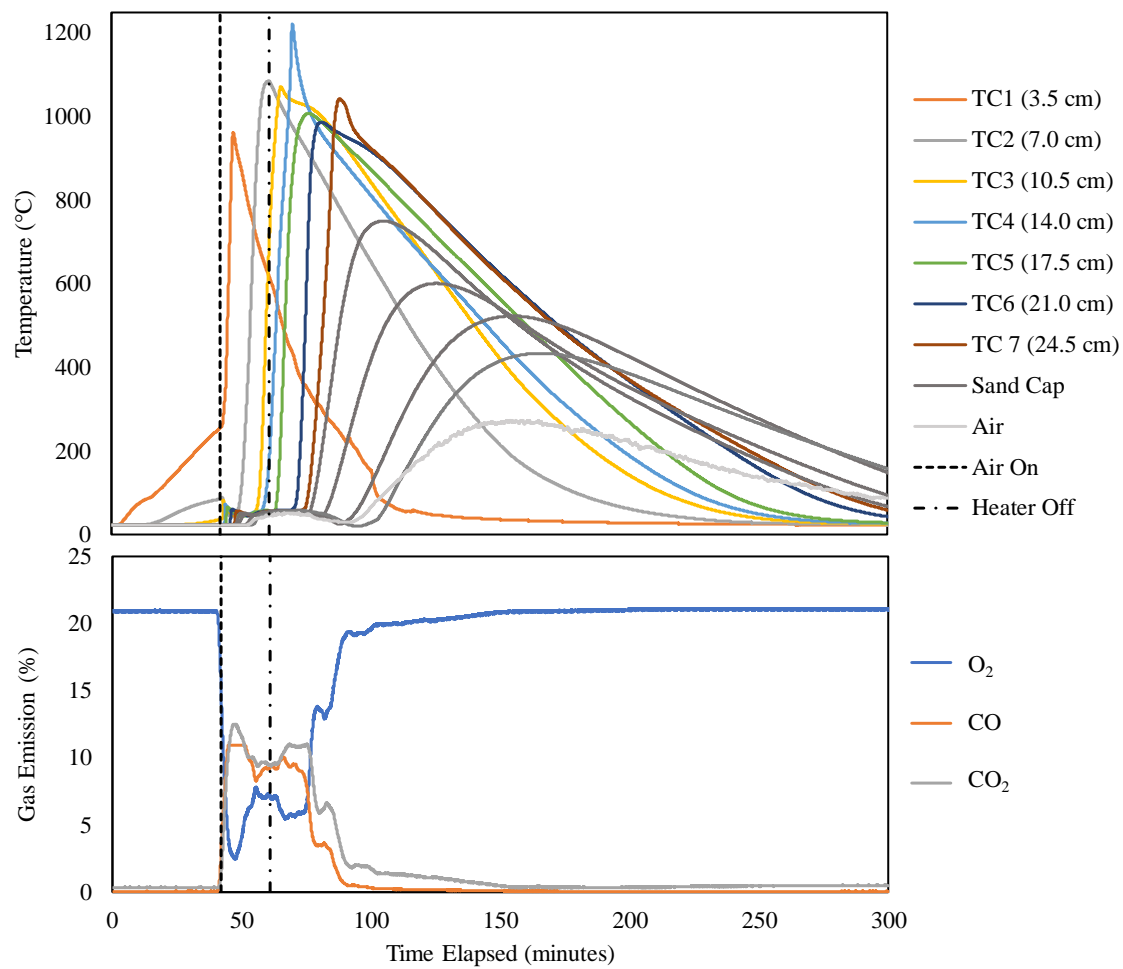
Figure I.19: Thermocouple and gas profiles for S-3 using 50 g GAC/kg sand and an air flux of 5.0 cm/s.

S-4

GAC Concentration: 51 g GAC/1 kg sand
Air Flux: 5.0 cm/s
Average Peak Temperature: 1060 ± 53˚C
Smouldering velocity: 0.73 ± 0.15 cm/min
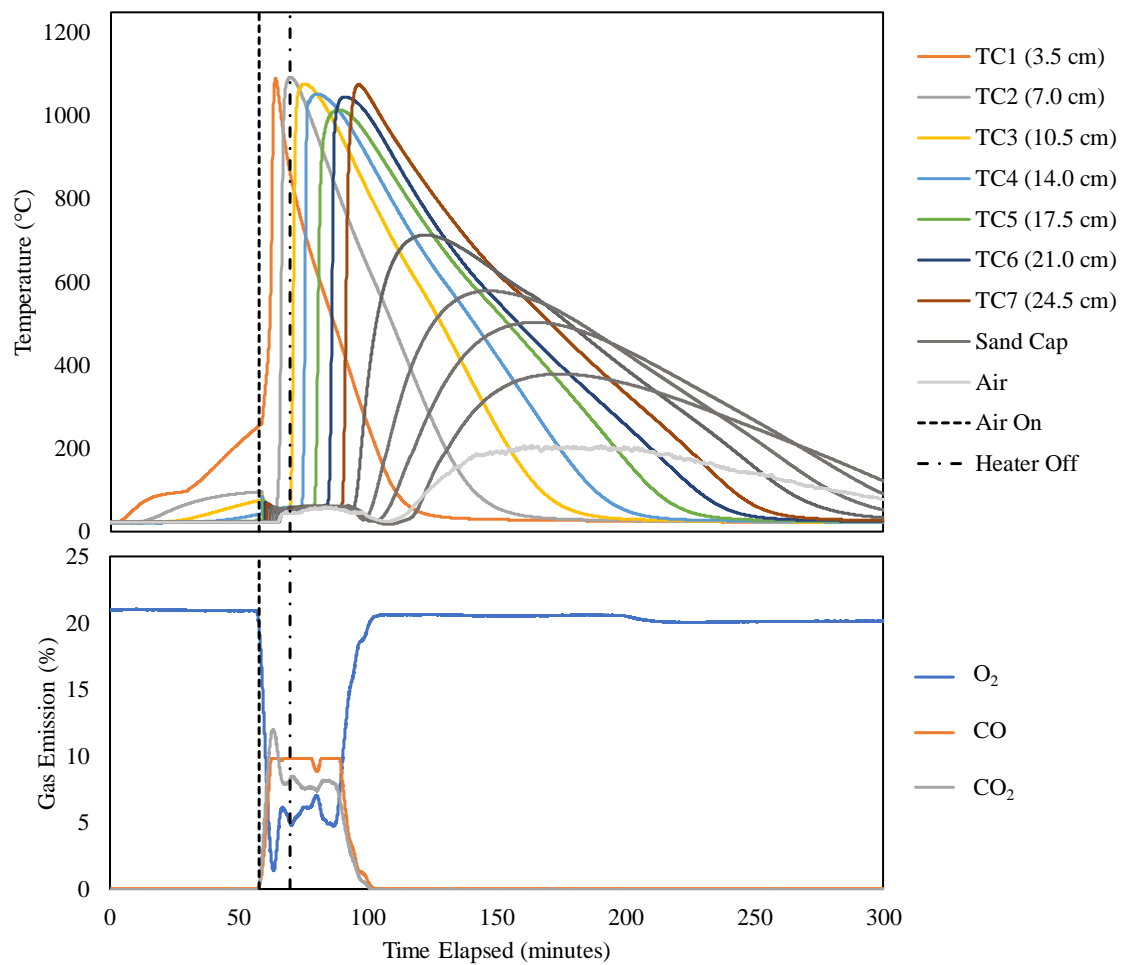
Figure I.20: Thermocouple and gas profiles for S-4 using 51 g GAC/kg sand and an air flux of 5.0 cm/s.

Appendix J: Relationship Between Air Flux & Front Velocity
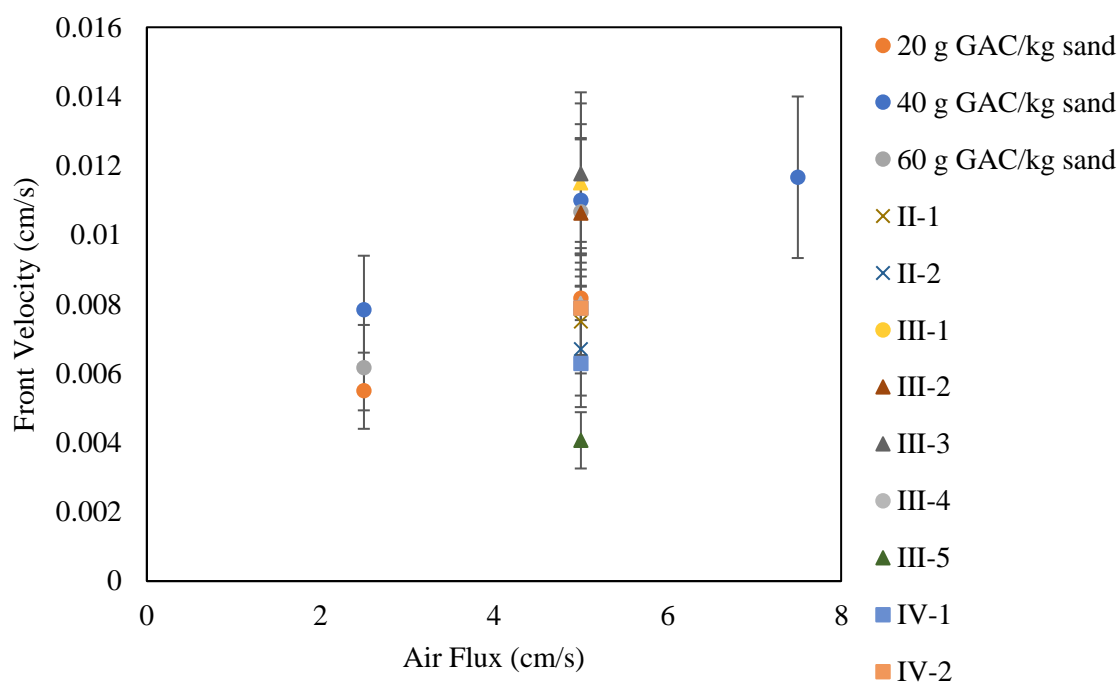
Figure J.1: Relationship between the air flux and front velocity for all experiments completed.

Appendix K: PFOS Concentrations in Stock Solution

Table K.1: Average PFOS Concentration in Stock Solution Before Adding GAC and
After GAC Was Removed

Experiment	Before Adding GAC (mg PFOS/L)	After Removing GAC (mg PFOS/L)
II-1	180.5	0.0954
II-2	190.8	0.1288

Appendix L: PFAS Concentrations Before and After Smouldering Treatment

Table L.1: PFAS Concentrations Before and After Smouldering Treatment for All Experiments Conducted

Experiment		PFBA (mg/kg)	PFPeA (mg/kg)	PFBS (mg/kg)	PFHxA (mg/kg)	PFHpA (mg/kg)	PFHxS (mg/kg)	PFOA (mg/kg)	PFNA (mg/kg)	PFOS (mg/kg)	PFDA (mg/kg)	PFUnA (mg/kg)	PFDoA (mg/kg)	PFOSA (mg/kg)
Contaminated GAC														
II-1	Pre-treatment[b]	B.D.L.[a]	B.D.L.	B.D.L.	B.D.L.	B.D.L.	B.D.L.	B.D.L.	B.D.L.	182.1	B.D.L.	B.D.L.	B.D.L.	B.D.L.
	Post-treatment	B.D.L.	B.D.L.	B.D.L.	B.D.L.	B.D.L.	B.D.L.	B.D.L.	B.D.L.	B.D.L.	B.D.L.	B.D.L.	B.D.L.	B.D.L.
II-2	Pre-treatment[b]	B.D.L.	B.D.L.	B.Q.L.	B.D.L.	B.D.L.	0.195	B.D.L.	B.D.L.	197.7	B.D.L.	B.D.L.	B.D.L.	B.D.L.
	Post-treatment	B.D.L.	B.D.L.	B.D.L.	B.D.L.	B.D.L.	B.D.L.	B.D.L.	B.D.L.	0.431	B.D.L.	B.D.L.	B.D.L.	B.D.L.
Spiked Soil														
III-2[c]	Pre-treatment	n/a[d]	n/a	0.695	n/a	0.233	0.197	3.363	0.344	0.405	n/a	n/a	n/a	n/a
	Post-treatment	n/a	n/a	B.D.L.	n/a	B.D.L.	B.D.L.	$3.01 \times 10^{-4,\,e}$	B.D.L.	B.D.L.[f]	n/a	n/a	n/a	n/a
III-3	Pre-treatment	B.D.L.	B.D.L.	0.089	B.D.L.	0.220	0.171	2.442	0.158	0.216	1.25×10^{-3}	B.D.L.	B.D.L.	B.D.L.
	Post-treatment	B.D.L.	B.D.L.	B.D.L.	B.D.L.	B.D.L.	B.D.L.	B.D.L.	B.D.L.	B.D.L.	B.D.L.	B.D.L.	B.D.L.	B.D.L.
III-4	Pre-treatment	B.D.L.	B.D.L.	0.126	B.D.L.	0.313	0.219	3.006	0.185	0.322	B.D.L.	B.D.L.	B.D.L.	B.D.L.
	Post-treatment	B.D.L.	B.D.L.	B.D.L.	B.D.L.	B.D.L.	B.D.L.	B.D.L.	B.D.L.[g]	B.D.L.[g]	B.D.L.	B.D.L.	B.D.L.	B.D.L.
III-5	Pre-treatment	1.73×10^{-3}	B.D.L.	0.074	B.D.L.	0.108	0.069	2.386	0.095	0.162	B.D.L.	B.D.L.	B.D.L.	B.D.L.
	Post-treatment	B.D.L.	B.D.L.	B.D.L.[h]	B.D.L.	B.D.L.	B.D.L.	B.D.L.	B.D.L.	B.D.L.[h]	B.D.L.	B.D.L.	B.D.L.	B.D.L.
Contaminated Field Soil														
IV-1	Pre-treatment	B.Q.L.	B.Q.L.	B.Q.L.	B.Q.L.	B.Q.L.	0.017	0.002	B.Q.L.	0.353	B.Q.L.	B.Q.L.	B.Q.L.	B.Q.L.
	Post-treatment	B.D.L.	B.D.L.	B.D.L.	B.D.L.	B.D.L.	B.Q.L.	B.Q.L.	B.D.L.	B.Q.L.	B.D.L.	B.D.L.	B.D.L.	B.D.L.
IV-2	Pre-treatment	2.84×10^{-3}	B.D.L.	3.29×10^{-4}	B.D.L.	B.D.L.	5.12×10^{-3}	B.D.L.	B.D.L.	0.092	B.D.L.	B.D.L.	B.D.L.	B.D.L.
	Post-treatment	B.D.L.	B.D.L.	B.D.L.	B.D.L.	B.D.L.	B.D.L.	B.D.L.	B.D.L.	B.D.L.	B.D.L.	B.D.L.	B.D.L.	B.D.L.

[a]B.D.L = 0.0004 mg/kg, B.Q.L. = 0.001 mg/kg

[b]Concentration was calculated using the concentration of the stock solution before and after the GAC was added. Concentration reported applies to the GAC and sand used for the experiment.

[c]Samples analyzed by SGS AXYS Analytical Services Ltd.

[d]n/a indicates PFAS compound was not analyzed for in the sample.

[e]Two post-treatment samples had a PFOA concentration of 5.08×10^{-4} mg/kg and 2.96×10^{-4} mg/kg, the third post-treatment sample was B.D.L.

[f]One post-treatment sample had a PFOS concentration of 2.25×10^{-4} mg/kg. When averaged, the three samples were below the detection limit.

[g]One post-treatment sample had a PFOS concentration of 3.08×10^{-3} mg/kg and another had 3.37×10^{-3} mg/kg PFNA. The average of the three post-treatment samples was below the average detection limit.

[h]One post-treatment sample had a PFOS concentration of 5.02×10^{-4} mg/kg and a different post-treatment sample had PFBS concentration of 1.27×10^{-4} mg/kg. The average of the three post-treatment samples was below the detection limit for both compounds.

Appendix M: PFAS Observed in Rinses of Emissions Glassware

Table M.1: Basic Methanol Rinse Results for Experiments II-1 and III-3 (B.D.L. = 0.0004 mg/L & B.Q.L. = 0.001 mg/L)

Experiment	Sample Name	PFBA (ppb)	PFPeA (ppb)	PFBS (ppb)	PFHxA (ppb)	PFHpA (ppb)	PFHxS (ppb)	PFOA (ppb)	PFNA (ppb)	PFOS (ppb)	PFDA (ppb)	PFUnA (ppb)	PFDoA (ppb)	PFOSA (ppb)
II-1	Blank Rinse	3.17	B.D.L.	B.D.L.	B.D.L.	B.D.L.	B.D.L.	B.Q.L.	B.D.L.	B.Q.L.	B.D.L.	B.D.L.	B.D.L.	B.D.L.
	Tubing Rinse - Pre-test	3.71	B.D.L.	B.D.L.	19.56	B.D.L.	B.D.L.	B.D.L.	B.D.L.	2.17	B.D.L.	B.D.L.	B.D.L.	B.D.L.
	Tubing Rinse - 1	1.47	B.D.L.	B.D.L.	B.D.L.	B.D.L.	B.D.L.	B.D.L.	B.D.L.	1.47	B.D.L.	B.D.L.	B.D.L.	B.D.L.
	Glass Piece 1 - Pre-test	3.06	B.D.L.	B.D.L.	B.D.L.	B.D.L.	B.D.L.	B.Q.L.	B.D.L.	1.90	B.D.L.	B.D.L.	B.D.L.	B.D.L.
	Glass Piece 1 - 1	1.45	B.D.L.	B.D.L.	B.D.L.	B.D.L.	B.D.L.	B.D.L.	B.D.L.	1.78	B.D.L.	B.D.L.	B.D.L.	B.D.L.
	Glass Piece 2 - Pre-test	n/a	n/a	n/a	n/a	n/a	n/a	n/a	n/a	n/a	n/a	n/a	n/a	n/a
	Glass Piece 2 - 1	2.35	B.D.L.	B.D.L.	B.D.L.	B.D.L.	B.D.L.	B.D.L.	B.D.L.	1.37	B.D.L.	B.D.L.	B.D.L.	B.D.L.
	XAD 1 Rinse - Pre-test	1.90	B.D.L.	B.D.L.	32.18	B.D.L.	B.D.L.	B.D.L.	B.D.L.	4.10	B.D.L.	B.D.L.	B.D.L.	B.D.L.
	XAD 1 Rinse - 1	B.Q.L.	B.D.L.	B.D.L.	2.87	B.D.L.	B.D.L.	B.D.L.	B.D.L.	2.60	B.D.L.	B.D.L.	B.D.L.	B.D.L.
	XAD 2 Rinse - Pre-test	n/a	n/a	n/a	n/a	n/a	n/a	n/a	n/a	n/a	n/a	n/a	n/a	n/a
	XAD 2 Rinse - 1	1.44	B.D.L.	B.D.L.	B.D.L.	B.D.L.	B.D.L.	1.28	B.D.L.	1.97	B.D.L.	B.D.L.	B.D.L.	B.D.L.
	Impinger Top Rinse - Pre-test	2.40	B.D.L.	B.D.L.	26.92	B.D.L.	B.D.L.	B.D.L.	B.D.L.	2.89	B.D.L.	B.D.L.	B.D.L.	B.D.L.
	Impinger Top Rinse - 1	1.57	B.D.L.	B.D.L.	3.04	B.D.L.	B.D.L.	B.D.L.	B.Q.L.	1.36	B.D.L.	B.D.L.	B.D.L.	B.D.L.
	Impinger Bottom Rinse - Pre-test	2.70	B.D.L.	B.D.L.	32.00	B.D.L.	B.D.L.	1.10	B.D.L.	1.85	B.D.L.	B.D.L.	B.D.L.	B.D.L.
	Impinger Bottom Rinse - 1	n/a	n/a	n/a	n/a	n/a	n/a	n/a	n/a	n/a	n/a	n/a	n/a	n/a
	Glass Piece 3 - Pre-test	2.98	B.D.L.	B.D.L.	30.89	B.D.L.	B.D.L.	B.D.L.	B.D.L.	8.62	B.D.L.	B.D.L.	B.D.L.	B.D.L.
	Glass Piece 3 - 1	1.41	B.D.L.	B.D.L.	17.99	B.D.L.	B.D.L.	B.Q.L.	B.D.L.	B.Q.L.	B.D.L.	B.D.L.	B.D.L.	B.D.L.
	Glass Piece 4 - Pre-test	n/a	n/a	n/a	n/a	n/a	n/a	n/a	n/a	n/a	n/a	n/a	n/a	n/a
	Glass Piece 4 - 1	B.D.L.	B.D.L.	B.D.L.	5.12	B.D.L.	B.D.L.	B.D.L.	B.D.L.	B.Q.L.	B.D.L.	B.D.L.	B.D.L.	B.D.L.
III-3	Blank Rinse	B.D.L.	0.00	B.D.L.	B.D.L.	B.D.L.	B.D.L.	B.D.L.	B.D.L.	B.D.L.	B.D.L.	B.D.L.	B.D.L.	0.00
	Tubing Rinse - Pre-test	B.D.L.	0.00	B.D.L.	B.D.L.	0.09	B.D.L.	B.D.L.	B.D.L.	B.D.L.	B.D.L.	B.D.L.	B.D.L.	0.00
	Tubing Rinse - 1	B.D.L.	0.10	B.D.L.	0.88	0.10	B.D.L.	B.D.L.	B.D.L.	B.D.L.	0.15	B.D.L.	B.D.L.	0.00
	Glass Piece 1 - Pre-test	B.D.L.	0.18	B.D.L.	B.Q.L.	0.10	B.D.L.	B.D.L.	B.D.L.	B.D.L.	0.24	B.D.L.	B.D.L.	0.00
	Glass Piece 1 - 1	B.D.L.	0.16	B.D.L.	B.D.L.	0.10	B.D.L.	B.D.L.	B.D.L.	B.D.L.	B.D.L.	B.D.L.	0.05	0.00
	Glass Piece 2 - Pre-test	B.D.L.	0.34	B.D.L.	B.D.L.	B.D.L.	B.D.L.	B.D.L.	B.D.L.	B.D.L.	0.11	B.D.L.	B.D.L.	0.00
	Glass Piece 2 - 1	B.D.L.	0.29	B.D.L.	B.D.L.	B.D.L.	B.D.L.	B.D.L.	B.D.L.	B.D.L.	B.D.L.	B.D.L.	B.D.L.	0.00
	XAD 1 Rinse - Pre-test	B.D.L.	0.00	B.D.L.	1.32	B.D.L.	B.D.L.	B.D.L.	B.D.L.	B.D.L.	0.13	B.D.L.	B.D.L.	0.00
	XAD 1 Rinse - 1	B.D.L.	0.08	B.D.L.	B.Q.L.	B.D.L.	B.D.L.	0.81	B.D.L.	B.D.L.	B.Q.L.	B.D.L.	0.07	0.00
	XAD 2 Rinse - Pre-test	B.D.L.	0.24	B.D.L.	1.39	B.D.L.	B.D.L.	B.D.L.	B.D.L.	B.D.L.	B.D.L.	B.D.L.	B.D.L.	0.00
	XAD 2 Rinse - 1	B.D.L.	1.02	B.D.L.	B.Q.L.	B.D.L.	B.D.L.	B.D.L.	B.D.L.	B.D.L.	B.Q.L.	B.D.L.	B.D.L.	0.00
	Impinger Top Rinse - Pre-test	B.D.L.	0.16	B.Q.L.	1.86	0.13	B.D.L.	B.D.L.	B.D.L.	B.D.L.	0.12	B.D.L.	B.D.L.	0.00
	Impinger Top Rinse - 1	B.D.L.	0.14	B.Q.L.	B.D.L.	0.08	B.D.L.	B.D.L.	B.D.L.	B.D.L.	B.D.L.	B.D.L.	0.06	0.00
	Impinger Bottom Rinse - Pre-test	B.D.L.	0.00	B.Q.L.	1.61	B.D.L.	B.D.L.	B.D.L.	B.D.L.	B.D.L.	B.Q.L.	B.D.L.	B.D.L.	0.00
	Impinger Bottom Rinse - 1	B.D.L.	0.15	B.D.L.	B.Q.L.	B.D.L.	B.D.L.	B.D.L.	B.D.L.	B.D.L.	B.Q.L.	B.D.L.	B.D.L.	0.00
	Glass Piece 3 - Pre-test	B.D.L.	0.14	B.D.L.	3.43	B.D.L.	B.D.L.	B.D.L.	B.D.L.	B.D.L.	B.Q.L.	B.D.L.	B.Q.L.	0.00
	Glass Piece 3 - 1	B.D.L.	0.14	B.D.L.	1.36	B.D.L.	B.D.L.	B.D.L.	B.D.L.	B.D.L.	B.Q.L.	B.D.L.	B.D.L.	0.00
	Glass Piece 4 - Pre-test	B.D.L.	1.43	B.D.L.	B.D.L.	B.D.L.	B.D.L.	B.D.L.	B.D.L.	B.D.L.	B.D.L.	B.D.L.	B.D.L.	0.00
	Glass Piece 4 - 1	B.D.L.	0.29	B.D.L.	B.Q.L.	B.D.L.	B.D.L.	B.D.L.	B.D.L.	B.D.L.	B.D.L.	B.D.L.	B.Q.L.	0.00

Appendix N: PFAS Captured in PFAS Emissions

Table N.1: PFAS Captured for Experiments Using Impingers Containing KOH Solution

Experiment	Sample	PFBA (ng/L)	PFPeA (ng/L)	PFBS (ng/L)	PFHxA (ng/L)	PFHpA (ng/L)	PFHxS (ng/L)	PFOA (ng/L)	PFNA (ng/L)	PFOS (ng/L)	PFDA (ng/L)	PFUnA (ng/L)	PFDoA (ng/L)	PFOSA (ng/L)
Spiked Soil														
	Impinger 1	32.1	16.1	B.D.L.	19.4	28	B.D.L.	12	B.D.L.	B.D.L.	B.D.L.	B.D.L.	B.D.L.	NR
III-2[a]	Impinger 2	B.D.L.	B.D.L.	B.D.L.	B.D.L.	B.D.L.	B.D.L.	B.D.L.	B.D.L.	B.D.L.	B.D.L.	B.D.L.	B.D.L.	NR
	Impinger 3	B.D.L.	B.D.L.	B.D.L.	B.D.L.	B.D.L.	B.D.L.	14	B.D.L.	B.D.L.	B.D.L.	B.D.L.	B.D.L.	NR
	Impinger 4	B.D.L.	B.D.L.	B.D.L.	B.D.L.	B.D.L.	B.D.L.	6	B.D.L.	B.D.L.	B.D.L.	B.D.L.	B.D.L.	NR
Contaminated Field Soil														
	Impinger 1	B.D.L.	B.D.L.	B.D.L.	B.D.L.	B.D.L.	B.D.L.	B.D.L.	B.D.L.	B.D.L.	B.D.L.	B.D.L.	B.D.L.	B.D.L.
	Impinger 2	B.D.L.	B.D.L.	B.D.L.	B.D.L.	B.D.L.	B.D.L.	B.D.L.	B.D.L.	B.D.L.	B.D.L.	B.D.L.	B.D.L.	B.D.L.
IV-1	Impinger 3	B.D.L.	B.D.L.	B.D.L.	B.D.L.	B.D.L.	B.D.L.	B.D.L.	B.D.L.	B.D.L.	B.D.L.	B.D.L.	B.D.L.	B.D.L.
	Impinger 4	B.D.L.	B.D.L.	B.D.L.	B.D.L.	B.D.L.	B.D.L.	B.D.L.	B.D.L.	B.D.L.	B.D.L.	B.D.L.	B.D.L.	B.D.L.
	Impinger 5	B.D.L.	B.D.L.	B.D.L.	B.D.L.	B.D.L.	B.D.L.	B.D.L.	B.D.L.	B.D.L.	B.D.L.	B.D.L.	B.D.L.	B.D.L.

[a]PFPeS, PFHpA, PFTrDA, PFTeDA were also analyzed. All were B.D.L. (<0.0004 mg/L)

Table N.2: PFAS Captured for Experiments Using Two XAD Tubes & One Impinger

Experiment	Sample Name	PFBA (mg/kg)	PFPeA (mg/kg)	PFBS (mg/kg)	PFHxA (mg/kg)	PFHpA (mg/kg)	PFHxS (mg/kg)	PFOA (mg/kg)	PFNA (mg/kg)	PFOS (mg/kg)	PFDA (mg/kg)	PFUnA (mg/kg)	PFDoA (mg/kg)	PFOSA (mg/kg)
Contaminated GAC														
II-1	XAD 1 - GAC	6.70×10^{-1}	1.93×10^{-1}	B.D.L.	7.28×10^{-2}	B.D.L.	B.D.L.	B.D.L.	B.D.L.	B.D.L.	B.D.L.	B.D.L.	B.D.L.	B.D.L.
	XAD 1 - Mineral wool	B.D.L.	B.D.L.	B.D.L.	B.D.L.	B.D.L.	B.D.L.	B.D.L.	B.D.L.	3.72×10^{-1}	B.D.L.	B.D.L.	B.D.L.	B.D.L.
	XAD 2 - GAC	B.D.L.	B.D.L.	B.D.L.	B.D.L.	B.D.L.	B.D.L.	B.D.L.	B.D.L.	B.D.L.	B.D.L.	B.D.L.	B.D.L.	B.D.L.
	XAD 2 - Mineral wool	B.D.L.	B.D.L.	B.D.L.	B.D.L.	B.D.L.	B.Q.L.	5.83×10^{-2}	B.D.L.	1.05×10^{-1}	B.D.L.	B.D.L.	B.D.L.	B.D.L.
	Impinger - GAC	B.D.L.	B.D.L.	B.D.L.	B.D.L.	B.D.L.	B.D.L.	B.D.L.	B.D.L.	B.D.L.	B.D.L.	B.D.L.	B.D.L.	B.D.L.
II-2	XAD 1 – GAC[a]	6.61×10^{-1}	2.87×10^{-1}	B.D.L.	1.20×10^{-1}	8.41×10^{-2}	B.D.L.	1.38×10^{-2}	B.D.L.	4.60×10^{-2}	B.D.L.	B.D.L.	B.D.L.	B.D.L.
	XAD 1 - Mineral wool	7.83×10^{-3}	B.Q.L.	B.Q.L.	B.Q.L.	B.D.L.	6.90×10^{-3}	B.D.L.	B.D.L.	9.27×10^{-1}	B.D.L.	4.43×10^{-3}	B.D.L.	B.D.L.
	XAD 2 - GAC	B.D.L.	B.D.L.	B.D.L.	B.Q.L.	B.D.L.	B.D.L.	B.D.L.	B.D.L.	B.Q.L.	B.D.L.	B.Q.L.	B.D.L.	B.D.L.
	XAD 2 - Mineral wool	1.01×10^{-2}	B.Q.L.	B.D.L.	1.54×10^{-2}	1.35×10^{-2}	6.22×10^{-3}	2.61×10^{-2}	1.53×10^{-2}	1.68	7.27×10^{-3}	5.10×10^{-3}	5.62×10^{-3}	B.D.L.
	Impinger - GAC	B.D.L.	B.D.L.	B.D.L.	B.D.L.	B.D.L.	B.D.L.	B.D.L.	B.D.L.	B.D.L.	B.D.L.	3.10×10^{-3}	B.D.L.	B.D.L.
Spiked Soil[b]														
III-3	XAD 1 - GAC	B.D.L.	$9.96E \times 10^{-3}$	B.D.L.	1.85×10^{-2}	9.60×10^{-3}	B.D.L.	9.19×10^{-3}	B.D.L.	B.D.L.	B.D.L.	B.D.L.	B.D.L.	B.D.L.
	XAD 1 - Mineral wool	B.D.L.	1.02×10^{-2}	5.20×10^{-3}	8.24×10^{-3}	1.25×10^{-2}	B.Q.L.	1.80×10^{-2}	3.98×10^{-3}	6.65×10^{-3}	2.87×10^{-3}	B.D.L.	2.50×10^{-3}	B.D.L.
	XAD 2 - GAC	B.D.L.	B.D.L.	B.D.L.	B.D.L.	8.18×10^{-4}	B.D.L.	B.D.L.	B.D.L.	B.D.L.	B.D.L.	B.D.L.	B.D.L.	B.D.L.
	XAD 2 - Mineral wool	B.D.L.	B.D.L.	5.65E-03	B.Q.L.	8.52E-03	B.Q.L.	3.20×10^{-2}	1.09×10^{-2}	6.17×10^{-3}	6.71×10^{-3}	B.D.L.	3.08×10^{-3}	B.D.L.
	Impinger - GAC	B.Q.L.	1.01×10^{-2}	B.D.L.	B.Q.L.	1.12×10^{-3}	B.D.L.	B.Q.L.	B.D.L.	B.D.L.	B.D.L.	B.D.L.	B.D.L.	B.D.L.
III-4	XAD 1 - GAC	B.D.L.	B.Q.L.	B.D.L.	2.61×10^{-2}	B.D.L.	B.D.L.	B.D.L.	B.D.L.	B.Q.L.	B.D.L.	B.D.L.	B.D.L.	B.D.L.
	XAD 1 - Mineral wool	B.D.L.	B.D.L.	B.Q.L.	B.D.L.	B.D.L.	B.Q.L.	B.D.L.	1.60×10^{-2}	9.85×10^{-1}	B.D.L.	B.D.L.	B.D.L.	B.D.L.
	XAD 2 - GAC	B.D.L.	B.D.L.	B.D.L.	B.D.L.	B.D.L.	B.D.L.	B.D.L.	B.D.L.	B.D.L.	B.D.L.	B.D.L.	B.D.L.	B.D.L.
	XAD 2 - Mineral wool	B.D.L.	B.D.L.	B.D.L.	B.Q.L.	B.D.L.	B.Q.L.	B.D.L.	B.Q.L.	2.36×10^{-1}	B.D.L.	B.D.L.	B.D.L.	B.D.L.
	Impinger - GAC	B.D.L.	B.D.L.	B.D.L.	B.D.L.	B.D.L.	B.D.L.	B.D.L.	B.D.L.	B.D.L.	B.D.L.	B.D.L.	B.D.L.	B.D.L.
III-5	XAD 1 - GAC	8.31×10^{-3}	B.D.L.	B.D.L.	B.D.L.	B.D.L.	B.D.L.	B.D.L.	B.D.L.	B.D.L.	B.D.L.	B.D.L.	B.D.L.	B.D.L.
	XAD 1 - Mineral wool	5.03×10^{-2}	B.D.L.	B.D.L.	B.D.L.	B.D.L.	B.D.L.	B.D.L.	B.D.L.	2.10	B.D.L.	B.D.L.	B.D.L.	B.D.L.
	XAD 2 - GAC[c]	NR	NR	NR	NR	NR	NR	NR	NR	NR	NR	NR	NR	NR
	XAD 2 - Mineral wool	1.12×10^{-1}	B.D.L.	B.D.L.	B.D.L.	B.D.L.	B.D.L.	B.Q.L.	B.Q.L.	2.26×10^{-1}	B.D.L.	B.D.L.	B.D.L.	B.D.L.
	Impinger - GAC	4.37×10^{-3}	B.D.L.	B.D.L.	B.D.L.	B.D.L.	B.D.L.	B.D.L.	B.D.L.	B.D.L.	B.D.L.	B.D.L.	B.D.L.	B.D.L.
Contaminated Field Soil														
IV-2	XAD 1 - GAC	4.89×10^{-3}	B.D.L.	B.D.L.	B.D.L.	B.D.L.	B.D.L.	B.D.L.	B.D.L.	B.D.L.	B.D.L.	B.D.L.	B.D.L.	B.D.L.
	XAD 1 - Mineral wool	5.23×10^{-3}	B.D.L.	B.D.L.	B.D.L.	B.D.L.	B.D.L.	B.D.L.	1.19×10^{-1}	B.D.L.	B.D.L.	B.D.L.	B.D.L.	B.D.L.
	XAD 2 - GAC	B.D.L.	B.D.L.	B.D.L.	B.D.L.	B.D.L.	B.D.L.	B.D.L.	2.36×10^{-3}	B.D.L.	B.D.L.	B.D.L.	B.D.L.	B.D.L.
	XAD 2 - Mineral wool	8.38×10^{-3}	B.D.L.	B.D.L.	B.D.L.	B.D.L.	B.D.L.	B.D.L.	9.77×10^{-1}	B.D.L.	B.D.L.	B.D.L.	B.D.L.	B.D.L.
	Impinger - GAC	6.17×10^{-3}	B.D.L.	B.D.L.	B.D.L.	B.D.L.	B.D.L.	B.D.L.	B.D.L.	B.D.L.	B.D.L.	B.D.L.	B.D.L.	B.D.L.

[a]Additional analysis was completed for shorter-chain compounds: TFA = 1.80 mg/kg and PFPA = 3.25 mg/kg.

[b]XAD and impinger samples were not analyzed for experiment III-1.

[c]Sample results were not reported.

Appendix O: Soluble Fluoride Results

Table O.1: Soluble Fluoride Results

Sample	Soluble Fluoride (mg/kg)
Spiked Soil	
Blank Topsoil	B.D.L.
III-4 Pre-treatment	B.D.L.
III-4 Post-treatment	B.D.L.
III-5 Pre-treatment	B.D.L.
III-5 Post-treatment	B.D.L.
Contaminated Field Soil	
IV-1 Pre-treatment	B.D.L.
IV-2 Pre-treatment	B.D.L.
IV-2 Pre-treatment (duplicate)	B.D.L.
IV-2 Post-treatment	B.D.L.

Curriculum Vitae

Name:	Alexandra Lorna Duchesne

Post-secondary Education and Degrees:
The University of Western Ontario
London, Ontario, Canada
2012-2017 B.E.Sc.

Honours and Awards:
Province of Ontario Graduate Scholarship
2017-2018

Eric and Ruby Chung Award Graduate Scholarship
2018

Province of Ontario Graduate Scholarship (declined)
2018-2019

NSERC Canada Graduate Scholarship
2018-2019

Related Work Experience:
Teaching Assistant
The University of Western Ontario
2018-2019

Lecture Assistant
The University of Western Ontario
2017-2019